ENVIRONMENTAL CHAMBER STUDIES OF OZONE IMPACTS OF COATINGS VOCs

Final Report to the

California Air Resources Board
Contract No. 07-339

By

William P. L. Carter

May 11, 2011

Center for Environmental Research and Technology
College of Engineering
University of California
Riverside, California 92521

ABSTRACT

An environmental chamber and modeling study was conducted to reduce uncertainties in atmospheric ozone impacts for volatile organic compounds (VOCs) emitted from coatings. Some coatings VOCs (Texanol® and low-aromatic petroleum distillates) have near-zero or negative incremental ozone reactivities in chamber experiments, but calculations show positive ozone impacts in the atmosphere. Modeling indicated that experiments with increased light intensity and added H_2O_2 should give reactivities that better correlate with those in the atmosphere. After upgrading our chamber's light source, experiments to test the new method performed as expected, and gave good correlations between experimental and atmospheric MIR values for the VOCs tested. These experiments also appear to be more sensitive to effects of VOCs on secondary organic aerosol (SOA) formation than previous experiments. Such experiments should be included in future environmental chamber reactivity studies, though other types of experiments are also needed for adequate mechanism evaluation.

Experiments were also conducted to assess ozone impacts of ethyl methyl ketone oxime (EMKO), and soy ester solvents. The EMKO results indicated it has both radical sinks and NO_x sources in its mechanism, and has no measurable impact on SOA formation. The EMKO mechanism that simulated the data gave a negative MIR of -1.27 gm O_3 /gm VOC, but positive MOIR and EBIR values of 0.41 and 1.14, respectively. This has implications about the use of the MIR scale for such compounds. The experiments to assess soy ester reactivity were not successful because of the low volatility of the constituents, but uncertainties concerning atmospheric availability are probably more important.

ACKNOWLEDGEMENTS AND DISCLAIMERS

This work was funded by the California Air Resources Board (CARB) through contract number 07-339. The environmental chamber experiments were carried out at the College of Engineering Center for Environmental Research and Technology (CE-CERT) by Shunsuke Nakao, Kathy Cocker, Wendy Goliff, Dylan Switzer, Christoper Clark, Xiaochen Tang or Ping Tang, with assistance from Kurt Bumiller, and Charles Bufalino. Mr. Dennis Fitz provided assistance in administration of this project. Dr. Gookyoung Heo provided valuable assistance in the preparation of this report. Helpful discussions with Dr. Roger Atkinson and Dr. David Cocker are also acknowledged.

TABLE OF CONTENTS

LIST OF TABLES

LIST OF FIGURES

LIST OF FIGURES (continued)

EXECUTIVE SUMMARY

Background

Coatings use involves emissions of volatile organic compounds (VOCs) into the atmosphere, where they can contribute to the formation of ground-level ozone. VOCs differ in their effects on ozone formation, and the Maximum Incremental Reactivity (MIR) scale has been used to quantify this. MIR values are not measured experimentally, but are calculated using models for airshed conditions and atmospheric chemical mechanisms for the VOCs' reactions. Therefore, the validity of the MIR values depends on the validity of the mechanisms used in the models, which need to be tested experimentally. One problem is that some important coatings VOCs, namely Texanol® and various petroleum distillates, have been found to have very low or negative effects on ozone formation in environmental chamber experiments but are calculated to have positive MIR values in the atmosphere. Although the mechanisms used to calculate the MIR values for these VOCs fit these chamber data reasonably well, these differences lead to uncertainties concerning the credibility and applicability of the use of the chamber data to evaluate atmospheric mechanisms. In addition, there are coatings compounds for which environmental chamber data are not available and whose mechanisms and MIR values are unknown or highly uncertain.

This report describes results of a project we carried out to address these research needs. We conducted a modeling assessment, chamber facility upgrades, and experiments to develop and test new types of chamber experiments that give reactivity results that correspond better to those calculated for the atmosphere. In addition, experiments were conducted or attempted to assess the atmospheric ozone impact of ethyl methyl ketone oxime (EMKO), and soy ester solvents, both of which are found in coatings emissions surveys in California but have not been studied previously.

Methods

All experiments were carried out using the UCR EPA chamber and model calculations were carried out using the SAPRC-07 chemical mechanism used to derive the current MIR scale. The modeling assessment of chamber vs. atmospheric reactivities involved simulating reactivity results of various types of chamber experiments and comparing them with atmospheric MIR values, and calculating how the impacts of various aspects of VOC oxidation mechanism affect these results. Initial calculations indicated that increasing light intensity and run duration should result in better correlations between chamber and atmospheric reactivities, so additional banks of blacklights were added to increase the light intensity in our reactivity experiments by a factor of ~3, and attempts were made to increase the irradiation time in our experiments. Most of the experiments for this project were carried out with the increased light intensity, but experimental problems prevented us from increasing the duration of the irradiation beyond 6-8 hours. The reactivity experiments with EMKO and representative soy ester constituents employed the same methodology as in our previous chamber reactivity studies, except with the higher light intensity.

Results and Discussion

The results of the modeling assessment of reactivity experiments indicated that increasing the light intensity and adding H_2O_2 as a radical initiator resulted in experiments that gave very good correlations between chamber and atmospheric reactivities for non-aromatic coatings constituents, and reasonably good correlations for most others. We then tested this method by conducting such experiments

for n-butane, n-octane, m-xylene Texanol®, and representative petroleum distillate samples, and the results were generally as predicted. For the non-aromatic materials the correlation coefficient between chamber reactivities and atmospheric MIR was 82%, and the correlation is higher if aromatics are included. The results suggested that the current mechanism may underestimate reactivities for aromatics, but this is indicated by other data as well. The new experiments also appear to be more sensitive to effects of the test compounds on particle matter (PM) formation than the previous types of experiments.

The experiments with EMKO indicate that it has both strong radical sinks and NO_x sources in its mechanism. The mechanism developed to simulate these data predicted relatively high negative MIR values for the atmosphere, but significantly positive reactivities under NO_x - limited conditions. This made EMKO unusual in having reactivity characteristics more like NO_x than most VOCs, and has implications concerning the use of the MIR scale when regulating such compounds.

We were unable to obtain useful data to reduce reactivity estimates for the soy ester mixtures because of the low volatilities of their major chemical constituents and our inability to obtain commercial samples of more volatile chemically similar analogues. We did obtain data suggesting that current estimated mechanisms may somewhat overestimate reactivities of saturated fatty esters, but these are expected to make only minor contributions to the overall soy ester reactivity.

Conclusions and Recommendations

It is concluded that use of the new reactivity experiments with higher light intensity and added H_2O_2 solves the problems of inconsistencies between chamber and atmospheric reactivities that was observed previously for compounds like Texanol® and petroleum distillates that are important in coatings. This gives more credibility to reactivity results that have been obtained previously. These new experiments, which also appear to be potentially more useful than previous experiments for assessing effects of VOCs on SOA formation, therefore should be included in the suite of experiments used to evaluate mechanisms for reactivity assessment. However, other types of experiments are also needed to fully evaluate the mechanisms. The minimum set of mechanism evaluation experiments should also include the previous types of MIR (higher NO_x) experiments that are more sensitive to radical termination effects, and experiments to test mechanisms under NO_x - limited conditions that are not well tested by experiments designed to simulate conditions of the MIR scale.

The reactivity results for EMKO allow this compound to be added to the MIR and other reactivity scales. However, its unusual reactivity characteristics reveal a problem with the use of the MIR scale for regulatory applications. The purpose of the MIR scale is to quantify the maximum ozone impact of the compounds, and this is the case for most VOCs. But this is not the case for EMKO, which has a negative MIR but quite high positive reactivities for low NO_x conditions. This means that reactivities in the MIR scale cannot be the only basis for making exemption decisions for VOCs, and that the results for EMKO may need to be taken into account when the reactivity scale used in regulatory applications is updated.

With regard to the soy ester materials, whose reactivities we were unable to assess for this project, it should be pointed out that uncertainties in the reaction mechanism and MIR are not the most important considerations. The availability of these low volatility compounds to undergo gas-phase reactions to form ozone in the atmosphere is the much greater uncertainty. It is reasonable to expect that at least some of the soy ester constituents may eventually make it to the gas phase and undergo reaction if given enough time, but it is also reasonable to expect that the fraction available for reaction will be less than 100%. The availability factor is probably much more uncertain than the currently estimated MIR, and should be a higher research priority for soy esters and other low volatility materials.

INTRODUCTION

Coatings use involves emissions of volatile organic compounds (VOCs) into the atmosphere, where they can react and contribute to the formation of ground-level ozone. Since ground-level ozone exceeds air quality standards in many areas of the United States, ozone reduction is a major reason that coatings VOCs are subject to regulatory action. However, the impact of VOC emissions on ozone formation is complex, depending significantly on the nature of the VOC and the environmental conditions under which the VOC reacts. This needs to be taken into account when developing cost-effective control strategies for coatings VOCs. Otherwise, costly VOC regulations may have relatively little impact on meeting air quality standards, and opportunities for effective VOC control may be missed.

When assessing effects of VOC control strategies on ozone, the only practical way to take all the complex environmental and chemical factors into account is to use air quality models to predict the effects of emissions changes on air quality. Such models require appropriate representation of emissions, ambient conditions, and the physical and chemical transformations that occur in the atmosphere. A critical component of such models with regard to predictions of effects of VOCs on ozone formation is the chemical mechanism, which is the component in the model that represents the chemical transformations by which VOCs cause ozone formation. If significant portions of the chemical mechanism are incorrect or incomplete, then inappropriate VOC control strategies may result.

The atmospheric reactions by which VOCs cause ozone formation are complex and have many types of uncertainties. For this reason the chemical mechanisms used in airshed models cannot be relied upon to give correct predictions unless they have been adequately tested against experimental data. Data from environmental chambers, where the chemical reactions by which VOCs contribute to ozone formation are studied under controlled conditions, currently provide the best way to test chemical mechanisms independently of the many other uncertainties in airshed models regarding emissions, meteorology, and other ambient conditions. Because of this, evaluation against environmental chamber data has been extensively relied upon in the development of current chemical mechanisms (Jeffries et al, 1992; Dodge, 2000)

The SAPRC-99 chemical mechanism (Carter, 2000a) has been the most widely used chemical mechanism in the United States for calculating relative impacts (reactivities) of VOCs on ozone formation, and is the basis of the Maximum Incremental Reactivity (MIR) ozone reactivity scale (Carter, 1994a) used in California regulations for alternative vehicle fuels (CARB, 1993) and aerosol coatings (CARB, 2000). This reactivity scale was also considered as a basis for reactivity-based regulations for architectural coatings VOCs (CARB, 2008). SAPRC-99 has subsequently been updated to the SAPRC-07 chemical mechanism (Carter, 2010a), and this has been used to derive updated MIR and other reactivity scales. The SAPRC-07 MIR scale has recently been implemented as part of California's reactivity-based regulations (Carter, 2010b, CARB, 2010), and the implementation of the SAPRC-07 mechanism in airshed models such as the Community Multiscale Air Quality model (CMAQ) is underway.

The validity of the MIR values for the various types of coatings VOCs depends on the validity of the mechanisms for compounds involved. As indicated above, these mechanisms are highly complex and need to be evaluated against environmental chamber data. For most of the major types of coatings VOCs, their representation in the SAPRC-07 mechanism has been shown to simulate the available environmental chamber data reasonably well (Carter, 2010a), giving us some confidence in the validity of their current MIR values. These include various alkane and aromatic mixtures as occur in petroleum distillates, and

various types of oxygenated compounds with glycol ether and ester groups, for which major representative compounds have been estimated, or experimentally evaluated estimation methods have been derived (e.g., see Carter, 2000a; Carter and Malkina, 2005; Carter, 2008, and references therein). However, coatings also include compounds for which environmental chamber data are not available, and for which data for chemically similar compounds are not sufficient to develop mechanisms. In these cases, MIR values are either highly uncertain or not available. Although many of these compounds are only minor constituents of most coatings, in some cases they are present in sufficient quantities that using high "upper limit" MIR values (e.g., see Appendix D of Carter, 2000a, updated as discussed by Carter, 2010b) significantly affect the reactivity estimates of the materials.

Uncertainties exist in reactivity estimates even for compounds that have been extensively studied. Although the SAPRC-07 mechanisms for the major coatings constituents were extensively evaluated against available environmental chamber data, limitations in the data have resulted in limitations in the extent to which the mechanisms have been evaluated, and therefore in the reliability of their reactivity values. Initially, most of the chamber experiments used for mechanism evaluation have been carried out under relatively high reaction concentrations, making extrapolations to concentrations representative of ambient conditions uncertain. Because of this, the "next generation" UCR EPA environmental chamber was constructed to permit mechanism evaluation experiments to be carried out at under more controlled conditions and at lower concentrations than previously possible (Carter, 2004, Carter et al, 2005a,b). This chamber has subsequently been used for evaluating mechanisms at lower NO_x concentrations than employed previously, for determining effects of changing total VOC and NO_x levels on ozone formation (Carter, 2004; Carter et al, 2005a,b) and for evaluating atmospheric ozone impacts of selected architectural coatings (Carter and Malkina 2005; Carter et al, 2005c) and pesticide VOCs (Carter and Malkina, 2007).

The results of experiments in the new chamber indicated that although the SAPRC-07 chemical mechanism generally performed satisfactorily in simulating O_3 under low NO_x conditions, and in simulating the ozone impacts of most of the coatings VOCs that were studied, some potentially significant problems remain. With regard to the mechanisms in general, they were found to consistently underpredict O_3 formation under conditions of relatively low VOC/NO_x ratios that are characteristic of conditions used to derive the MIR scale. These and other data indicate significant problems with current mechanisms for aromatic hydrocarbons. Although aromatic hydrocarbons are not important constituents in most coatings solvents (except as a minor component of some solvent-borne coatings), they are important constituents affecting atmospheric ozone formation, and mechanism errors for these highly reactive compounds could result in inappropriate control strategies being predicted for all VOCs, because they affect the chemical environment where the VOCs react. Although the aromatics mechanisms incorporated in SAPRC-07 represent an improvement over those in SAPRC-99 in many respects, most of these performance problems in simulating the available environmental chamber data still remain (Carter, 2010a).

With regard to most of the major coatings VOCs that were studied, the recent experiments indicated that in general the SAPRC-07 chemical mechanism performed reasonably well in simulating their incremental reactivities[1] observed in these experiments, once provision was made for the tendency of the general mechanism to underpredict O_3 in the experiments representing MIR conditions (Carter and Malkina 2005; Carter et al, 2005c; Carter, 2010a). However, a concern exists concerning how well the experiments represent ambient conditions, and therefore how useful they are in evaluating the

[1] The Incremental Reactivity of a compound is the change in ozone formed when a small amount is added to the chamber or atmospheric simulation, divided by the amount added

mechanisms under those conditions. In particular, many important types of coatings VOCs such as Texanol® and various petroleum distillates are observed to have very low or even negative effects on ozone formation in environmental chamber experiments but are predicted, using the same mechanism that accurately simulates these chamber data, to have a positive effect on ozone formation in the atmosphere.

The differences in the chamber and atmospheric results can be attributed to different sensitivities of atmospheric and chamber conditions to various aspects of the mechanisms of these compounds. Compounds such as Texanol® and the constituents of hydrocarbon solvents used with coatings tend to have negative impacts on ozone formation because they inhibit radical levels (and thus reduce O_3 formation from all VOCs present) while they have positive impacts on ozone because of the NO to NO_2 conversions by the radicals formed in their direct reactions, and the reactions of their major reactive oxidation products. These tend to have opposite effects, with the net reactivity tending to be driven by the balance between them. Carter and Malkina (2005) attributed the differences between chamber and atmospheric reactivities for such compounds to the negative radical inhibition effect being relatively more important in the chamber than the atmosphere, compared to the positive effect of the direct NO to NO_2 conversions. As discussed later in this report, an important factor contributing to these differences is the fact that the integrated OH radical levels are significantly lower in the incremental reactivity environmental chamber experiments used to evaluate the mechanisms than calculated for the atmospheric simulations used to calculate the MIR and other reactivity scales. If the integrated radical levels in the incremental reactivity chamber experiments could be increased, such as by increasing light intensity, duration of the experiment, or by adding radical initiators, then better correlations between environmental chamber and atmospheric reactivities may be obtained. This would result in increased confidence in the relevance of mechanism evaluation results to the atmospheric reactivity values used in regulatory applications.

Based on these considerations, the California Air Resources Board (CARB) contracted with the College of Engineering Center for Environmental Research and Technology (CE-CERT) at the University of California, Riverside (UCR) to carry out a project to address these research needs related to coatings VOC reactivity. This project had two major objectives. The first was to develop and test modifications to our incremental reactivity environmental chamber experiments whose results will give better correlations with incremental reactivities in the atmosphere, particularly for important coatings compounds such as Texanol® and primarily alkane petroleum distillates. This involved increasing the light intensity of our chamber experiments by adding more lights, investigating the feasibility of increasing the duration of our reactivity chamber experiments, and conducting reactivity experiments with H_2O_2 added as a radical initiator to increase integrated radical levels.

The second objective of this project was to reduce uncertainties in reactivity estimates for coatings VOCs of concern to the CARB for which mechanisms and reactivity estimates do not exist or are very uncertain. The compounds chosen for study were ethyl methyl ketone oxime (EMKO) and soy ester constituents, though only the work with EMKO was successful. This is in addition to conducting additional experiments with Texanol® and representative petroleum distillates using the new experimental approach developed for this project. The work carried out to address these objectives is documented in this report.

EXPERIMENTAL METHODS

Chamber Description

All of the environmental chamber experiments for this project were carried out using the UCR EPA environmental chamber. This chamber was constructed under EPA funding to address the needs for an improved environmental chamber database for mechanism evaluation (Carter et al, 1999, Carter, 2002). The objectives, design, construction, and results of the initial evaluation of this chamber facility are described in more detail elsewhere (Carter et al, 1999; Carter, 2002, 2004; Carter et al, 2005a,b). A brief description of the chamber is given below.

The UCR EPA chamber consists of two ~85,000-liter fluorinated ethylene propylene (FEP) Teflon® reactors located inside a 16,000 cubic ft temperature-controlled "clean room" that is continuously flushed with purified air. The clean room design is employed in order to minimize infiltration of background contaminants into the reactor due to permeation or leaks. Two alternative light sources can be used. The first consists of a 200 KW argon arc lamp with specially designed UV filters that give a UV and visible spectrum similar to sunlight. This light source could not be used for this project because it was not operational during this period. Banks of blacklights are also present to serve as a backup light source for experiments where blacklight irradiation is sufficient, and this was used for the experiments for this project because of availability and because use of blacklights was judged to be sufficient to satisfy the project objectives. These blacklights were upgraded as part of this project as discussed below. The interior of the enclosure is covered with reflective aluminum panels in order to maximize the available light intensity and to attain sufficient light uniformity, which is estimated to be ±10% or better in the portion of the enclosure where the reactors are located (Carter, 2002). A diagram of the enclosure and reactors is shown in Figure 1. The spectrum of the blacklight light source is given by Carter et al (1995).

The dual reactors are constructed of flexible 2 mil Teflon® film, which is the same material used in the other UCR Teflon chambers used for mechanism evaluation (e.g., Carter, 2000a, 2010a, and references therein). A semi-flexible framework design was developed to minimize leakage and simplify the management of large volume reactors. The Teflon film is heat-sealed into separate sheets for the top, bottom, and sides (the latter sealed into a cylindrical shape) that are held together and in place using bottom frames attached to the floor and moveable top frames. The moveable top frame is held to the ceiling by cables that are controlled by motors that raise the top to allow the reactors to expand when filled or lower the top to allow the volume to contract when the reactors are being emptied or flushed. These motors in turn are controlled by pressure sensors that raise or lower the reactors as needed to maintain slight positive pressure which contributes to preventing background contaminants from infiltrating into the chamber reactors. During experiments the top frames are slowly lowered to maintain a constant positive pressure as the reactor volumes decrease due to sampling or leaks. The experiment is terminated if the volume of one of the reactor reaches about 1/3 the maximum value, where the time this took varied depending on the amount of leaks in the reactor, but was greater than the duration of most of the experiments discussed in this report. Since at least some leaks are unavoidable in any large Teflon film reactor, the constant positive pressure is important to minimize the introduction of enclosure air into the reactor that may otherwise result.

As indicated in Figure 1, the floor of the reactors has openings for a high volume mixing system for mixing reactants within a reactor and also for exchanging reactants between the two reactors to

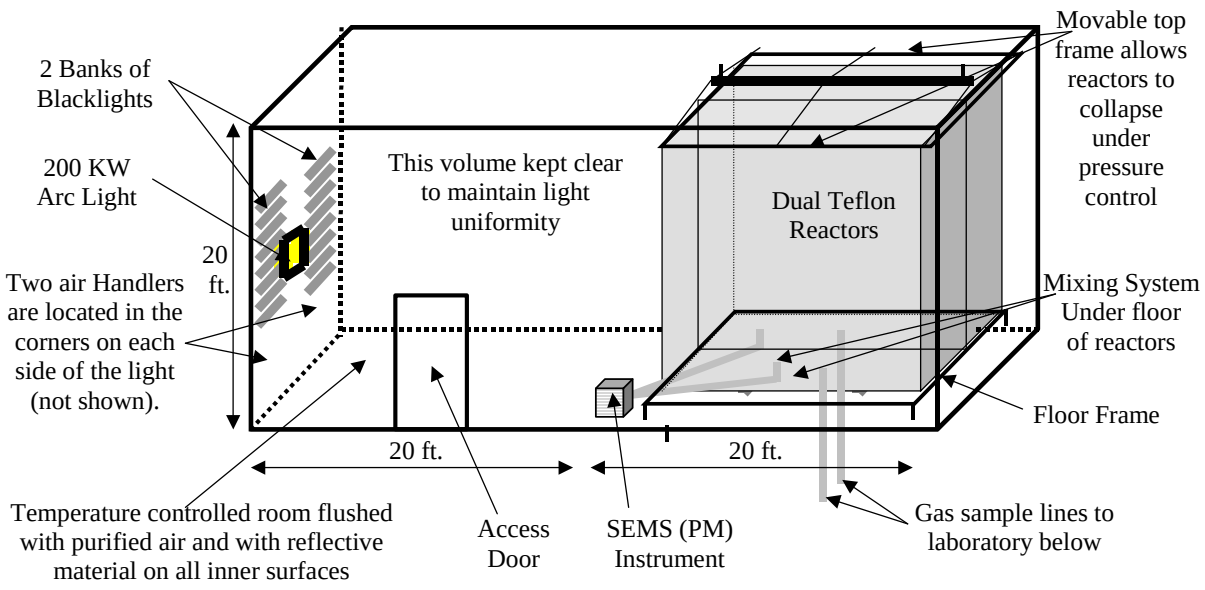

Figure 1. Schematic of the UCR EPA environmental chamber reactors and enclosure.

achieve equal concentrations in each reactor. This utilizes four 10" Teflon pipes with Teflon-coated blowers and flanges to either blow air from one side of a reactor to the other, or to move air between each of the two reactors. Teflon-coated air-driven metal valves are used to close off the openings to the mixing system when not in use, and during the irradiation experiments.

An air purification system (AADCO, Cleves, OH) that provides dry purified air at flow rates up to 1500 liters min^{-1} is used to supply the air to flush the enclosure and to flush and fill the reactors between experiments. The air is further purified by passing it through cartridges filled with Purafil® and heated Carulite 300® which is a Hopcalite® type catalyst, and also through a filter to remove particulate matter. The measured NO_x, CO, and non-methane organic concentrations in the purified air were found to be less than the detection limits of the instrumentation employed (see Analytical Equipment, below).

The chamber enclosure is located on the second floor of a two-floor laboratory building that was designed and constructed specifically to house this facility (Carter, 2002). Most of the analytical instrumentation is located on the ground floor beneath the chamber, with sampling lines leading down as shown in Figure 1.

Analytical Instrumentation

Table 1 gives a listing of the analytical and characterization instrumentation whose data were utilized for this project. Other instrumentation was available and used for some of these experiments, as discussed by Carter 2002 and Carter et al, 2005a, but the data obtained were not characterized for modeling and thus not used in the mechanism evaluations for this project. Table 1 includes a brief description of the equipment, species monitored, and their approximate sensitivities, where applicable. These are discussed further in the following sections.

Table 1. List of analytical and characterization instrumentation for the UCR EPA chamber.

Type	Model or Description	Species	Sensitivity	Comments
Ozone Analyzer	Dasibi Model 1003-AH. UV absorption analysis.	O_3	2 ppb	Standard monitoring instrument.
NO - NO_y Analyzer	TECO Model 42 C with chemiluminescent analysis for NO, NO_y is converted to NO by catalytic conversion.	NO NO_y	1 ppb 1 ppb	Useful for NO and initial NO_2 monitoring. Note that converter used for NO_2 analysis also converts peroxy acyl nitrates (PANs) and organic nitrates, so these are also detected as NO_2. Quartz fiber filters soaked in a 9% solution of NaCl and dried were used to remove HNO_3 prior to entering the converter, to avoid a non-quantitative interference by HNO.
CO Analyzer	Thermo Environmental Instruments Inc. Model 48 C	CO	50 ppb	Standard monitoring instrument
GC-FID Instruments	HP 6890 Series II GCs with dual columns, loop injectors and FID detectors. Controlled by computer interfaced to network.	VOCs	~10 ppbC	30 m x 0.53 mm GS-Alumina column used for the analysis of light hydrocarbons such as ethylene, propylene, *n*-butane and trans-2-butene and 30 m x 0.53 mm DB-5 column used for the analysis of C_{5+} alkanes and aromatics, such as toluene and *m*-xylene. Loop injection is suitable for low to medium volatility VOCs that are not too "sticky" to pass through valves.
GC-FID Instruments with cartridge sampling	Agilent 6890 GC with FID detection interfaced to a Gerstel TDS 3 ThermoDesorption System with Tenax-TA cartridge sampling or a ThermoDesorption System (CDS analytical, ACEM9305, Sorbent Tube MX062171) with Tenax-TA/Carbopack/ Carbosieve S111.	Lower Volatil-ity VOCs	~1 ppbC	Sample collection tubes were 10mm ID with a length of 200mm packed with 160 ml Tenax-TA. The tubes were thermally desorbed at 330°C The column used was a 50 m J&W Scientific DB-1701 with a bore of 0.032 inches and a 1 micron film thickness. This system was used for the analysis of Texanol® and for attempted analysis of the representative soy ester constituents. Since December 2010, sample collection tubes were packed with Tenax-TA/Carbopack/Carbosive S111. The tubes were thermally desorbed at 290°C. The column used was a 30 m Restek® Rtx-35 Amine (0.53 mm ID, 1.00 micron). This system was used for the analysis of Texanol®.
Gas Calibrator	Model 146C Thermo Environmental Dynamic Gas Calibrator	N/A	N/A	Used for calibration of NO_x and other analyzers. Instrument under continuous use.

Table 1 (continued)

Type	Model or Description	Species	Sensitivity	Comments
Data Acquisition Sytem	Windows PC with custom LabView software, 16 analog input, 40 I/O, 16 thermo-couple, and 8 RS-232 channels.	N/A	N/A	Used to collect data from most monitoring instruments and control sampling solenoids. In-house LabView software was developed using software developed by Sonoma Technology for ARB for the Central California Air Quality Study as the starting point.
Temperature sensors	Various thermocouples, radiation shielded thermocouple housing	Tempera -ture	~0.1 ^{o}C	Primary measurement is thermocouples inside reactor. However, comparison with temperature measurements in the sample line suggests that irradiative heating may bias these data high by ~2.5^{o}C. See text.
Scanning Mobility Particle Spectrometer (SMPS)	TSI 3080L column, TSI 3077 ^{85}Kr neutralizer, and TSI 3760A CPC. Instrument design, control, and operation Similar to that described in Cocker et al. (2001)	Aerosol number and size distribut-ions	Adequate	Provides information on size distribution of aerosols in the 28-730 nm size range, which accounts for most of the aerosol mass formed in our experiments. Data can be used to assess effects of VOCs on secondary PM formation.

Ozone, CO, NO, and NO_y (i.e., NO, NO_2 and other nitrogen-containing species that are converted to NO using a heated catalytic converter) were monitored using commercially available instruments as indicated in Table 1. The instruments were spanned for NO, NO_2, and CO and zeroed prior to most experiments using the gas calibration system indicated in Table 1, and a prepared calibration gas cylinder with known amounts of NO and CO. O_3 and NO_2 spans were conducted by gas phase titration using the calibrator during this period. Span and zero corrections were made to the NO, NO_2, and CO data as appropriate based on the results of these span measurements, and the O_3 spans indicated that the UV absorption instrument was performing within its specifications.

Organic reactants other than the EMKO and complex petroleum distillate mixtures were analyzed by gas chromatography (GC) with flame ionization detector (FID) as described elsewhere (Carter et al, 1995; see also Table 1). The surrogate gaseous compounds ethylene, propylene, n-butane and trans-2-butene were monitored by using 30 m megabore GS-Alumina column and the loop sampling system. The second signal of the same GC outfitted with FID, loop sampling system and 30 m megabore DB-5 column was used to analyze the liquid surrogate components toluene, *n*-octane, and *m*-xylene. The sampling methods employed for injecting the sample with the test compounds on the GC column depended on the volatility or “stickiness” of the compounds.

Both the GC instruments were controlled and their data were analyzed using HPChem software installed on a dedicated PC. The GC's were spanned using the prepared calibration cylinder with known amounts of ethylene, propane, propylene, *n*-butane, *n*-hexane, toluene, *n*-octane and *m*-xylene in ultrapure nitrogen. Analyses of the span mixture were conducted approximately every day an experiment was run, and the results were tracked for consistency.

The surrogate components analyzed by the above system were calibrated by repeated analysis of a standard mixture containing these compounds, and verified by injecting and sampling known amounts of the compound in a calibration chamber of known volume. The amounts of gaseous compounds injected

were determined by vacuum methods, using an MKS Baratron precision pressure gauge, and bulbs of known volume, determined by weighing when filled with water. The amounts of liquid compounds injected were determined by measuring amounts injected using microliter syringes. The volumes of the calibration chambers were determined by injecting and analyzing compounds whose analyses have been calibrated previously.

The isomers of Texanol® were also monitored by GC-FID, except in this case by using Tenax cartridge sampling with thermal desorption as described in Table 1. This method was also employed when doing experiments with ethyl methyl ketone oxime (EMKO) and representative soy ester constituents, but the compounds were either not detected or the analysis was found not to be quantitative. Therefore, for modeling purposes the amounts of these compounds added to the experiments were computed based on the amounts injected and the volumes of the reactors.

Most of the instruments, other than the GCs and aerosol instrument, were interfaced to a PC-based computer data acquisition system under the control of a LabView program written for this purpose. These data, and the GC data from the HP ChemStation computer, were collected over the CE-CERT computer network and merged into Excel files that were used for applying span, zero, and other corrections, and preparation of the data for modeling.

Sampling Methods

Samples for analysis by the continuous monitoring instrument were withdrawn alternately from the two reactors and zero air, under the control of solenoid valves that were in turn controlled by the data acquisition system discussed above. For most experiments the sampling cycle was 5 minutes for each reactor, the zero air, or (for control purpose) the chamber enclosure. The program controlling the sampling sent data to the data acquisition program to indicate which reactor was being sampled, so the data could be appropriately apportioned when being processed. Data taken less than 3-4 minutes after the sample switched were not used for subsequent data processing. The sampling system employed is described in more detail by Carter (2002).

Samples for GC analysis of surrogate compounds were taken at approximately every 20-minute directly from each of the reactors through the separate sample lines attached to the bottom of the reactors, as shown in Figure 1. The GC sample loops were flushed for a desired time with the air from reactors using a pump. Samples for analysis of Texanol® and attempted analysis for other low-volatility VOCs were taken by using Tenax cartridges that were then thermally desorbed onto the GC for analysis.

Characterization Methods

Use of chamber data for mechanism evaluation requires that the conditions of the experiments be adequately characterized. This includes measurements of temperature, humidity, and light intensity and spectral distribution, and wall effects characterization. Wall effects characterization is discussed in detail by Carter (2004) and updated by Carter and Malkina (2005) and Carter (2010a), and most of that discussion is applicable to the experiments for this project. The instrumentation used for the other characterization measurements is briefly summarized in Table 1, and these measurements are discussed further below.

Temperature. Air temperature was monitored during chamber experiments using calibrated thermocouples attached to thermocouple boards on our computer data acquisition system. The temperature in each of the reactors was continuously measured using relatively fine gauge thermocouples that were located ~1’ above the floor of the reactors. These thermocouples were not shielded from the

light, though it was expected that irradiative heating would be minimized because of their small size. Experiments where the thermocouple for one of the reactors was relocated to inside the sample line indicated that radiative heating is probably non-negligible, and that a correction needs to be made for this by subtracting ~2.5^{o}C from the readings of the thermocouples in the reactors. This is discussed by Carter (2004).

The temperature was not varied for the experiments carried out for this project. For all experiments the average temperature was in the range of 296-300^{o}K, with the average being 298±1^{o}K.

Light Spectrum and Intensity. The spectrum of the light source in the 300-850 nm region has been measured using a LiCor LI-1800 spectroradiometer, which is periodically calibrated at the factory (e.g., see Carter et al, 2005). Based on previous extensive measurements the spectrum of the blacklight light was assumed to be constant, and was not measured during the time period of this project. The method used to derive the light intensity using the blacklight light source was based on that discussed by Carter et al (2005), updated as described by Carter and Malkina (2007). Briefly, the absolute light intensity is measured by carrying out NO_2 actinometry experiments periodically using the quartz tube method of Zafonte et al (1977) modified as discussed by Carter et al (1995). In most cases the quartz tube was located in front of the reactors. Since this location is closer to the light than the centers of the reactors, the measurement at this location is expected to be biased high, so the primary utility of these data are to assess potential variation of intensity over time. However, several special actinometry experiments were previously conducted where the quartz tube was located inside the reactors, to provide a direct measurement of the NO_2 photolysis rates inside the reactors. The results of these measurements were used to derive a correction factor of 0.698 to derive NO_2 photolysis rates in the reactor from those measured in front of the reactor (Carter et al, 2005c). The trend of in-reactor and corrected in-front-of-reactor actinometry results over blacklight run number (the number of runs conducted using blacklights) were then used to derive an assigned NO_2 photolysis rate as a function of blacklight run number. Results of actinometry measurements carried out during the course of this project are given in the "Characterization results" section, below.

As discussed below, additional blacklights were added to the chamber as part of this project. The light intensity was measured once the construction of the new lights were completed using the quartz tube method discussed above, both inside and outside the reactors. Since the same type of blacklight bulbs (115W Osram Sylvania 350 BL; part no. 25251) was used with the new lights as those already in the chamber, we assume that the spectral distribution of the light source did not change.

Experimental Procedures

The reaction bags were collapsed to the minimum volume by lowering the top frames, and then emptied and refilled at least six times after each experiment, and then were filled with dry purified air on the night before each experiment. Span measurements were generally made on the continuously measuring instruments prior to injecting the reactants for the experiments. The reactants were then injected through Teflon injection lines (that are separate from the sampling lines) leading from the laboratory on the first floor to the reactors on the second floor. The common reactants were injected in both reactors simultaneously, and were mixed by using the reactor-to-reactor exchange blowers and pipes for 10 minutes. The valves to the exchange system were then closed and the other reactants were injected to their respective sides and mixed using the in-reactor mixing blowers and pipes for 1 minute. The contents of the chamber were then monitored for at least 30 minutes prior to irradiation, and samples were taken from each reactor for GC analysis to get stabilized initial concentrations and air temperatures inside the reactors.

Once the initial reactants are injected, stabilized, and sampled, the blacklights are turned on to begin the irradiation. During the irradiation the contents of the reactors are kept at a constant positive pressure by lowering the top frames as needed, under positive pressure control, to minimize infiltration of background contaminants into the reactors. The reactor volumes therefore decrease during the course of the experiments, in part due to sample withdrawal and in part due to small leaks in the reactors. A typical irradiation experiment ended after about 6 hours, by which time the reactors are typically down to about half their fully filled volume. Larger leaks are manifested by more rapid decline of reactor volumes, and the run is aborted early if the volume declines to about 1/3 the maximum. This was not the case for most of the experiments discussed in this report. After the irradiation the reactors were emptied and filled six times as indicated above.

The procedures for injecting the various types of reactants were as follows. NO and NO_2 were prepared for injection using a vacuum rack. Known pressures of NO, measured with MKS Baratron capacitance manometers, were expanded into Pyrex bulbs with known volumes, which were then filled with nitrogen (for NO) or purified air (for NO_2). In order to maintain constant NO/NO_2 ratios, the same two bulbs of a specified volume were utilized in most of experiments. The contents of the bulbs were then flushed into the reactor(s) with nitrogen. For experiments with added CO, CO was purified by passing it through an in-line activated charcoal trap and flushing it into the reactor at a known rate for the amount of time required to obtain the desired concentration. Measured volumes of volatile liquid reactants were injected, using a micro syringe, into a 2 ft long Pyrex injection tube surrounded with heat tape and equipped with one port for the injection of the liquid and other ports to attach bulbs with gas reactants. For injections into both reactors (e.g., NO_x and base ROG surrogate components in incremental reactivity experiments), one end of the injection tube was attached to the "T"-shape glass tube (equipped with stopcocks) that was connected to reactors and the other end of injection tube was connected to a nitrogen source. The injections into a single reactor (e.g., for an amine in the reactivity experiments) was similar except the "T" tube was not used.

The procedures for injection of the hydrocarbon surrogate components were as follows. A cylinder containing n-butane, trans-2-butene, propylene and ethylene in nitrogen, was used for injecting the gaseous components of the surrogate. The cylinder was attached to the injection system and a gas stream was introduced into reactors at controlled flow for a certain time to obtain desired concentrations. A prepared mixture with the appropriate ratios of toluene, n-octane and m-xylene was utilized for injection of these surrogate components, using the procedures as discussed above for pure liquid reactants. All the gas and liquid reactants intended to be the same in both reactors were injected at the same time. The injection consisted of opening the stopcocks and flushing the contents of the bulbs and the liquid reactants with nitrogen, with the liquid reactants being heated slightly using heat tape that surrounded the injection tube. The flushing continued for approximately 10 minutes.

Injection of low-volatility compounds such as Texanol® and methyl decanoate into the chambers was carefully performed using a heated oven through heated transfer line maintained at a temperature higher than oven for 30 minutes. The oven temperature can be adjusted, and a temperature of 60°C was used for Texanol® experiments performed in December, 2010 and January, 2011. The glass manifold inside the oven was packed with glass wool to increase the mass transfer surface area. Nitrogen (N_2) was used as the carrier gas.

Light Source Upgrades

As part of our efforts to increase integrated radical levels in our reactivity chamber experiments, the maximum intensity of our blacklight light source was increased by adding additional banks of blacklights. The new banks of lights were separately switched, allowing experiments to be carried out using the same blacklight intensity as employed previously, as well as experiments with the higher

intensity that resulted when all the lights were turned on. Although switches allowed for using some but not all of the new banks of lights, for this project the only lighting options employed were experiments with only the old lights carried out to reproduce the lighting in previous experiments, and experiments with all of the old and new lights carried out to utilize the maximum possible light intensity.

The same type of blacklights (115W Osram Sylvania 350 BL; part no. 25251) was purchased and installed using additional steel structures to secure newly added 192 blacklight bulbs and their associated bulb holders, ballasts and wires. They are located on the same wall as the previously existing blacklights, as shown on Figure 1. The previously existing 80 blacklights are located symmetrically (i.e., left and right sides) around the arc lamp, and, after addition of 192 new blacklights, 136 blacklights are located on each side of the arc lamp symmetrically. These efforts to upgrade the light system took longer and cost more than anticipated when the project was proposed. As discussed below, this upgrade resulted in an increase of k1 (photolysis frequency of NO_2) from 0.13 min^{-1} to 0.40 min^{-1}.

Materials

The sources of the NO, CO and the various base case surrogate compounds came from various commercial vendors as employed in previous projects at our laboratory. CO (Praxair, CP grade) was scrubbed with carbon charcoals before injection into the reactors to remove carbonyl (C=O) -containing compounds produced by reaction of CO and the cylinder surface. NO_2 was generated by chemical conversion of NO (Matheson, UHP grade). Ethyl methyl ketone oxime (CAS no. 96-29-7), methyl decanoate (CAS no. 110-42-9), and methyl linoleate (CAS no. 112-63-0) were purchased from Sigma Aldrich, and Texanol® (CAS no. 25265-77-4) was obtained from Eastman Chemicals.

Experiments were also carried out utilizing several of the hydrocarbon solvents we studied previously (Carter and Malkina, 2005). These are summarized on Table 2. These were obtained from the American Chemistry Council (ACC) or member companies during the course of the study of Carter and Malkina (2005) and were stored under refrigeration in sealed glass containers since the time they were acquired. The compositions of these mixtures used for modeling are given in Table A-1 of the Supplementary Materials. They were derived as discussed by Carter and Malkina (2005), based on results of analyses provided to us by the ACC (Jaques, 2003, 2004).

Table 2. Petroleum distillate samples utilized in reactivity experiments for this project

Designation	Description	CARB Bin
ASTM-1C	Dearomatized Mixed Alkanes, Primarily C_{10}-C_{12} mixed alkanes	11
ASTM-1B	Reduced Aromatics Mineral Spirits, Primarily C_{10}-C_{12} mixed alkanes with 6% aromatics.	14
ASTM-1A	Regular mineral spirits, Primarily C_{10}-C_{12} mixed alkanes with 19% aromatics.	15
Aromatic-100	Primarily C_9-C_{10} alkylbenzenes	22

MODELING METHODS

Chemical Mechanism

Base Mechanism

The starting point for the chemical mechanism evaluated in this work is the SAPRC-07 chemical mechanism as documented and listed by Carter (2010a). Files and software implementing this chemical mechanism are available at the SAPRC mechanism web site at http://www.cert.ucr.edu/~carter/SAPRC.

As discussed previously (Carter, 2000a,b, 2010a), the SAPRC mechanisms consist of a "base mechanism" that represents the reactions of the inorganic species and common organic products and lumped organic radical model species and "operators", and separate mechanisms for the initial reactions of the many types of other organic compounds that are not in the base mechanism. The compounds, or groups of compounds, that are not included in the base mechanism but for which mechanism assignments have been made, are referred to as detailed model species. These include all the base ROG surrogate constituents and the compounds whose reactions were modeled in this work. These compounds can either be represented explicitly, with separate model species with individual reactions or sets of reactions for each, or using lumped model species similar to those employed in the "fixed parameter" version of SAPRC (Carter, 2000b, 2010a). The latter approach is useful when modeling complex mixtures in ambient simulations or simulations of experiments with complex mixtures, but the other approach, representing each compound explicitly, is more appropriate when evaluating mechanisms for individual compounds or simple mixtures. This is because the purpose of mechanism evaluations against chamber data is to assess the performance of the mechanism itself, not to assess the performance of lumping approaches. The latter is most appropriately assessed by comparing simulations of explicit and condensed versions of the same mechanism in ambient simulations.

In view of this, when modeling the environmental chamber experiments, all of the organic constituents of the base ROG surrogate were represented explicitly using separate model species for each compound. In addition, the individual test compounds were also represented explicitly when simulating experiments with those compounds. The only exception was test compounds that were complex mixtures, such as those listed in Table 2, above. In this case, separate lumped model species were employed to represent the compounds in the mixtures. In addition, lumped model species were used to represent the base case ambient reactive organic gas (ROG) mixture in the atmospheric reactivity simulations. In those cases, the kinetic and mechanistic parameters of those lumped model species were derived based on the specific compounds in the mixtures they were representing. (The composition of the base ROG mixture used in the atmospheric reactivity simulations is given in Table A-1 of the Supplementary Materials and is the same as employed previously (Carter, 1994a, 2000a, 2010a). This gives the least approximate representation of the atmospheric reactions of these compounds within the framework of the SAPRC-07 chemical mechanism.

Except for EMKO, whose mechanism was developed for this project and is discussed separately below, the mechanisms used for the model simulations of the chamber experiments or atmospheric reactivities were the same as given by Carter (2010a).

Mechanisms for "Pure Mechanism" Species for n-Octane

"Pure mechanism" species were used in order to assess how different experimental or environmental conditions affect relative contributions of different aspects of the mechanisms to

incremental reactivity. A pure mechanism species is a model species representing only a single aspect of a VOC's mechanism. If the VOC reacts only with OH, in SAPRC-07 its mechanism is represented by the lumped process

$$OH + VOC \rightarrow yr1\ rad1 + yr2\ rad2 + \ldots\ yp1\ prod1 + yp2\ prod2 + \ldots,$$

where rad1, prod1, etc. refer to the radical and non-radical products, and yr1, yp1, etc. are their respective yields. If we define R.rad1, as pure mechanism species representing the net effect of conversion of OH to the radical product rad1, and P.prod1 as the pure mechanism species representing the net effect of the formation of product prod1 (and likewise for rad2, prod2, etc.), then the net effect of the VOC's reactions is exactly the same as the mixture of these pure mechanism species with relative amounts equal to their yields. Since incremental reactivities of mixtures are linear combinations of incremental reactivities of the constituents (for the limit of small amount of VOC added), the incremental reactivity of the VOC can be given by

$$IR(VOC) = yr1 \times IR(R.rad1) + yr2 \times IR(R.rad2) + \ldots + yp1 \times IR(R.prod1) + yp2 \times IR(P.prod2) + \ldots$$

where IR refers to incremental reactivity. This permits the relative contribution of each aspect of the mechanism to the overall reactivity of the VOC to be assessed.

For this work, we assessed contributions of various aspects of the mechanism of n-octane to its incremental reactivity in the atmosphere and in simulated environmental chamber experiments. n-Octane was chosen because its reactivity has been well studied experimentally, it is representative of the alkanes in petroleum distillates such as those used for coatings, and because it is measured and calculated to have negative reactivities in our past chamber experiments but positive reactivities in the atmosphere. Similar results are expected for other coatings VOCs where this is a concern. The SAPRC-07 representation of n-octane's mechanism is as follows,

$$N\text{-}C8 + OH = 0.646\ xHO2 + 0.354\ \{RO2XC + zRNO3\} + 1.432\ RO2C + 0.024\ xRCHO + 0.622\ xPROD2 + yR6OOH$$

For the purpose of reactivity analysis under MIR conditions, the contribution of yR6OOH can be ignored because it represents effects of peroxy + HO_2 reactions, which are important only under very NO_x-limited conditions. The effects of the other reactions are represented by the following pure mechanism species, whose rate constants with OH are the same as that for n-octane, and whose mechanisms are as follows:

$$R.HO2 + OH \rightarrow xHO2$$
$$R.RNO3 + OH \rightarrow RO2XC + zRNO3$$
$$P.RCHO + OH \rightarrow OH + xRCHO$$
$$P.PROD2 + OH \rightarrow OH + xPROD2$$
$$P.RO2C + OH \rightarrow OH + RO2C$$
$$P.RO2XC + OH \rightarrow OH + RO2XC$$

The first two reactions represent the effects of conversion of OH radicals to other radical species in the reactions, and rest represent effects of the formation of the products or the NO to NO_2 conversion or NO loss operators (RO2C and RO2XC) alone. For the presentation of the results, the reactivity contributions are classified as follows:

NO to NO_2 conversions: 0.646 MR(R.HO2) + 1.432 MR(P.RO2C)
Nitrate formation: 0.354 [MR(R.RNO3) + MR(P.RO2XC)]
Product formation: 0.024 MR(P.RCHO) + 0.622 MR(P.PROD2)

Here, MR refers to mechanistic reactivity, which is the same as incremental reactivity except it is relative to the amount of test VOC reacted in the simulation, rather than the amount added.

Mechanism for Ethyl Methyl Ketone Oxime (EMKO)

The only compound whose mechanism was developed or modified specifically for this project was ethyl methyl ketone oxime (EMKO), $CH_3CH_2C(CH_3)=NOH$. No information could be found concerning its atmospheric reaction mechanism or reaction rates for this compound, and the only relevant information for related compounds we could find was from Horne and Norrish (1970), who measured UV absorption cross sections and the OH radical rate constant for formaldoxime ($CH_2=NOH$) and acetaldoxime ($CH_3CH=NOH$). The absorption cross section data indicate that photolysis of these compounds is negligible under atmospheric conditions, but reaction with OH occurred at significant rates, with the measured rate constants being 6.3×10^{-13} and 2.2×10^{-12} cm^3 $molec^{-1}$ s^{-1} for formaldoxime and acetaldoxime, respectively. No information was obtained concerning the mechanism, other than NO being observed as a product of the reaction (in the absence of O_2) with yields not quantified. Horne and Norrish (1970) attributed the reaction to abstraction from the =CH2 or =CH groups, and the significant differences in the rate constants for the two compounds suggest that the reaction is not simply abstraction from OH, unless the overall process involves first the addition to the double bond. However, the kinetic and product data do not rule out the reaction proceeding by OH addition to the double bond, and that appears to us to be more likely than abstraction from the vinylic hydrogens.

We assume that the major atmospheric reaction of EMKO is with OH radicals, either by hydrogen atom abstraction or addition to the C=N double bond. Possible initial reaction pathways are as follows:

$$CH_3CH_2C(CH_3)=NOH + OH \rightarrow H_2O + \cdot CH_2CH_2C(CH_3)=NOH \quad (1)$$
$$CH_3CH_2C(CH_3)=NOH + OH \rightarrow H_2O + CH_3CH_2C(CH_2\cdot)=NOH \quad (2)$$
$$CH_3CH_2C(CH_3)=NOH + OH \rightarrow H_2O + CH_3CH(\cdot)C(CH_3)=NOH \quad (3)$$
$$CH_3CH_2C(CH_3)=NOH + OH \rightarrow CH_3CH_2C(CH_3)(OH)N(\cdot)OH \quad (4)$$
$$CH_3CH_2C(CH_3)=NOH + OH \rightarrow CH_3CH_2C(CH_3)(\cdot)N(OH)OH \quad (5)$$

From group additivity estimates associated with the mechanism generation system (Carter, 2000a, 2010a), assuming that the substituent effect for C=N is the same as that assigned to C=C, we estimate that the rate constants for pathways 1-3 are 1.7×10^{-13}, 1.4×10^{-13} and 9.4×10^{-13} cm^3 $molec^{-1}$ s^{-1}, respectively, yielding a total rate constant of 1.25×10^{-12} cm^3 $molec^{-1}$ s^{-1} for these three processes.

We estimate the total rate constant for the addition reactions (pathways 4 and 5) based on ratios of OH addition to C=C and C=N bonds, assuming that addition to the C=N bond is the only significant process in the reactions of OH with formaldoxime and acetaldoxime. The ratios of OH additions to the double bonds in $CH_2=NOH$ relative to ethene and $CH_3CH=NOH$ relative to propene are 0.075 and 0.085, respectively, which are reasonably consistent and suggest a ratio of 0.08 may give a reasonable estimate of the OH + oxime addition rate constant relative to the addition to the C=C double bond in the analogous 1-alkene. Therefore, from the rate constant for addition of OH to isobutene, the analogous alkene for EMKO, we estimate that the total rate constant for processes (4+5) is 4.04×10^{-12} cm^3 $molec^{-1}$ s^{-1}. (The rate constants for OH addition to the alkenes are based on the total rate constants assigned for the SAPRC-07 chemical mechanism (Carter, 2010a), minus the estimated rate constant for C-H abstraction for propene and isobutene, which is minor).

These estimated rate constants mean that abstraction from C-H is estimated to occur about 25% of the time, with the remainder by reaction with the C=NOH group. We use the estimated mechanism for the process (3), the major C-H abstraction process, to estimate the subsequent reactions for all abstraction routes. The subsequent reactions are expected to be

$$CH_3CH(\cdot)C(CH_3)=NOH + O_2 \rightarrow CH_3CH(OO\cdot)C(CH_3)=NOH$$

$$CH_3CH(OO\cdot)C(CH_3)=NOH + NO \rightarrow NO_2 + CH_3CH(O\cdot)C(CH_3)=NOH$$
$$CH_3CH(O\cdot)C(CH_3)=NOH + O_2 \rightarrow HO_2 + CH_3COC(CH_3)=NOH$$

For implementing in the SAPRC-07 chemical mechanism, we approximate the subsequent reactions of $CH_3COC(CH_3)=NOH$ using the model species PROD2 (used to represent reactions of the higher ketones), so the overall process is formation of HO_2 and PROD2 following an NO to NO_2 conversion. In terms of SAPRC-07 model species, this corresponds to:

$$EMKO + OH \rightarrow RO2C + xHO2 + xPROD2$$

The mechanism following reaction at the C=NOH group is more difficult to estimate. Although a number of speculative possibilities could be proposed, as discussed below the results of the incremental reactivity environmental chamber experiments with EMKO can only be simulated if it is assumed that the overall process involves radical termination and regeneration of NO_x. The most reasonable explanation for this is to assume that the OH + EMKO adduct somehow decomposes or rearranges to form H_2O + $CH_3CH_2C(CH_3)=NO\cdot \leftrightarrow CH_3CH_2C(CH_3)(\cdot)N=O$, i.e., having the same net effect as abstraction from the OH group. This could then react to form methyl ethyl ketone (MEK) and NO_2 via

$$CH_3CH_2C(CH_3)(\cdot)N=O + O_2 \rightarrow CH_3CH_2COCH_3 + NO_2$$

In terms of SAPRC-07 model species, this is represented as

$$OH + EMKO \rightarrow MEK + NO2$$

The estimated rate constant and mechanism for the reaction at C=NOH is highly uncertain, but as discussed below this gives best fits to environmental chamber reactivity data obtained as part of this project. The data are not even approximately fit if the reaction did not involve radical termination and NO_x formation, and if the rate constant were adjusted to optimize fits to our reactivity data the result would be essentially the same as our estimate. Unfortunately, we were not able to monitor the consumption rate of EMKO in our experiments due to the limitations of our GC system in quantitatively detecting EMKO, so the total rate constant could not be determined experimentally.

Combining these two processes, we obtain the following as the overall mechanism in terms of SAPRC-07 model species, with a total rate constant of 5.3×10^{-12} cm^3 $molec^{-1}$ s^{-1}.

$$OH + EMKO \rightarrow 0.24\ \{RO2C + xHO2 + xPROD2\} + 0.76\ \{MEK + NO2\}$$

Reaction with O_3 and NO_3 radicals is assumed to be negligible.

Adjusted Aromatics Mechanism

As discussed by Carter (2010a) and also below, the SAPRC-07 chemical mechanism has a consistent bias towards underpredicting O_3 formation in reactive organic gas (ROG) surrogate - NO_x experiments at lower ROG/NO_x ratios. This is attributed to problems with the aromatics mechanisms since the aromatics (specifically toluene and m-xylene) have the most uncertain mechanisms of the various surrogate components, and this bias is not seen when simulating results of surrogate - NO_x experiments that do not contain aromatics. This is despite the fact that the aromatics mechanisms are derived to give good fits to O_3 formation in aromatic - NO_x experiments without other VOCs present, though it should be noted that mechanisms that fit O_3 in these aromatic - NO_x experiments tend to underpredict aromatic consumption rates (i.e., OH radical levels) in those experiments. Although we are attempting to develop new aromatics mechanisms that do not have these problems, we have been unsuccessful in solving this problem during the course of this project.

This underprediction bias affects model simulations of the relatively low ROG/NO_x incremental reactivity experiments designed to represent MIR conditions. This bias would in part be cancelled out

when evaluating test VOC mechanisms by modeling incremental effects of test VOC additions in these experiments, since it should affect the base case and added test VOC experiment by approximately the same amount. However, the bias may not be exactly cancelled out, especially if the presence of the test VOC changes the extent of the bias by changing the effective ROG/NO_x ratio, as would occur when relatively large amounts of test VOC is added. It would provide a better and probably less biased test of the mechanism if the mechanism could at least simulate the base case experiment without bias.

In order to address this problem for the purpose of testing mechanisms for test VOCs against the chamber data, we developed "adjusted aromatics" versions of the mechanisms for the aromatic surrogate components toluene and m-xylene where this underprediction bias in predictions of O_3 formation, NO oxidation, and radical levels in the base case surrogate experiments is reduced. This adjustment is done by increasing the effective quantum yields of the model species used to represent the photoreactive non-α-dicarbonyl aromatics fragmentation to minimize the biases in simulations of NO oxidation and O_3 formation rates in the surrogate experiments carried out for this project. The reactions of these species are represented by the AFG1 and AFG2 model species, which have the same mechanism except that AFG1 has a quantum yield of 1 and AFG2 has a quantum yield of 0, and the AFG1/AFG2 ratio is adjusted to give best fits to the environmental chamber data. This is equivalent to adjusting the quantum yield of the compounds represented by AFG1 and AFG2. For the adjusted aromatics mechanism, the bias in simulating the surrogate - NO_x experiments was found to be minimized if the AFG1 yields were increased by a factor of 1.9, and the AFG2 yields were reduced to either zero or such that the AFG1+AFG2 yields were the same as in the unadjusted mechanism, whichever was larger. This gave the following overall mechanisms for toluene and m-xylene:

TOLUENE + OH = 0.312 {OH + AFG3} + 0.181 {HO2 + CRES} + 0.454 {RO2C + xHO2} + 0.054 {RO2XC + zRNO3} + 0.238 xGLY + 0.151 xMGLY + 0.065 xBALD + 0.371 xAFG1 + 0.020 xAFG2 + 0.073 yR6OOH + 0.435 yRAOOH

M-XYLENE + OH = 0.239 {OH + AFG3} + 0.159 {HO2 + CRES} + 0.52 {RO2C +xHO2} + 0.082 {RO2XC + zRNO3} + 0.100 xGLY + 0.380 xMGLY + 0.041 xBALD + 0.638 xAFG1 + 0.047 yR6OOH + 0.555 yRAOOH

The effects on the model simulations are discussed in the mechanism evaluation section of this report.

It is important to recognize that the purpose of deriving this mechanism is to evaluate abilities of mechanisms to predict effects of added test compounds to incremental reactivity experiments without complications arising from biases in model simulations of the base case experiment. Since these adjusted mechanisms are not consistent with results of aromatics - NO_x experiments, they are not considered suitable for use in atmospheric models, or for estimating reactivities for the aromatics themselves. Model simulations of the reactivity experiments were conducted using both the standard and adjusted aromatics experiments, and in most cases the results of both are shown. A comparison of the reactivity simulations with the adjusted and unadjusted mechanisms is useful in providing information on the effects of this base case mechanism bias on the mechanism evaluation results.

Simulation Inputs and Procedures

Simulations of Chamber Experiments

The procedures used in the model simulations of the environmental chamber experiments for this project were based on those discussed in detail by Carter (2004) and were employed in more recent studies (Carter and Malkina, 2005, 2007; Carter, 2008 and references therein), except as indicated below. Carter (2004) should be consulted for details of the characterization model and chamber effects parameters employed. The temperatures used when modeling were the averages of the temperatures measured in the reactors, corrected as discussed by Carter (2004). The temperature was not varied and averaged 298±1^{o}K for the experiments for this project. The photolysis rates were derived from the NO_2

photolysis rates assigned for the experiment, the spectral distribution for the blacklight source employed, and absorption cross sections and quantum yields in the SAPRC-07 chemical mechanism employed. The NO_2 photolysis rates were assigned 0.13 min^{-1} for the experiments with the original blacklights and 0.40 min^{-1} with both the original and newly added lights. The blacklight spectral distribution given by Carter et al (1995) was found to be appropriate for the blacklights in this chamber and was therefore used when modeling the blacklight runs discussed in this report.

The chamber effects parameters used when modeling the experiments in this chamber were the same as those given by Carter (2004) except for the HONO offgasing parameters, which were derived based on results of characterization runs carried out in conjunction with these experiments. As discussed by Carter (2004), the chamber effects model currently used for this chamber represents both the chamber radical source and background NO_x offgasing by HONO offgasing, whose magnitude is determined by the chamber effects parameter RN-I, which is the ratio of the HONO offgasing rate to the NO_2 photolysis rate. The RN-I parameter that best fits the characterization data tends to vary over time depending on the conditions of the chamber, and the results of the characterization experiments applicable to modeling the experiments discussed in this report, and the assignment of the RN-I values used, are given in the Characterization Results section, below.

The initial reactant concentrations used in the model simulations were based on the measured values except for EMKO, the representative soy ester compounds, and the hydrocarbon mixtures listed on Table 2, for which no reliable quantitative analytical method was available during the course of this project. In those cases, the amounts of the compounds injected into the experiments, and the volumes of the reactors were used to calculate the initial concentrations used for modeling. Although the reactors are flexible, their initial volumes were very consistent from run to run because of the use of the pressure control system when filling the reactor to its maximum volume prior to the reactant injections (see Chamber Description section, above, and Carter, 2004).

A number of test simulations of idealized or hypothetical experiments were carried out as part of our assessment of factors that affect differences between reactivities measured in chamber experiments and reactivities measured in the atmosphere. The light intensity, run duration, and initial reactant concentrations that were varied are given in conjunction with the discussion of the results of the simulations. The speciation of the base reactive organic gas (ROG) mixture was derived by averaging the measured relative contributions of the constituents from a number of experiments, and is given in Table A-1of the Supplementary Materials. The initial NO_x was represented as 70% NO and 30% NO_2, which is typical of NO_x injections for the incremental reactivity experiments. The chamber effects inputs were the same as used in the simulations of actual experiments except for the HONO offgasing parameter, where a representative value of 12 ppt was used for RN-I. Dilution was assumed to be negligible. For reactivity calculations simulating chamber experiments, the amount of test VOC added was determined such that the amount estimated to react during the course of the simulation was 50 ppb. This is sufficient to obtain a measurable response in reactivity results for most VOCs. However, for reactivity calculations to assess mechanistic contributions to reactivity, the amount of test VOC added was reduced to an estimated 0.5 ppb reacted to approximate true incremental reactivity, since the analysis method is only valid for the limit of small amounts of test VOC added.

For the simulations of the environmental chamber experiments, reactivity is defined in terms of the effect on NO oxidation + O_3 formation, or changes in the quantity

$$\Delta([O_3]\text{-}[NO]) = ([O_3]^{final} - [O_3]^{initial}) + ([NO]^{initial} - [NO]^{final})$$

As discussed previously, the processes responsible for O_3 formation are manifested as NO consumption when NO is in excess, so $\Delta([O_3]\text{-}[NO])$ gives a measure of reactivity that is useful even in high NO_x experiments where O_3 is suppressed by excess NO.

The performance of the model in simulating final $\Delta([O_3]\text{-}[NO])$ yields and formation rates were also used as a basis of evaluating mechanism performance in simulating the base case surrogate - NO_x experiments and for the purpose of developing the adjusted aromatics mechanism. The model performance in simulating final $\Delta([O_3]\text{-}[NO])$ yields was derived from experimental and calculated $\Delta([O_3]\text{-}[NO])$ yields at the last hour of the experiment. The $\Delta([O_3]\text{-}[NO])$ formation rates were found by the model performance in simulating $\Delta([O_3]\text{-}[NO])$ at the time that the rate of change of $\Delta([O_3]\text{-}[NO])$ is at a maximum in the experiment, which generally is when $\Delta([O_3]\text{-}[NO])$ is around half its maximum or final value. In both cases, model bias is defined as the difference between modeled and experimental results, divided by the experimental value.

For some incremental reactivity experiments, reactivity was also defined in terms of effects of the added test compound on integrated OH radical levels, or IntOH. The integrated OH radical levels are not measured directly, but can be derived from the amounts of consumption of reactive VOCs that react only with OH radicals. In particular,

$$\text{IntOH}_t = \frac{\ln([\text{tracer}]_0 / [\text{tracer}]_t) - Dt}{\text{kOH}^{\text{tracer}}}$$

where $[\text{tracer}]_0$ and $[\text{tracer}]_t$ are the initial and time t concentrations of the compound used as the OH tracer, $\text{kOH}^{\text{tracer}}$ is its OH rate constant, and D is the dilution rate in the experiments. The latter is small and can be neglected in experiments where IntOH is reported here. For our incremental reactivity experiments, the base ROG surrogate component m-xylene is the most reactive compound in the experiment that reacts only with OH radicals, and was therefore used as the OH tracer to derive the IntOH data. The m-xylene OH radical rate constant used in this analysis was 2.31×10^{-11} cm^3 $molec^{-1}$ s^{-1} (Atkinson and Arey, 2003). Such data could not be obtained for all experiments because of GC problems in some cases and interferences with the test compound or its products in the GC analysis of m-xylene in some other cases.

Atmospheric Reactivity Simulations

Atmospheric reactivity model simulations were carried out to derive MIR and other atmospheric reactivity values for the compound EMKO that was studied for this project, and also to assess factors affecting differences between reactivities in the atmosphere and those measured in environmental chamber experiments. The scenarios and methods used were the same as those used when calculating the MIR and other atmospheric ozone reactivity scales, and were described previously (Carter, 1994a,b 2000a, 2010a). The base ROG constituents were represented using the lumping procedures incorporated in the condensed version of the SAPRC-07 mechanism (Carter, 2010a). Note that this differs from the treatment of the base ROG mixture used in the environmental chamber simulations, where each compound was represented explicitly. However, the individual compounds whose reactivities were being assessed were represented explicitly, as was the case for the simulations of the chamber experiments. The mechanism used for EMKO is discussed above, and the mechanisms for the other compounds are given by Carter (2010a). Note that the adjusted aromatics mechanism was not used for any of the atmospheric reactivity simulations discussed in this work.

Note that reactivities are defined in terms of effects on maximum O_3 in calculations of atmospheric reactivity scales, not in terms of effects on $\Delta([O_3]\text{-}[NO])$ as used in the simulations of chamber experiments. This is because $\Delta([O_3]\text{-}[NO])$ measure does not have a straightforward relationship to chemical processes in scenarios where NO_x emissions are occurring. In addition, ozone is the quantity of interest in atmospheric simulations, and scenarios where NO_x is sufficient excess to suppress O_3 formation are generally not of interest.

MODELING ASSESSMENT OF CHAMBER VS. ATMOSPHERIC REACTIVITIES

Background and Objectives

Incremental reactivity experiments consist of irradiations of a reactive organic gas (ROG) surrogate mixture in the presence of NO_x both with and without an added test compound in order to determine the effect of the added compound on O_3 formation and other measures of reactivity. However, it is not practical to duplicate in an environmental chamber experiment all the factors affecting VOC reactivity in the atmosphere, so incremental reactivities measured in chamber experiments would be different from incremental reactivities in the atmosphere, such as MIR values. Even if it were practical to derive an experiment to sufficiently duplicate chemical conditions used to calculate MIR or other atmospheric reactivity scales, it would still not be possible to directly measure true incremental reactivities, because that is defined for the limit of a small amount of the test VOC added, while larger amounts have to be added in experiments to obtain a measurable effect of the VOC addition. Therefore, the purpose of the experiments is not to measure atmospheric reactivity, but to test the ability of the model to calculate it under chemical conditions approximating those in the atmosphere.

For this purpose, the incremental reactivity chamber experiments do not have to exactly duplicate the exact magnitudes of reactivities in the atmosphere, but they at least have to be sensitive to the same aspects of the mechanisms that affect atmospheric reactivities, in order for these mechanistic aspects to be adequately tested. Alternatively, a set of different experiments can be employed to test different aspects of the mechanisms, and if sufficiently comprehensive they could test the aspects that affect atmospheric reactivities under various conditions. In practice, we have used two types of experiments for this purpose, relatively low ROG and high NO_x experiments approximating MIR conditions, and higher ROG and/or lower NO_x experiments to test the behavior of the mechanisms under NO_x limited conditions. Together these types of experiments have been used as the basis for evaluating the ability of mechanisms to predict incremental reactivities in the atmosphere.

Unfortunately, for many compounds that are of interest in coatings applications, such as Texanol® and C_{10}-C_{12} primarily alkane petroleum distillates, the incremental reactivities in chamber experiments tend to be near zero or negative while those calculated for MIR and other atmospheric reactivity scales are positive. This is despite the fact that the mechanisms predicting the positive atmospheric reactivities also successfully simulate the results of the experiments where negative reactivities are observed. This is shown on Figure 2, which gives experimental and calculated ozone formation + NO oxidation results for selected incremental reactivity experiments for selected compounds in the SAPRC-07 mechanism evaluation dataset. All these compounds have about the same atmospheric MIR value, but the incremental reactivities in the chamber experiments vary greatly, from positive for n-butane, approximately zero for Texanol®, and negative for n-octane and the ASTM-1B mixture containing mixed C_{10}-C_{12} alkanes.

While this can be explained mechanistically (as discussed below), it gives concerns about how well the experiments are simulating the chemical conditions in the atmosphere, and the credibility of the evaluation of the mechanism against chamber data. Therefore, designing incremental reactivity experiments that give better correlations with atmospheric incremental reactivities would provide a more realistic mechanism evaluation, and also improve the credibility of the evaluation as a whole.

Previous calculations carried out at the time that this project was proposed indicated that one important source for the difference between atmospheric and chamber reactivities is the fact that the integrated OH radical levels were about a factor of 9 lower in simulations of chamber experiments

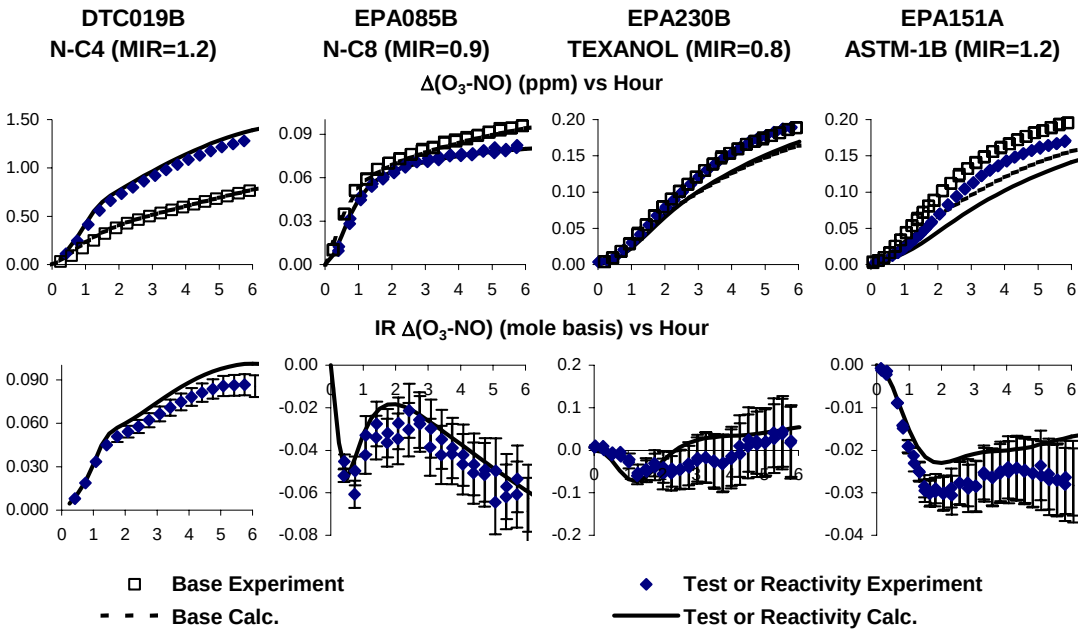

Figure 2. Experimental and calculated results ozone formation + NO oxidation results of selected incremental reactivity experiments for selected compounds, showing the atmospheric MIR values (in moles O_3 per mole VOC) for the selected compounds.

simulating MIR conditions compared to those occurring in scenarios representing those used to calculate the MIR scale. The higher integrated radical levels in the atmospheric simulations increase the overall extent of reaction and thus increase the relative importance of secondary reactions of oxidation products to the O_3 formation process. This is shown on Figure 3, taken from the proposal for this project, which plots SAPRC-99 model calculations of the relative importance of formation of the oxidized products represented by the PROD2 model species to NO to NO_2 conversion reactions in the initial reactions, against integrated OH levels for various atmospheric and environmental chamber reactivity simulations. (These were calculated using "pure mechanism" species reactivities, similar to those discussed above in the Modeling Methods section.) This is consistent with results of updated calculations carried out for this project that are discussed below, and clearly indicates that integrated OH levels in our previous experiments are much lower than in the atmospheric models used to calculate the MIR and other reactivity scales, and that increasing the integrated OH levels should result in experiments where the relative importance of secondary reactions become comparable to that calculated for the atmosphere.

Figure 3 also shows that it may be possible to design experiments with higher integrated OH levels where oxidation product contributions to reactivity are more consistent with atmospheric conditions. The changes included increasing radical levels by either increasing the light intensity, increasing run duration, adding various types of radical initiators or increasing radical initiation processes, or a combination of these. However, not all the modifications that were investigated can be achieved in practice at an affordable cost. The extent to which the modifications would actually improve correlations between atmospheric and chamber reactivities, and the practicality of implementing these approaches in actual experiments, was not fully investigated. In this section we present the results of additional and updated calculations to assess factors affecting differences in chamber and atmospheric reactivities, and alternative practical experimental approaches to reduce these differences.

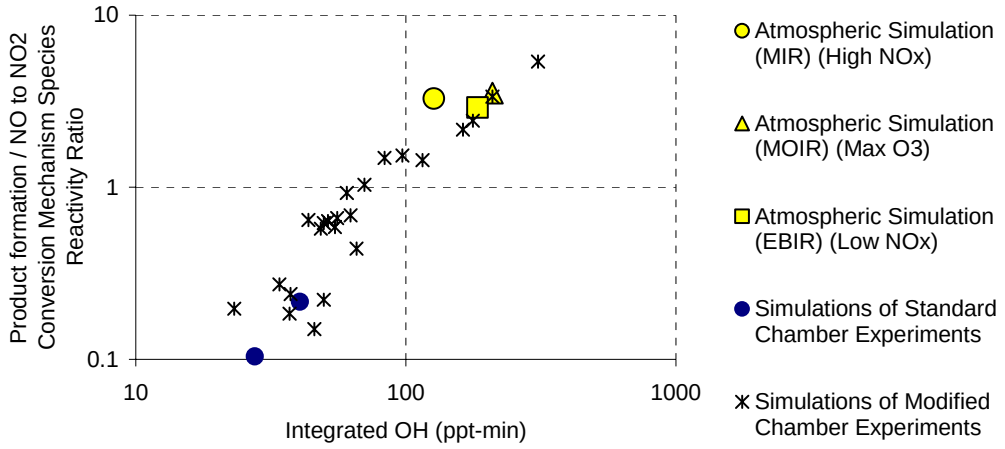

Figure 3. Plots of ratios of incremental reactivities of mechanism species representing secondary product reactions to those representing NO to NO_2 conversions in the primary reactions against integrated OH levels in various atmospheric and environmental chamber simulations. Calculated using the SAPRC-99 mechanism. (From the project proposal.)

Methods

Table 3 summarizes inputs and selected outputs (discussed below) of a series of idealized environmental chamber experiments utilized in this investigation of how to improve correlations between experimental and atmospheric reactivities. These chamber scenarios allow an assessment of effects of increasing light intensity, increasing run duration, and adding radical initiators in environmental chamber experiments. The specific scenarios are as follows:

Cham 1: Previous MIR Reactivity Experiments. This chamber experiment scenario represent the conditions of the incremental reactivity experiments designed to represent MIR conditions that we have been extensively utilizing in the past in reactivity studies with various compounds using the UCR EPA environmental chamber (Carter, 2010a and references therein; Carter, 2008, 2009a,b,c; Carter and Malkina, 2005, 2007; Carter et al, 2005c, 2010). The initial reactant concentrations are averages from many experiments and the light source consisted of blacklights with an intensity corresponding to an NO_2 photolysis rate (k1) of 0.13 min^{-1}, which is representative of most of these experiments. Although a smaller number of reactivity experiments have also been conducted using the arc light source with k1 of 0.26 min^{-1} in some of the earlier studies, the reactivity results were generally consistent with those for the experiments carried out using blacklights.

It should be pointed out that the previous reactivity studies also included experiments under lower NO_x and/or higher base case reactive organic gas (ROG) conditions to evaluate mechanisms under more NO_x - limited conditions. However, while these are useful for mechanism evaluation, they do not represent MIR conditions as well, and reactivities in these experiments correlate much more poorly with atmospheric MIR (or even MOIR and EBIR) than the results of the MIR experiments. Therefore, chamber experiments simulating NO_x - limited are not included in this investigation. However, experiments simulating NO_x - limited conditions are critical for any comprehensive mechanism evaluation, and must be included as part of any mechanism evaluation study along with experiments simulating MIR conditions.

Table 3. Summary of inputs and selected outputs for the atmospheric and chamber scenarios used to assess factors affecting reactivity.

Scenario ID and description	Atm. MIR Averaged Conditions MIR [a]	Cham 1 Previous MIR reactivity experiments	Cham 2 MIR experiments with higher light intensity	Cham 2T MIR experiments with more lights and longer time	Cham 2H MIR experiments with added H_2O_2 (as used)	Cham 2H+ MIR experiments with more added H_2O_2
			Conditions			
Initial NO_x (ppb)	[b]	30	50	50	60	60
Initial ROG (ppmC)	[b]	0.55	0.50	0.50	0.25	0.25
Initial H_2O_2 (ppb)					125	200
NO_2 Photolysis rate (min^{-1})	0.23-0.71	0.131	0.401	0.401	0.401	0.401
Duration (hours)	10	6	6	12	6	6
HONO input/k1 (ppt) [c]	0	12	12	12	12	12
			Results			
Integrated OH (ppt-min)	108	12	29	72	74	110
Correlation with Atmospheric MIR						
All Example VOCs [d]	100%	82%	89%	83%	88%	80%
Alkane, etc. [e]	99%	74%	85%	88%	95%	93%
Alkenes	100%	75%	85%	77%	73%	59%
Aromatics	100%	92%	96%	97%	96%	95%
Mechanistic Reactivities of "pure mechanism" species [f]						
NO to NO2 conversion	1.05	0.87	0.64	0.57	0.65	0.62
Nitrate formation	-2.73	-9.41	-6.45	-4.34	-1.19	-0.97
RCHO formation	4.16	0.15	0.74	1.06	1.28	0.99
PROD2 formation	2.91	0.10	0.35	0.81	1.11	1.16

[a] Atmospheric reactivity scenario representing the average of the conditions of all the 39 city-specific scenarios used to calculate the MIR reactivity scale. See Carter (1994b) for details of the inputs. Reactivities calculated for this scenario are very close to those calculated for the MIR scale, but not exactly the same (see Table A-2 in the Supplementary Materials).

[b] NO_x and VOCs are both present initially and emitted throughout the day. See note [a].

[c] Chamber effects parameter representing HONO offgasing, which provides the background radical and NO_x source, where k1 is the NO_2 photolysis rate assigned for the experiments. Other chamber effects parameters are the same as used when modeling all chamber experiments for this project.

[d] See Table A-2 in the Supplementary Materials for the list of representative VOCs used and their calculated incremental reactivities for the various scenarios.

[e] These also include other compounds with similar mechanisms to alkanes, such as alcohols, ethers, esters, glycols, etc. Most non-aromatic compounds in coatings solvents fall into this category.

[f] Molar mechanistic reactivities (moles O_3 formed / moles compound reacted) calculated for pure mechanism species with OH radical rate constant of n-octane. See discussion of the pure mechanism species for n-octane in the Modeling Methods section for details. Calculated for small amount of test VOC added for the purpose of mechanistic parameter analysis. These pure model species reactivities were calculated using the rate constant for n-octane, but are not strongly dependent on the rate constant and are at least approximately applicable to other compounds where these processes occur.

Cham 2. MIR Experiments with Higher Light Intensity. As discussed in the Experimental Methods section above, one of the accomplishments of this project was to enhance the blacklight light source in our chamber to increase the light intensity as quantified by the NO_2 photolysis rate (k1) from 0.13 min^{-1} to 0.40 min^{-1}, an increase by a factor of 3. This chamber experiment scenario represents conditions of MIR experiments that can be conducted in our chamber with the upgraded light system without increasing the run duration and adding radical initiators. Because of the higher light intensity, maximum incremental reactivity (MIR) conditions are calculated to occur at higher NO_x levels and/or lower base case ROG levels than was the case for our previous experiments. This is because increasing the light intensity increases the overall reactivity of the system in a qualitatively similar manner as increasing the ROG/NO_x ratio. Calculations indicated that increasing the initial NO_x from 30 to 50 ppb and reducing the initial ROG slightly should result in near MIR conditions. Such experiments were in fact carried out for this project, and are discussed in the Experimental Results section, below.

Cham 2T. MIR Experiments with Higher Light Intensity and Longer Run Duration. This chamber experiment scenario is the same as Cham 2, above, but with the experiment duration increased from 6 to 12 hours to increase the integrated OH radical levels (the integral of OH radical levels over time) by increasing the run time. Thus a comparison of these two scenarios indicates the effects of experiment run time on reactivity results with all else held constant. Although we attempted to conduct 12-hour experiments as discussed in the Experimental Results section, we were unable to conduct such long duration experiments during the course of this project because of experimental problems. However, we have successfully conducted 12+ hour experiments in the past, so in principle this type of chamber experiment is feasible.

An alternative method to conduct experiments with longer run duration is to conduct experiments with controlled dilution to make up for any leakage of the reactor during the course of the irradiation. In order for this to work, the dilution has to be controlled and reproducible and exactly the same in both the base case and added test VOC experiments when irradiated simultaneously in both reactors. As discussed in the Experimental Results section we found this to be difficult in practice, and different dilution rates were obtained in the two reactors despite equal pressure on the reactors and equal flow rates of dilution air into the reactors. In addition, calculations indicate that if the dilution is too great then the difference in O_3 formation in the base case and added test VOC experiment become too small to reliably measure with reasonable amounts of an added test VOC. Therefore, we did not investigate further the option of increasing run duration by increasing dilution to make up for chamber leakage. As with the other chamber simulation scenarios listed on Table 3, the Cham 2T scenario involves no dilution.

Cham 2H. MIR Experiments with Added H_2O_2. This chamber experiment scenario, along with the Cham 2H+ scenario discussed below, involves increasing the integrated radical levels by adding H_2O_2 as a radical initiator. The results can be compared with those of the Cham 2 scenario, which employs the same light intensity and run duration. The added radical initiator causes the MIR conditions to occur at lower ROG/NO_x ratios, so the initial NO_x and ROG levels also had to be modified. Calculations such as those discussed below indicate that the best correlations with atmospheric MIR values occur if the H_2O_2/Base ROG ratio is approximately 0.5 mole/moleC. Near MIR conditions occur if NO_x is increased to 60 ppb and the base ROG is decreased to 0.25 ppmC.

H_2O_2 was chosen as the radical initiator because we have had extensive experience in using it as a reactant to generate OH radicals in chamber experiments to study formation of secondary organic aerosol (SOA) in the absence of NO_x (e.g., Song et al, 2007). Although we do not have methods to monitor H_2O_2 in the gas phase, model simulations can successfully simulate results of H_2O_2 experiments with VOCs with known mechanisms by using the initial concentration calculated from the volume and concentration of H_2O_2 injected and the volume of the reactors. HONO or methyl nitrite could also be used as radical initiators, but both are also NO_x sources and affect the system in that way, HONO is difficult to

quantitatively synthesize in the absence of NO, NO_2 and other impurities in the amounts required, and calculations indicate that experiments with methyl nitrite tend to be less sensitive to added VOCs. Another option to increase radical initiation is to use higher UV intensity to enhance formation of O^1D from the photolysis of O_3, and add humidity to enhance its reaction with H_2O to form OH radicals. However, calculations indicate that this does not provide as large an increase in integrated OH levels under the conditions of our simulated chamber experiments as other methods, and changing the lights to enhance the UV is expensive and results in distributions of photolysis rates that are less representative of atmospheric conditions. Therefore, we conclude that addition H_2O_2 is the best practical option for enhancing radical levels using radical initiators.

Because as discussed below reactivities measured in this type of chamber experiment are predicted to give the best correlations with atmospheric MIR values for the types of compounds important in coatings applications, we conducted a number of experiments using this method as part of this project, and the results of experiments with representative previously studied compounds were generally consistent with model predictions. This is discussed in the Experimental Results section, below.

Cham 2H+. MIR Experiments with More Added H_2O_2. Although the Cham 2H scenario gave the best correlation with atmospheric MIR of all alternatives examined, as shown on Table 3, it still gave somewhat lower integrated OH levels than in atmospheric MIR scenarios. Therefore, the Cham 2H+ chamber experiment scenario was used to investigate the effect of increasing the added H_2O_2 from 125 to 200 ppb to attain approximately the same integrated OH as the scenario representing atmospheric MIR conditions. All the other conditions are the same as in the Cham 2H scenario. No reactivity experiments were conducted for this project using this amount of added H_2O_2, though there is no practical reason why they could not be conducted if desired.

As discussed in the Modeling Methods section, above, the chamber reactivity simulations were conducted with the amount of the test VOC in the simulations being sufficient to obtain experimentally measured differences in O_3 formation. However, for the purpose of assessing reactivity contributions using pure model species mechanistic reactivities, it is necessary that the simulated experiments represent true incremental reactivity conditions, i.e., the amount of added test VOC needs to be small. Therefore, for calculating relative contributions to reactivity of various aspects of the mechanism, the reactivities of the pure mechanism species were calculated for small amounts of test VOC added. See footnote [f] to Table 3 and the discussion of mechanisms for pure model species in the Modeling Methods section for more details concerning the mechanism contribution calculations.

n-Octane was chosen as the representative compound to assess mechanistic contributions to reactivity because it is a well-studied example of a compound with negative reactivities in chamber experiments and positive reactivities in the atmosphere, and is a representative of the types of alkanes present in petroleum distillate mixtures. Similar results would have been obtained if another alkane or a glycol ether or ester such as a Texanol® isomer had been chosen, because they have the same types of reaction mechanisms in terms of their overall reaction processes as represented in the SAPRC mechanisms.

For comparison purposes, Table 3 also summarizes the conditions and selected results of a scenario representing atmospheric MIR conditions. As discussed previously (Carter, 1994a,b, 2000a, 2010a), the actual MIR scale is calculated using the averages of incremental reactivities in the 39 city-specific scenarios with NO_x inputs adjusted to yield MIR conditions, and this is the scale used for comparisons with the reactivities calculated for the various experimental scenarios. However, for assessing mechanistic effects using reactivity calculations of pure mechanism species, it is more straightforward to use a single scenario, so the “averaged conditions” MIR scenario is used for this purpose. This is a single scenario with most inputs derived by averaging those for the 39 city-specific

scenarios, and with NO_x inputs adjusted to yield MIR conditions for that scenario. As indicated on Table 3 and also Table A-2, incremental reactivities for this scenario are very close to those in the actual MIR scale, so the mechanistic contributions calculated for it should be a good indication of atmospheric MIR conditions in general.

Results

The integrated OH levels, correlations of chamber reactivity with the atmospheric MIR scale for selected representative compounds, and mechanistic reactivities for various processes in the n-octane photooxidation mechanism are summarized in the "results" section of Table 3. Figure 4 gives plots of contributions of various aspects of n-octane's oxidation mechanism against the integrated OH levels in the simulation, and Figure 5 shows a comparison of the relative importance of these overall processes to n-octane's overall reactivity.

Consistent with the modeling studies conducted previously, the integrated OH levels in the previous MIR experiments are calculated to be almost an order of magnitude lower than in the atmospheric MIR conditions. Increasing the light intensity by a factor of ~3 results in a factor of 2.4 increase in the integrated OH levels, and doubling the duration of the experiment causes another factor of 2.4 increase in the integrated OH levels, though the result is still somewhat lower (by ~33%) than the integrated OH levels in the atmospheric simulation. Adding H_2O_2 at a level of 50% of the carbon in the base ROG on a molar basis causes the same increase in integrated OH. Increasing H_2O_2 by 60% caused a ~50% increase in integrated OH and achieved nearly the same level as in the MIR scenario.

Figure 4 shows that the effects on reactivity of formation of the organic products represented by RCHO (higher aldehydes) and PROD2 (higher ketones and other less photoreactive oxygenates) increase with increasing integrated OH, consistent with the previous results shown on Figure 3, above. Increasing the run duration in the Cham 2T scenario has almost exactly the same impact on both integrated radical levels and relative contributions of both PROD2 and RCHO formation as adding H_2O_2 in the Cham 2H scenario. However, the correlation is not perfect, increasing the H_2O_2 levels from that of the Cham 2H scenario to Cham 2H+ does not yield a corresponding increase in the relative contribution of RCHO formation, and relative contribution of PROD2 formation actually decreases. (See the "Results" section of Table 3 for additional information.)

Figure 4 shows that increasing the integrated OH level has the opposite effect on the relative contribution of organic nitrate formation in the RO_2 + NO reactions, though again the correlation is not perfect. This is a different type of chemical process than organic product formation, since it involves radical termination as well as organic nitrate formation. The radical termination process is by far the more important factor under MIR conditions, as indicated by the net negative effect of these processes on overall reactivity. This is because of the high sensitivity of O_3 formation under MIR conditions to reaction rates and radical levels. In this case, increasing the integrated OH level by adding the H_2O_2 has a much larger effect in decreasing the importance of nitrate formation than increasing the light intensity or run duration, though the effect seems to level off when the H_2O_2 is increased beyond the levels in the 2H scenario. Adding radical initiators to the experiment tends to make the system less radical limited, and therefore the effects of radical termination processes are reduced, though apparently there is a point beyond which further increasing radical initiators has less of an effect. Increasing light intensity and run duration also increases the importance of radical initiation processes since there is more reactivity or time to cause formation of radical initiating photoreactive oxidation products. But this is a secondary effect and the effect on the relative importance of termination processes is consequently lower.

Figure 5 compares the contributions of the various aspects of the n-octane mechanism to its overall reactivity in the various scenarios. Note that "product formation" refers to the sum of the effects of

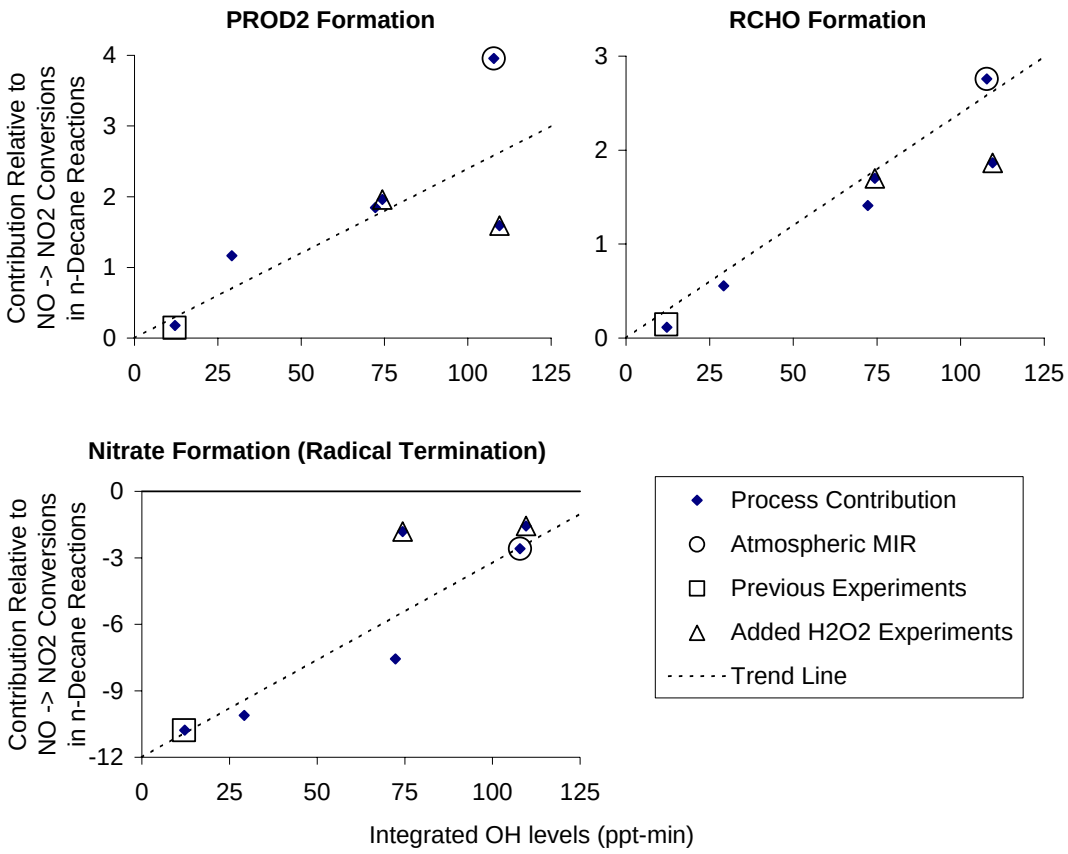

Figure 4. Plots of relative contributions of various aspects of n-octane's photooxidation mechanism against integrated OH levels for the atmospheric MIR and various chamber reactivity scenarios.

formation of RCHO and PROD2, and "nitrate formation" includes the effects of the radical termination involved in the nitrate formation process, and the sign has been changed to allow easier comparisons with the total positive contributions, which is the sum of the effects of product formation and NO to NO_2 conversions. For the atmospheric MIR scenario the organic product formation has a very similar contribution to reactivity as the NO to NO_2 conversions, and together they have about three times the magnitude as that of the negative effects of nitrate formation, resulting in a net positive reactivity for this scenario. In contrast, for the conditions of both the previous chamber experiments and also the experiments with the higher light intensity, the effect of product formation is minor (essentially negligible in the case of Cham 1), and the negative effect of the nitrate formation is much greater, both contributing to the relatively high net negative reactivities calculated for n-octane for those experiments. Increasing the light intensity increases product contribution by a relatively large factor but it is still relatively small, and it causes only a relatively small decrease in the magnitude of the negative effect of nitrate formation. Increasing the duration of the experiment causes a further increase in the contribution of organic formation and a further decrease in the magnitude of the negative effect of nitrate formation, with the change in the effect on nitrate formation being the more important factor affecting the net reactivity. However, the relative importance of nitrate formation is still almost 3 times greater in the Cham 2T scenario than for atmospheric MIR, and the net reactivity for n-octane is still calculated to be negative in the chamber experiment, though much less so.

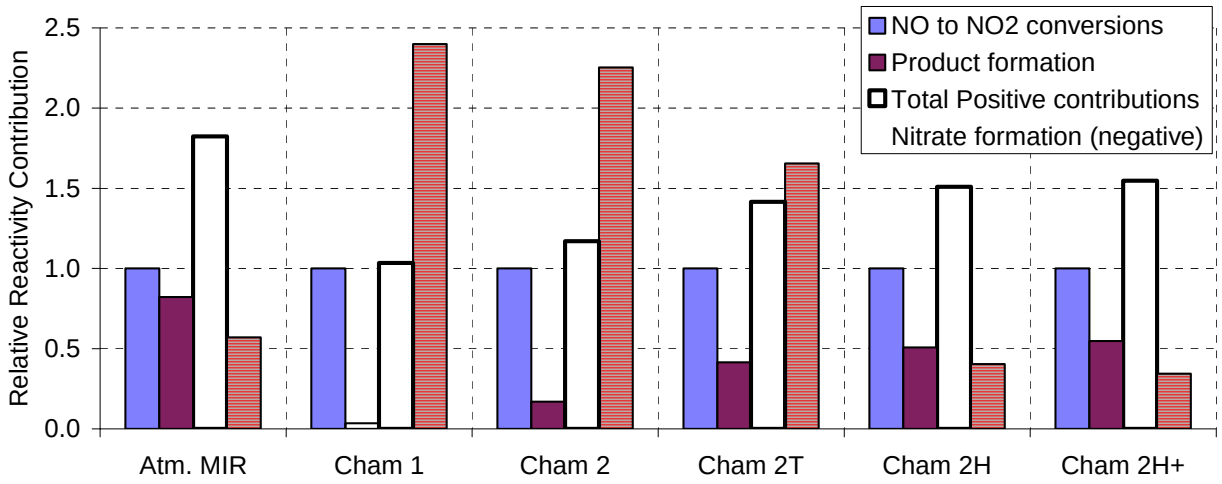

Figure 5. Relative contributions of various aspects of the n-octane mechanism to calculated mechanistic reactivities of n-octane for various types of incremental reactivity chamber experiments and atmospheric MIR. Contributions are normalized to the contributions of the NO to NO_2 conversions..

Adding H_2O_2 tends to increase the relative effect of product formation slightly more than doubling the reaction time, but its major effect is significantly reducing the contribution of nitrate formation to levels even lower than atmospheric MIR. This is because in addition to increasing the integrated radical levels, adding radical initiators also decreases the sensitivity of the experiment to other processes involving radical initiation and termination because it makes the system less radical limited. The overall effect in this case is that the net reactivity of n-octane in the added H_2O_2 chamber experiments becomes positive, as is the case for atmospheric conditions.

Based on these results we would expect the Cham 2H or Cham 2H+ to give better correlations with atmospheric reactivity for compounds like n-octane, though the addition of H_2O_2 does not increase the product contribution quite enough and decreases the nitrate contribution excessively compared to atmospheric MIR. The Cham 2H and Cham 2H+ appear to be about the same in terms of relative contributions to n-octane reactivity, but Table 3 indicates that adding the H_2O_2 beyond the level of the 2H scenario causes reduced correlations with atmospheric MIR. This is probably because the reduced sensitivity of the higher H_2O_2 scenario to radical initiation and termination processes causes somewhat higher relative reactivities for radical terminating compounds such as alkanes and somewhat lower relative reactivities of radical initiating compounds such as aromatics, relative to atmospheric MIR conditions. For this reason, the amount of H_2O_2 added in the Cham 2H appears to be closer to optimal.

Figure 6 shows plots of the relative incremental reactivities of 80 representative compounds and mixtures of various types calculated for selected simulated environmental chamber scenarios against their corresponding relative reactivities in the atmospheric MIR scale. The incremental reactivities are relative to the incremental reactivity of the base ROG mixture used to calculate the atmospheric reactivity scale, to place the magnitudes of the atmospheric and chamber reactivities on the same basis. The plots on the left show the data for all the compounds and the plots on the right have smaller scales to show the data for the alkane-like and other less reactive compounds and mixtures more clearly. The specific compounds and mixtures used, and their incremental reactivities for these and the other scenarios, are listed in Table A-2 in the Supplementary Materials.

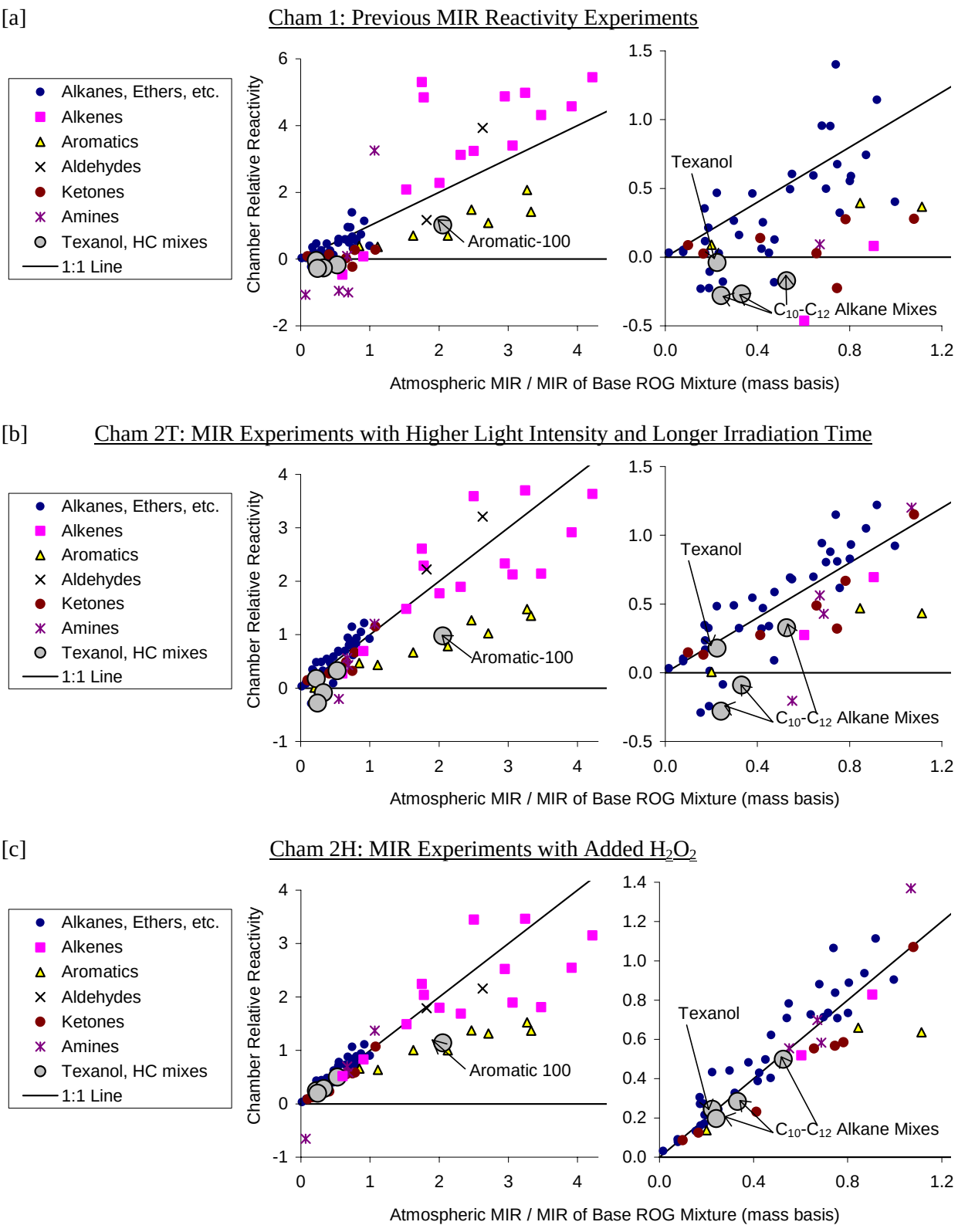

Figure 6. Plots of incremental reactivities for selected compounds and mixtures calculated for the conditions of various types of incremental reactivity chamber experiments designed to represent MIR conditions against atmospheric reactivities in the MIR scale..

Figure 6a shows that reactivities calculated for the conditions of the previous MIR experiments generally correlate with atmospheric MIR, particularly for the more reactive compounds, but there is considerable scatter and as discussed above, a number of important compounds with positive MIR's have negative reactivities in the experiments. Texanol® has a chamber reactivity of approximately zero and the mineral spirits and other alkane mixtures have negative chamber reactivities, despite their positive atmospheric MIR's. The mechanistic reasons for this are discussed above. The highest molecular weight alkenes also have negative chamber reactivities and positive atmospheric MIR's. The correlations are relatively good for the lower molecular weight alkenes and the aromatics, though the aromatics tend to fall below the 1:1 line. The mechanistic reasons for this have not been investigated.

Figure 6b shows that for experiments with higher light intensity and longer run duration the correlations between chamber and atmospheric reactivity are improved significantly for the less reactive compounds but not greatly changed for the more reactive compounds. The correlations for the alkane-like compounds and mixtures, and also the high molecular weight alkenes, are improved considerably, with the relative reactivity of Texanol® being almost the same in the chamber as the atmosphere. The scatter for the higher alkenes is not significantly improved, but the points are now closer to the 1:1 line. However, there are still alkane and alkane-like compounds and mixtures with negative chamber reactivities, with n-octane, discussed above, being an example. In addition, there is relatively little change in the relative chamber reactivities of the aromatics.

Figure 6c shows that for the experiments with the added H_2O_2 the correlations are significantly improved for the lower reactivity compounds, though there is relatively little improvement in the correlations for the more reactive compounds compared to the experiments with higher light intensity and longer run duration. This type of experiment performs particularly well for alkane and alkane-like compounds of relevance to coatings reactivity assessment, with Texanol® and the representative primarily alkane petroleum distillate mixtures all falling very close to the 1:1 line. On the other hand, the correlations for the aromatics are essentially unaffected, and the correlations for the alkenes are not quite as good as for the 2T experiments, and there are more alkenes below the 1:1 line than above it. Thus for the alkenes and the aromatics there is relatively little advantage over using added H_2O_2 compared to increasing the irradiation time, and vise-versa.

Plots of chamber vs. atmospheric reactivities are not shown for the Cham 2H+ experiments with additionally added H_2O_2 because they are very similar to those for the Cham 2H experiments shown in Figure 6c. However, there is a greater tendency for the points for the alkane-like compounds, including Texanol® and the representative primarily alkane petroleum distillate mixtures to be above the 1:1 line, the extent that the aromatics are below the 1:1 line is slightly greater, and there is also somewhat greater scatter for the alkenes, compared to the Cham 2H experiments with less added H_2O_2. For this reason we conclude that the relative amount of H_2O_2 added in the Cham 2H+ is less optimal than is the case for the Cham 2H runs.

Based on the results of this modeling analysis, we chose surrogate - NO_x + H_2O_2 experiments corresponding to the Cham 2H scenarios as the basis for experimental evaluations for this project. Reactivity experiments with the higher light intensity were also carried out, for comparison purposes with the previous experiments and for mechanism evaluation. We also attempted experiments with longer run duration for comparison purposes but we were unsuccessful because of experimental problems. These experimental evaluations, and the results obtained, are discussed in the following section.

EXPERIMENTAL AND MECHANISM EVALUATION RESULTS

Summary of Experiments and Characterization Results

A chronological listing of the environmental chamber experiments carried out for this project is given in Table A-3 of the Supplementary Materials. These included experiments to evaluate the upgraded blacklight light source and to investigate other potential modifications of the experimental methods, experiments with the test compounds of interest for this study, experiments to evaluate the use of the surrogate - NO_x + H_2O_2 to measure incremental reactivities, and appropriate characterization and control experiments needed for the data to be useful for mechanism evaluation. The "Results" column of Table A-3 summarizes relevant results of the individual characterization or method evaluation experiments, and gives the tables or figures where results of surrogate or reactivity experiments are presented. The results of the experiments to evaluate or investigate experimental modifications and the characterization results are discussed in the remainder of this section. The results of the surrogate and reactivity experiments for mechanism and method evaluation are discussed in the sections following this.

Investigation of Chamber and Experimental Method Upgrades

Light Upgrades. The major upgrade to the facility that was accomplished during the course of this project was the construction of additional banks of blacklights to permit experiments to be conducted with higher light intensities more representative of conditions used to calculate atmospheric reactivity scales. This upgrade was completed before any experiments were carried out for this project, and resulted in approximately a factor of 3 increase in the maximum light intensity available for our chamber experiments. This is discussed in the "Blacklight Characterization" section below. As indicated on Table A-3, most of the experiments were carried out using the enhanced light intensity, though several were carried out using only the original lights for characterization purposes.

Although the blacklight upgrade accomplished its goals, the cost and time required was greater than originally anticipated when the budget and schedule for this project was developed. For this reason, we were not able to conduct quite as many mechanism or method evaluation experiments that were originally planned. Nevertheless, we were able to conduct a significant number of useful experiments with the upgraded lights, as discussed in the remainder of this report.

Attempts to Increase Run Duration without Dilution. In addition to the light upgrades, we also investigated methods to increase the duration of the experiments in order to achieve integrated radical levels closer to those in atmospheric reactivity simulations. Although we have been able to conduct irradiations of 12 hours or more in the past, for most of this project we were unable to conduct experiments with such long durations because of leaks in the Teflon® reactors. As discussed in the Experimental Methods section, the UCR EPA chamber is designed such that sampling or leakage of the reactors causes the reactor volumes to decrease rather than the reactor contents to be diluted or contaminated with outside air, so leakage does not affect the validity of the results for mechanism evaluation. However, once the reactor volume has reached a minimum level it cannot be reduced further and the experiment has to be terminated. In some cases during this project, the leakage was so extensive that experiments had to be terminated before the normal 6-hour irradiation time had elapsed.

Significant efforts were made to find and correct the leaks so longer run durations could be accomplished, but they were only partially successful. Leaks were found and repaired after the experiments with the worst leakage problems, problems causing leaks around the sampling system were corrected, and improvements to the system of clamping the Teflon® film together on the top and bottom

edges were made to reduce leakage there. However, run durations comparable to what was achieved previously were not achieved. Tests to try to isolate the location of the unknown leaks were inconclusive. It was eventually concluded that part of the problem may be due to damage to the framework holding Teflon® panes together during the course of the several years of operation of this chamber, and redesign and reconstruction of the framework may be needed. By the time this was concluded there was insufficient time and resources remaining in this project to carry out this redesign and reconstruction, and the possibility that it may still not solve the problem cannot be ruled out.

It was eventually found that run times of up to 8 hours could be routinely accomplished if the known leak sources were addressed and the pressure used to control when the top framework is lowered to reduce the volume when air is lost due to sampling or leakage is decreased. This method was used for the surrogate + H_2O_2 experiments that were carried out around the end of the project. Further decreases in the controlled reactor pressure would allow longer run times, but were not employed because they would also result in unacceptable dilution in the chamber during the experiments.

Characterization of Dilution Rates. It is always possible to carry out long duration experiments by diluting the chamber with purified air during the irradiations, as is necessary in experiments in chambers with rigid walls. This requires that dilution rates be routinely characterized during the course of the experiments by adding inert tracers whose rates of consumption can be monitored precisely. We had not routinely used inert tracers in our experiments prior to this project, but they are clearly necessary to characterize experiments with controlled dilution, and would also be useful to verify that dilution is not occurring in experiments intended to be static, such as, for example, determining the minimum acceptable control pressure to extend irradiation time. To address this, during the course of this project we began routinely adding ~60 ppb perfluoro n-hexane (C_6F_{14}), an unreactive compound that can be monitored with high precision with GC-FID, to all of our irradiation experiments. The suitability of this compound as an unreactive tracer was verified by conducting a surrogate - NO_x + perfluorohexane experiment prior to conducting any other experiments for this project. As shown on Figure 7, the addition of large amounts of this tracer had no effects on measures of reactivity used in this study.

Attempts to Increase Run Duration with Controlled Dilution. In order for dilution to be useful as a means to extend the duration of incremental reactivity experiments, or to experimentally simulate the

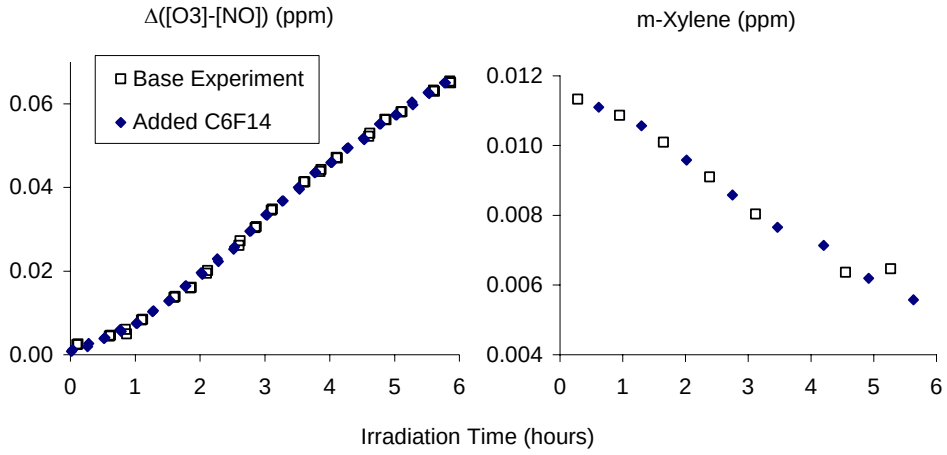

Figure 7. Effects of addition of ~3.5 ppm of perfluoro n-hexane on NO oxidation and O_3 formation and m-xylene consumption rates in the surrogate - NO_x + perflourohexane experiment EPA991.

effects of dilution on reactivity, it is necessary that the dilution rate be controlled, reproducible, and exactly the same in both reactors in the dual-reactor incremental reactivity experiments. If the reactor volumes are constant, then it is sufficient to control the rate of input of dilution air, and allow the excess air to escape to maintain constant chamber pressure. For implementing this for our experiments, mass flow controllers were acquired so that dilution air can be added at constant and controlled rates, and the plan was to keep the reactors at constant volume by filling them completely and allowing the excess air to exit the reactors through the leaks or if necessary vents added to maintain constant pressure. Previous experience has shown that reproducible volumes (measured by adding known amounts of compounds and measuring their concentrations) are obtained when the reactors are filled to their maximum extent at controlled pressures.

As shown in Table A-3, experiments were carried out early in this project to assess whether this plan for conducting experiments with controlled dilution would obtain satisfactory results. CO and perfluorohexane were injected into both reactors and the reactors were continuously diluted with pure air introduced at a constant rate measured by a mass flow controller. CO was continuously monitored for 22 to 68 hours depending on the experiment, and perfluorohexane was also monitored periodically and gave similar results as the CO data. The lights were kept off during these tests, and for the initial tests the air handlers used to control the temperature in the enclosure during irradiations were turned on in order to simulate the irradiation conditions. For the first of these tests, which extended for 27 hours, the continuous CO data indicated dilution on Side A was 6.6%/hour and dilution on Side B was 9.0%/hour. The results of the second test, which extended for 68 hours, indicated dilution rates of 6.2%/hour in Side A and 8.2%/hour in Side B. This is not considered to be acceptable reproducibility or side equivalency to be satisfactory for incremental reactivity experiments for mechanism evaluation.

The unsatisfactory results of the first two tests were attributed to the action of the air movement caused by the air handlers on the flexible walls of the reactors, which had different effects on the two reactors. In particular, the air currents were such that reactor A impinged on Reactor B and caused the volume of Reactor A to increase at the expense of Reactor B. As shown on Figure 1, above, the design of the chamber is such that the two reactors are in contact with each other so there is nothing to prevent this from happening. This was investigated by conducting a third dilution test with the air handlers turned off to reduce the buffeting of air on the reactors. This test, which lasted for 22 hours, showed a dilution of 5.0%/hour in Reactor A and 5.7%/hour in reactor B. This showed somewhat better side equivalency but this approach is not a solution since use of the air handlers is necessary for irradiation experiments.

Since redesigning the reactor configuration would be costly and time consuming and since it was hoped that other approaches may give better results for conducting reproducible and controlled experiments with higher integrated radical levels, it was decided not to pursue further the approach of using controlled dilution to extend the duration of incremental reactivity experiments.

Blacklight Characterization

All of the experiments for this project were carried out using the blacklight light source that was upgraded as part of this project. The blacklights employed previously, and for a few experiments for this project, are referred to as the “old” or the “original” blacklights. As discussed above, the blacklight upgrade for this project consisted of adding several new banks of blacklights without removing the banks of blacklights that were previously in place, with the new banks of lights being controlled by separate switches. This allowed for the option of conducting experiments using only the old banks of lights in order to reproduce the light intensity of previous experiments, as well as using some or all of the new banks of lights in order to have enhanced light intensity. Thus, these are the only lighting conditions whose characterization will be discussed in this report.

Methods for characterizing the intensity of the blacklight light source were discussed by Carter et al (2005b), though some revisions were made as a result of subsequent measurements. NO_2 actinometry measurements were made using the quartz tube method of Zafonte et al (1977), modified as discussed by Carter et al (1995c), with the quartz tube both inside the reactors and also in front of the reactors. As discussed by Carter et al (2005c), for the original blacklights the results of these and other measures of light intensity with the original or old blacklights, indicated a steady decline in light intensity with time, with the results being best correlated with the "blacklight run count", which is the number of experiments carried out in the chamber using the blacklights, and is thus an indicator of the ageing of the lights due to use. However, after around early 2006, or around the time of run EPA500 or a blacklight run count of around 200, the light intensity appeared to level off at a NO_2 photolysis rate of around 0.13 min^{-1}. This is shown on Figure 8a, which gives plots of NO_2 photolysis rates measured or estimated for the reactors against the blacklight run count. The "reactor" values give the results of the in-reactor actinometry measurements, including the results of the in-chamber actinometry carried out during the period of this project (run EPA1138, see Table A-3), which is the last point shown on the figure. The "enclosure (adjusted)" values show the results of the measurements made in front of the reactor, adjusted by a factor of 0.698, which is the ratio of reactor to enclosure actinometry measurements made previously (Carter et al, 2005c).

The results of the NO_2 actinometry measurements made with all of the blacklights after the blacklights were upgraded for this project are shown on Figure 8b. The single "reactor" point shows the result of the in-chamber actinometry experiment EPA1138 (see Table A-3), which gave an NO_2 photolysis rate of 0.401 min^{-1} when all of the lights (old and new) are turned on. The "enclosure (adjusted)" points shown on Figure 8b are results of measurements made in front of the reactors, multiplied by a factor derived by a factor of 0.768, which is the ratio of the in-reactor actinometry measurement from EPA1138 to the average of the results of the measurements in front of the reactor. This enclosure vs. reactor correction factor of 0.768 is somewhat higher than the factor of 0.698 derived for the original lights; this could be due either to measurement uncertainty or the effect of the increased number of lights or their placement. In any case, the enclosure actinometry results indicate no significant change of light intensity with time when all the lights are employed, in contrast with the results with the original lights when they were new.

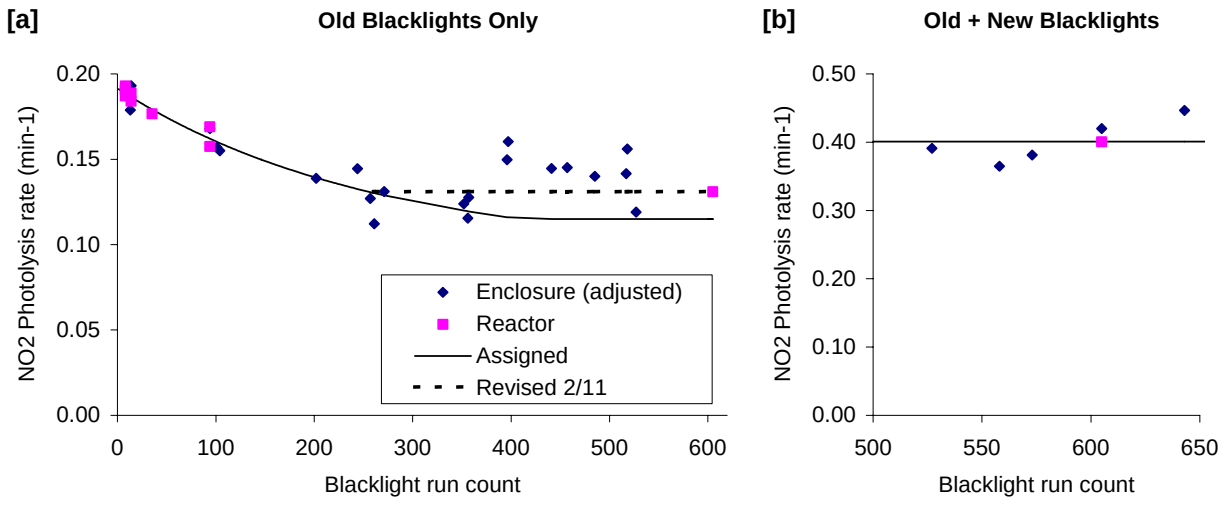

Figure 8. Plots of light intensity data used to assign NO_2 photolysis rates for the blacklight light source.

The lines on Figure 8 show the NO_2 photolysis rates that were assigned to the runs for modeling purposes. For all of the blacklights, a constant NO_2 photolysis rate of 0.401 min^{-1}, based on in-chamber actinometry measurement made during run EPA1138, is used. As discussed by Carter et al (2005b), for the old lights up to blacklight run count of around 400, the results are reasonably well fit by the empirical expression k_1 (min^{-1}) = 0.0958 x [1 + exp(-Blacklight Run Count x 0.003914)]. After that, the NO_2 photolysis rate was assumed to be constant at the value derived using this expression for a run count of around 400, or 0.115 min^{-1}, in modeling work reported previously (Carter, 2010a and references therein; Carter, 2008, 2009a,b,c; Carter et al, 2010). However, the results of the actinometry experiments carried out more recently indicate an average in-chamber NO_2 photolysis rate of about 0.13 min^{-1}, consistent with the results of the in-chamber measurement during EPA1138. Therefore, for this work and subsequent modeling work for these experiments, the NO_2 photolysis rate for experiments using the original blacklights that were previously assigned NO_2 photolysis rates lower than 0.13 min^{-1} are now assigned to values of 0.131 min^{-1}, based on the average of the adjusted enclosure measurements and the results of EPA1138. This is shown as the dotted line on Figure 8a.

The spectrum of the blacklights in this chamber has been measured periodically and is assumed to continue to be the same as the spectrum recommended by Carter et al (1995) for modeling blacklight chamber runs. There is no reason to expect the spectrum to change with the light upgrade made during this project, since the same type of lights is employed as the original lights.

Chamber Effects Characterization

Except as discussed below, the characterization results for the more recent experiments for this project are consistent with those discussed by Carter et al (2005c) and Carter and Malkina (2005, 2007), and the same characterization parameters were used for modeling. The most important chamber effect, and the only chamber effect parameter that was changed when modeling the experiments for this project, concerns the apparent HONO offgasing, which is believed to be responsible for both the chamber radical source and NO_x offgasing effects (Carter, 2004). This is represented in the chamber effects model by the parameter RN-I, which is the HONO offgasing rate used in the simulations divided by the light intensity as measured by the NO_2 photolysis rate. Figure 9 shows the HONO offgasing parameters that best fit the radical or NO_x - sensitive characterization experiments carried out during the period of the last three sets of reactors. Note that the experiments carried out for this project start at run EPA777, so the applicable characterization data for this project is for the last set of reactors shown on the figure.

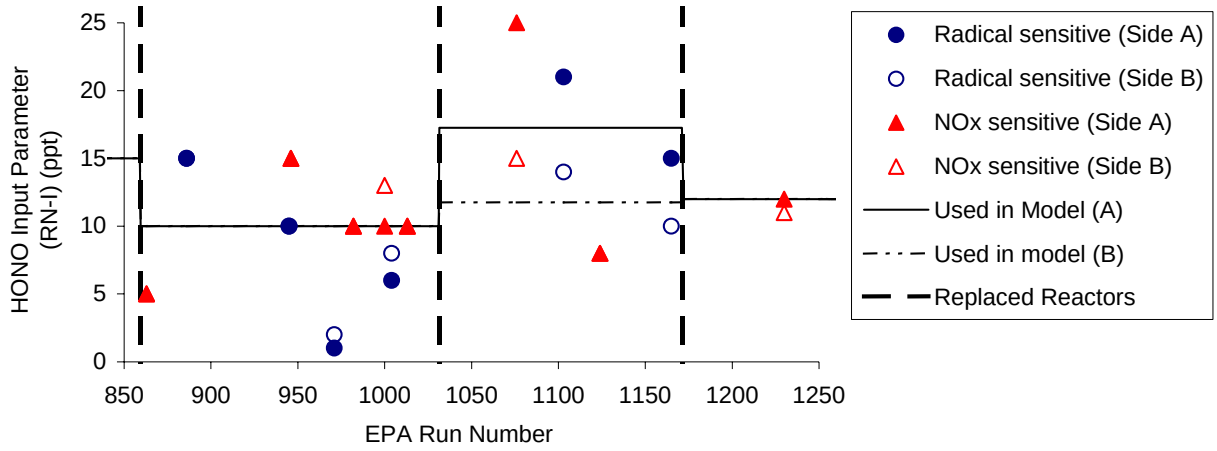

Figure 9. Plots of best fit HONO offgasing parameters against UCR EPA run number.

All the runs carried out for this project employed only the last two sets of reactors shown on Figure 9, the sets installed just before runs EPA1032 and EPA1172. For the first of these, two radical source and two NO_x offgasing characterization experiments were conducted, and generally consistent results were obtained. For the second of these, only one useable NO_x offgasing characterization experiment was conducted, indicating a NO_x offgasing rate within the range observed in previous characterization runs. A radical source characterization run, EPA1351, was also carried out using this reactor, but the results were rejected because the results were far outside the expected range, and experimental problems are suspected (see Table A-3), so the results were rejected. This makes the radical source and NO_x offgasing somewhat uncertain for this last reactor until more measurements are made, but most of the experiments using this reactor were surrogate - NO_x with added H_2O_2 experiments whose results are expected to be insensitive to this chamber effect, because NO_x is injected and the added H_2O_2 provides a much more important radical source than the chamber radical source.

Side equivalency test experiments, in which the same mixture is irradiated in both reactors, are carried out periodically as controls for the incremental reactivity experiments. Generally good side equivalency is observed for the gas-phase results, though sometimes one reactor is more favorable for particle formation than the other (Carter et al, 2005c). The results of the side equivalency test carried out during this project are summarized on Table A-3 and also in conjunction with the discussion of reactivity results discussed below. Except for run EPA1093, whose results are rejected because of probable problems with reactant injections and therefore is not listed on Table A-3, acceptable side equivalency was observed when such experiments were carried out during the course of this project.

Mechanism and Reactivity Assessment Evaluation Results

Table 4 lists the initial concentrations and selected gas-phase results for all the surrogate - NO_x experiments without added test compounds (base case reactivity and other surrogate experiments) carried out for this project, and Table 5 lists selected conditions and results for the incremental reactivity experiments. Experiments that were rejected because of experimental problems are not included in this listing. Additional results, and results of the model simulations of these experiments, are discussed below in the remainder of this section.

Surrogate - NO_x Experiments and Adjusted Aromatics Mechanism

The addition of the new lights meant that the conditions of the base case reactivity experiments would have to be modified if the new lights are employed, so a series of surrogate - NO_x and incremental reactivity experiments with previously studied compounds were carried out to evaluate the results and model performance. This resulted in a number of surrogate - NO_x experiments being carried out at varying initial NO_x and reactive organic gas (ROG) surrogate levels. The conditions and selected results of these experiments are summarized on Table 4, and the performance of the SAPRC-07 chemical mechanism in simulating the amounts and rates of O_3 formation and NO oxidation in these experiments is shown on Figure 10. The Δ([O3]-[NO]) model errors are shown as a function of the ROG/NO_x ratio multiplied by the NO_2 photolysis rate in order to place the results of experiments with different light intensities on approximately the same basis, since increasing the light intensity has a similar overall effect on reactivity as increasing the total VOC levels.

Figure 10 shows that the SAPRC-07 has a consistent bias towards underpredicting O_3 formation and NO oxidation at the lower ROG/NO_x ratios, though it gives satisfactory simulations of the higher ROG/NO_x runs that are more NO_x limited. This is similar to results of SAPRC-07 model simulations of previous surrogate - NO_x experiments carried out at the lower reactant concentrations used in our current experiments, and is attributed to problems with the aromatics mechanisms (Carter, 2010a). This

Table 4. Summary of initial concentrations and selected results of the surrogate - NO_x and surrogate - NO_x - H_2O_2 experiments without added test compounds.

Run	Hours	Initial (ppb or ppbC)			Ozone (ppb)		PM ($\mu g/m^3$)		Note
		NO_x	VOCs	H_2O_2	t=5 hr	Final	t=5 hr	Final	
Old blacklights only (lower light intensity)									
1088B	5	37	553		48	48	0.0	0.0	
1140B	7	26	556		67	88	-	-	
1145B	5	22	1053		88	88	0.2	0.2	
Experiments with NO_x = ~30 ppb, VOCs =~240 ppb, all blacklights (higher light intensity)									
1073B	7	31	241		46	67	-	-	
1079A	6	31	242		61	74	-	-	
1081B	9	31	245		65	109	0.3	0.2	
1083A	6	32	205		61	74	0.0	0.0	
1112A	6	24	236		95	113	0.0	0.0	Side Equivalency
1112B	6	24	236		93	110	0.1	0.0	
1177A	7	26	240		96	125	1.1	1.5	Side Equivalency
1177B	7	26	238		98	128	0.6	0.8	
Variable NO_x and VOC experiments, all blacklights									
1113A	6	56	680		205	231	0.0	0.0	
1128A	5	50	643		203	203	-	-	
1167B	5	50	677		186	186	0.0	0.0	
1133B	5	52	707		187	187	0.0	0.0	
1130B	3	53	773		-	156	-	0.0	
1164B	5	48	704		194	194	0.2	0.2	
1152B	5	42	638		194	194	0.5	0.5	
1113B	6	31	680		183	194	0.1	0.1	
1122A	7	27	611		173	195	-	0.0	
1122B	6	14	608		119	125	-	0.0	
1160A	5	14	713		125	125	0.1	0.1	
1139B	6	13	732		115	120	1.3	0.9	
Standard Surrogate + H_2O_2 experiments, all blacklights									
1338B	7	53	197	127	94	132	0.0	0.0	
1340B	8	60	186	127	100	153	0.0	0.0	
1343B	8	50	257	127	113	173	0.0	0.0	
1348B	8	70	284	127	127	196	0.0	0.0	
1349B	7	66	269	127	122	171	0.0	0.0	
1344B	9	55	208	127	121	196	0.0	0.0	
1345B	7	55	222	125	105	143	0.0	0.0	
1346B	8	42	204	125	84	131	0.0	0.0	
1347B	8	64	216	125	91	142	0.0	0.0	
1342B	8	63	217	127	83	130	0.0	0.0	
Variable NO_x and VOC surrogate + H_2O_2 experiments, all blacklights									
1339A	8	59	448	127	209	266	0.0	0.0	Side equivalency
1339B	8	62	448	127	214	270	0.0	0.0	

Table 5. Summary of conditions and selected results of the incremental reactivity experiments. See Table 4 for base case conditions and results.

Run	Hours	Base Case NOx (ppb)	Base Case ROG (ppmC)	Base Case O_3 (ppb)	Test VOCs added: Test Compound or Mixture	Test VOCs added (ppb)	Change $\Delta([O_3]-[NO])$ (ppb)	Change PM (μg/m3)
Experiments with old blacklights only (lower light intensity)								
1088A	5	37	0.55	48	Texanol®	102	12	0.7
1140A	7	26	0.56	88	Texanol®	93	10	0.0
1145A	5	23	0.96	88	EMKO	102	-18	1.2
Experiments with NO_x = ~30 ppb, VOCs =~240 ppb, all blacklights (higher light intensity)								
1079B	6	31	0.25	74	n-Butane	249	27	0.0
1083B	6	32	0.20	74	n-Butane	199	22	0.0
1073A	7	31	0.24	67	n-Octane	163	-6	0.0
1081A	9	31	0.19	109	Texanol®	51	17	0.3
Variable NO_x and VOC experiments, all blacklights								
1128B	5	50	0.63	203	n-Octane	188	-32	0.0
1133A	5	54	0.70	187	EMKO	102	-56	0.0
1130A	3	52	0.69	156	EMKO	59	-82	0.0
1139A	6	15	0.73	120	EMKO	102	71	0.5
1152A	5	42	0.64	194	Methyl Decanoate	57	-39	8.5
1160B	4	15	0.71	116	Methyl Decanoate	44	-34	8.3
1167A	5	50	0.67	186	Methyl Linoleate	50	-3	0.7
1164A	5	47	0.70	194	Methyl Linoleate	11	3	0.4
Surrogate + H_2O_2 experiments, all blacklights								
1338A	7	55	0.20	132	n-Octane	118	91	0.0
1340A	8	59	0.18	153	m-Xylene	14	90	0.1
1343A	8	49	0.25	173	Texanol®	102	66	1.3
1348A	8	69	0.28	196	Texanol®	102	73	0.0
1349A	7	66	0.27	171	Texanol®	102	79	0.2
1344A	9	54	0.21	196	ASTM-1A Mixture	504	49	7.6
1345A	7	54	0.22	143	ASTM-1B Mixture	804	64	9.4
1346A	8	45	0.20	131	ASTM-1C Mixture	495	48	4.1
1347A	8	64	0.21	142	Aromatic-100	113	105	0.5
1342A	8	62	0.21	130	Aromatic-100	1199	133	3.1

underprediction bias cancels out to some extent when modeling effects of added test compounds for the purpose of evaluating their mechanisms by comparing experimental and calculated incremental reactivities, but this bias is still a concern.

As discussed above in the discussion of the chemical mechanism in the Modeling Methods section, we developed an “adjusted aromatics” version of the SAPRC-07 chemical mechanism in order to determine mechanism performance for test compounds studied for this project using an unbiased base case mechanism. The yields of the model species representing uncharacterized photoreactive aromatic fragmentation products were increased by a factor of 1.9 in order to reduce the average bias in the

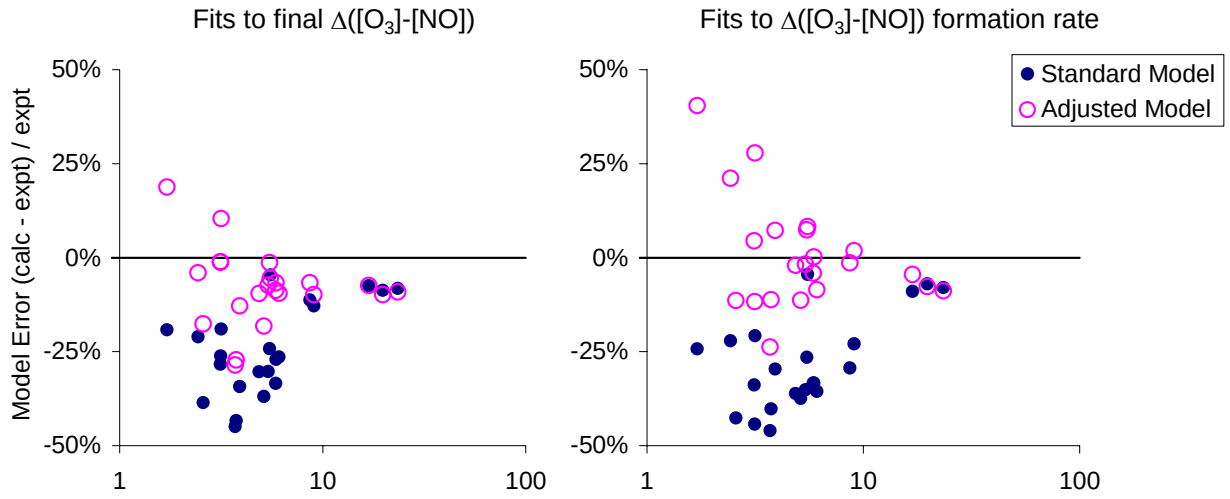

Figure 10. Plots of model errors for Δ([O3]-[NO]) formation and formation rates against NO_2 photolysis rate x surroage / NO_x ratios for the simulations of the surrogate - NO_x experiments using the standard and adjusted SAPRC-07 mechanisms.

simulations of $\Delta([O_3]-[NO])$ formation rates to zero. The performance of the adjusted mechanism in simulating these experiments is also shown on Figure 10. Although there is still run-to-run variability in the model performance, the adjustment significantly reduced the bias in the simulations of the final $\Delta([O_3]-[NO])$ yields as well as eliminating the average bias for the $\Delta([O_3]-[NO])$ formation rates.

A comparison of reactivity simulations using both the adjusted and unadjusted mechanism thus allows the effects of this potential source of bias to be assessed. For this reason, the model performance using both the adjusted and unadjusted mechanisms is shown in this report when presenting data to evaluate mechanisms of the test compounds.

Reactivity Results for Previously Studied Compounds with Varied Light Intensity

A number of incremental reactivity experiments with previously studied compounds were carried out for control purposes or to evaluate the use of reactivity experiments at higher light intensity, different base case ROG and NO_x conditions, and in a few cases longer run duration. These experiments, which utilized n-butane, n-octane, and Texanol® as the test compound, are summarized on Table 5, and reactivity data related to O_3 formation and NO oxidation are shown on Figure 11 and Figure 12. Results of model calculations using the standard and adjusted aromatics SAPRC-07 mechanism are also shown on these figures. Figure 11 also shows the results of the side equivalency experiments, and shows that good side equivalency was obtained.

The results of these experiments were generally similar to those obtained previously for these compounds, and reasonably consistent with model predictions. The only possible exception is the added Texanol® experiment EPA1088 (Figure 12), which was an attempt to replicate pervious Texanol® experiments carried out with the lower light intensity (Carter and Malkina, 2005). In the previous experiments the addition of Texanol® had no measurable effects on O_3 formation and NO oxidation, despite measurably suppressing integrated OH levels as indicated by the m-xylene data (Carter and Malkina, 2005). In this experiment, the addition of Texanol® had a measurable tendency to increase NO

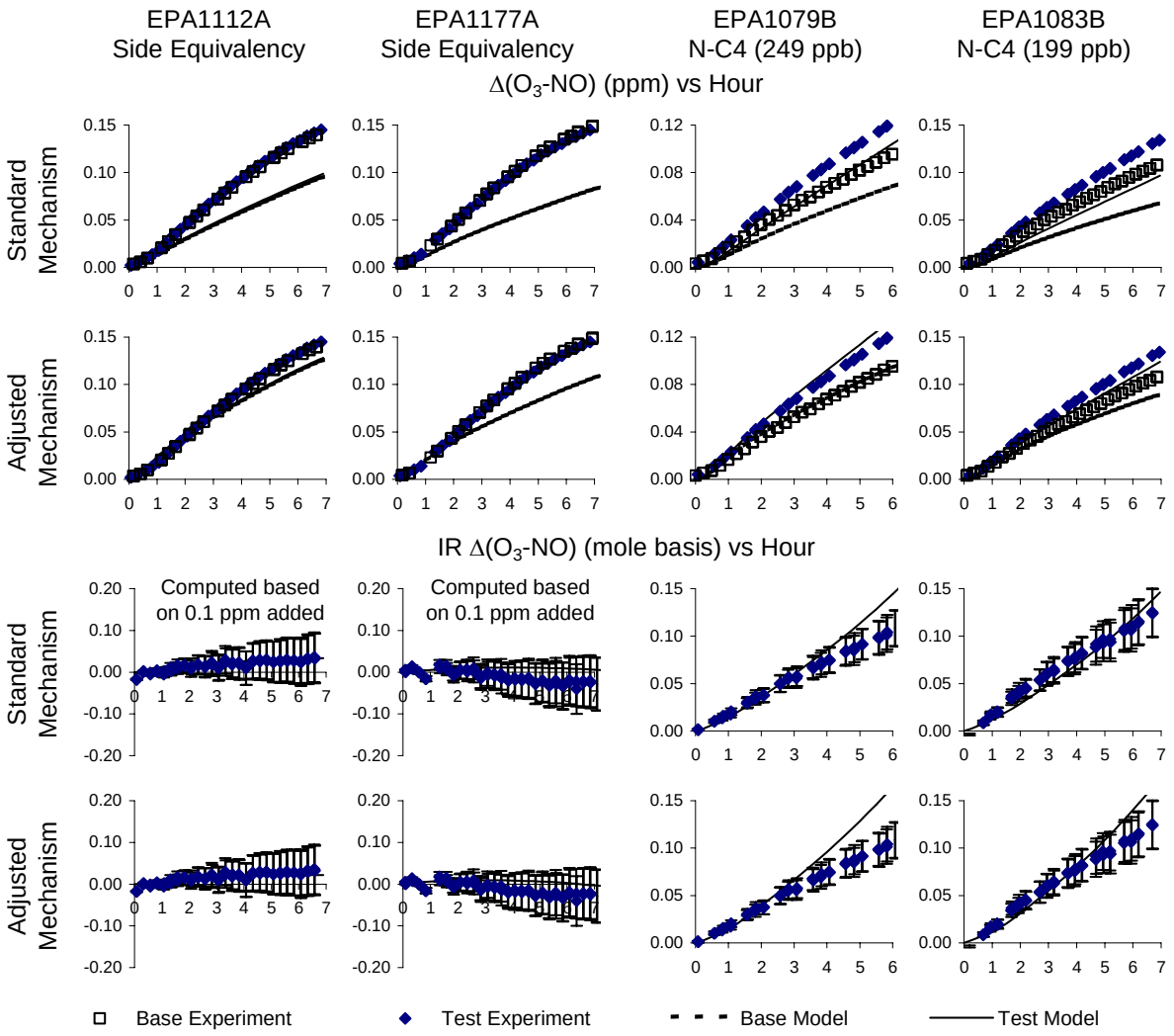

Figure 11. Plots of experimental and calculated $\Delta([O_3]-[NO])$ data for the surrogate - NO_x side equivalency tests and incremental reactivity experiments with n-butane.

oxidation and O_3 formation, more than predicted by the model, though the discrepancy was relatively small. The discrepancy was somewhat less in the subsequent added Texanol® experiment with the lower light intensity (EPA1140, also on Figure 12), where the results were somewhat more consistent with model predictions.

The experiments with added n-butane (Figure 11) and n-octane (Figure 12) carried out with the higher light intensity were qualitatively similar to experiments with the lower light intensity, with the chamber reactivity of n-butane being positive and the reactivity of n-octane being negative in all cases, as observed previously. There is an indication of the chamber reactivity of n-octane becoming less negative and approaching zero with longer irradiation times in run EPA1073 (Figure 12), which was the only experiment with that compound where the reaction time exceeded 6 hours. This is consistent with what would be expected based on the results of our modeling assessment of chamber vs. atmospheric

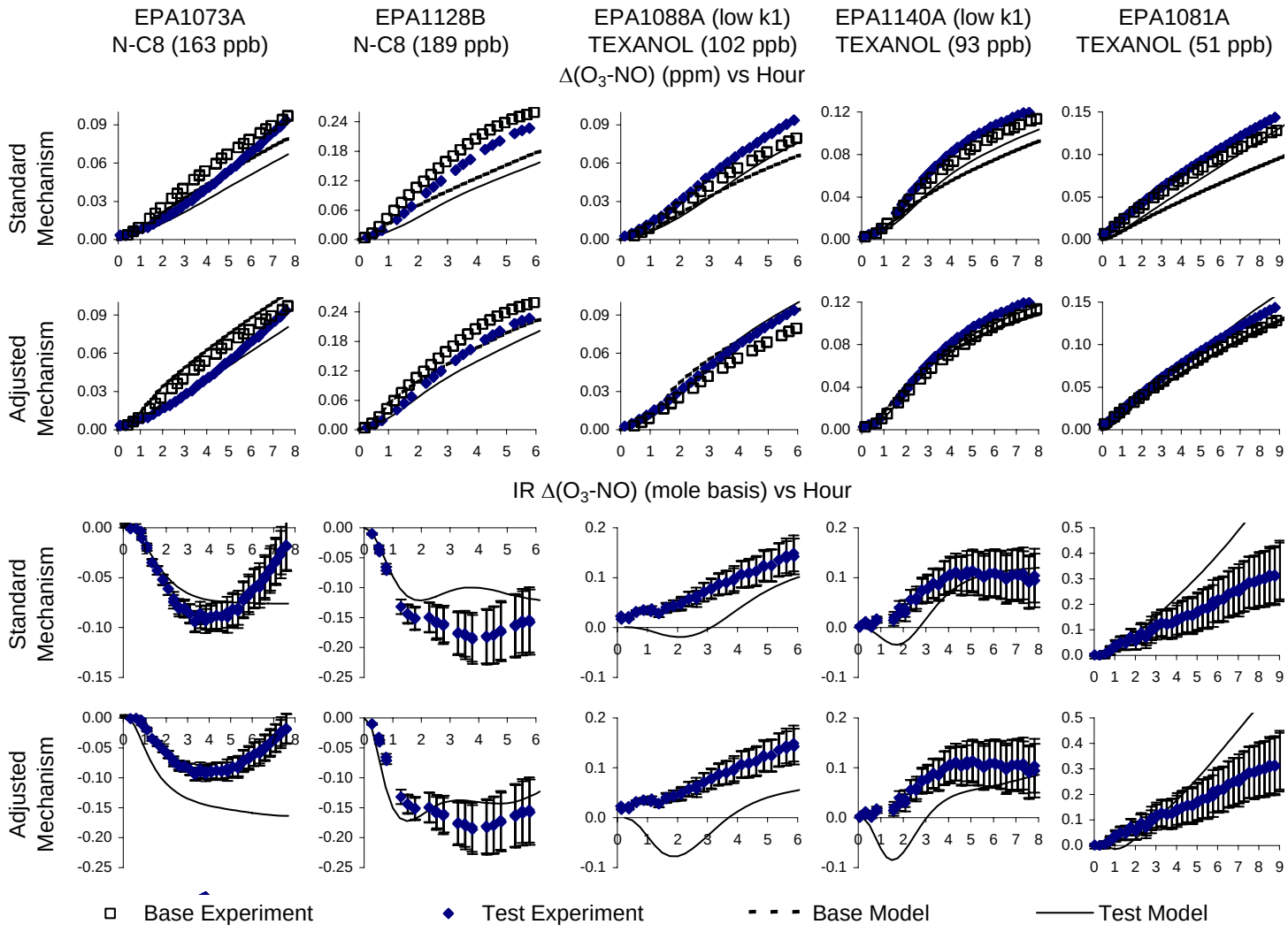

Figure 12. Plots of experimental and calculated $\Delta([O_3]-[NO])$ data for the surrogate - NO_x incremental reactivity with n-octane and Texanol®.

reactivities, discussed above, though the decrease in negative reactivity around the end of the experiment was not well simulated by either mechanism.

In the case of Texanol®, the incremental reactivity measured in the single experiment with the higher light intensity (EPA1081, shown on Figure 12) was about three times greater than observed in the experiments with the lower light intensity. The effects on the $\Delta([O_3]-[NO])$ data did not look any different in that experiment because the amount of Texanol® added was half that used in the other experiments, but the effect relative to the amount added was larger. This is also consistent with our expectations based on the results of our assessment of chamber vs. atmospheric reactivities

More experiments with the higher light intensity and longer run duration would have been useful to more completely assess our predictions that the incremental reactivities of compounds like n-octane and Texanol® would become more like those under atmospheric conditions, or at least less negative, under those conditions. However, it was not possible to assess this more completely because of problems with conducting experiments with longer run times, as discussed above. For this reason, most of our experimental evaluation of alternative reactivity measurement methods focused on the predictions that adding H_2O_2 to the surrogate - NO_x experiment would also give results that corresponded better to reactivities in the atmosphere. The results of our experimental evaluation of these types of experiments are discussed later in this report. First, however, we will discuss the experimental reactivity results for EMKO and the soy ester constituents, since these employed similar types of experiments as those discussed above.

Reactivity Results for EMKO

Because of cost overruns and our inability to obtain useful data to assess reactivities of soy esters (discussed below), ethyl methyl ketone oxime (EMKO) was the only new compound whose mechanism was developed and successfully evaluated as part of this study. A total of four successful incremental reactivity experiments with EMKO were carried out, one (EPA1145) with the lower light intensity under relatively NO_x - limited conditions, two (EPA1130 and EPA1133) representing MIR conditions, and one (EPA1139) representing more NO_x - limited conditions. The conditions and results of these experiments are summarized on Table 5, and concentration-time plots of selected results are shown on Figure 13.

The results clearly indicate that EMKO inhibits NO oxidation and O_3 formation in under VOC limited conditions, and also significantly decreases radical levels. This suggests that EMKO has strong radical sinks in its mechanism. On the other hand, the results also indicate that the addition of EMKO can actually increase O_3 yields under sufficiently NO_x - limited conditions. This is suggested in the results of EPA1145 where the O_3 in the added EMKO reactor approaches that of the base case reactor by the end of the experiment, and is clearly indicated in run EPA1139, where the final O_3 in the added EMKO reactor is significantly higher than on the base case side.

These results suggest a mechanism that both inhibits radicals and releases NO_x during the EMKO oxidation. For this reason, it is assumed that the major pathway when OH either abstracts from the NOH group or adds to the C=N double bond, is radical termination and NO_x producing, as discussed in the Modeling Methods section above. If this is assumed, the mechanism gives reasonably good fits to the incremental reactivity results, as shown on Figure 13a for the standard mechanism, Figure 13b for the adjusted aromatics mechanism, and Figure 13c for the simulations of integrated OH levels for both mechanisms. The magnitudes of the incremental reactivities are somewhat overpredicted in some experiments and somewhat underpredicted in others, but overall the reactivity results are simulated reasonably well without systematic biases. The reasonably good fits to the initial rates of NO oxidation

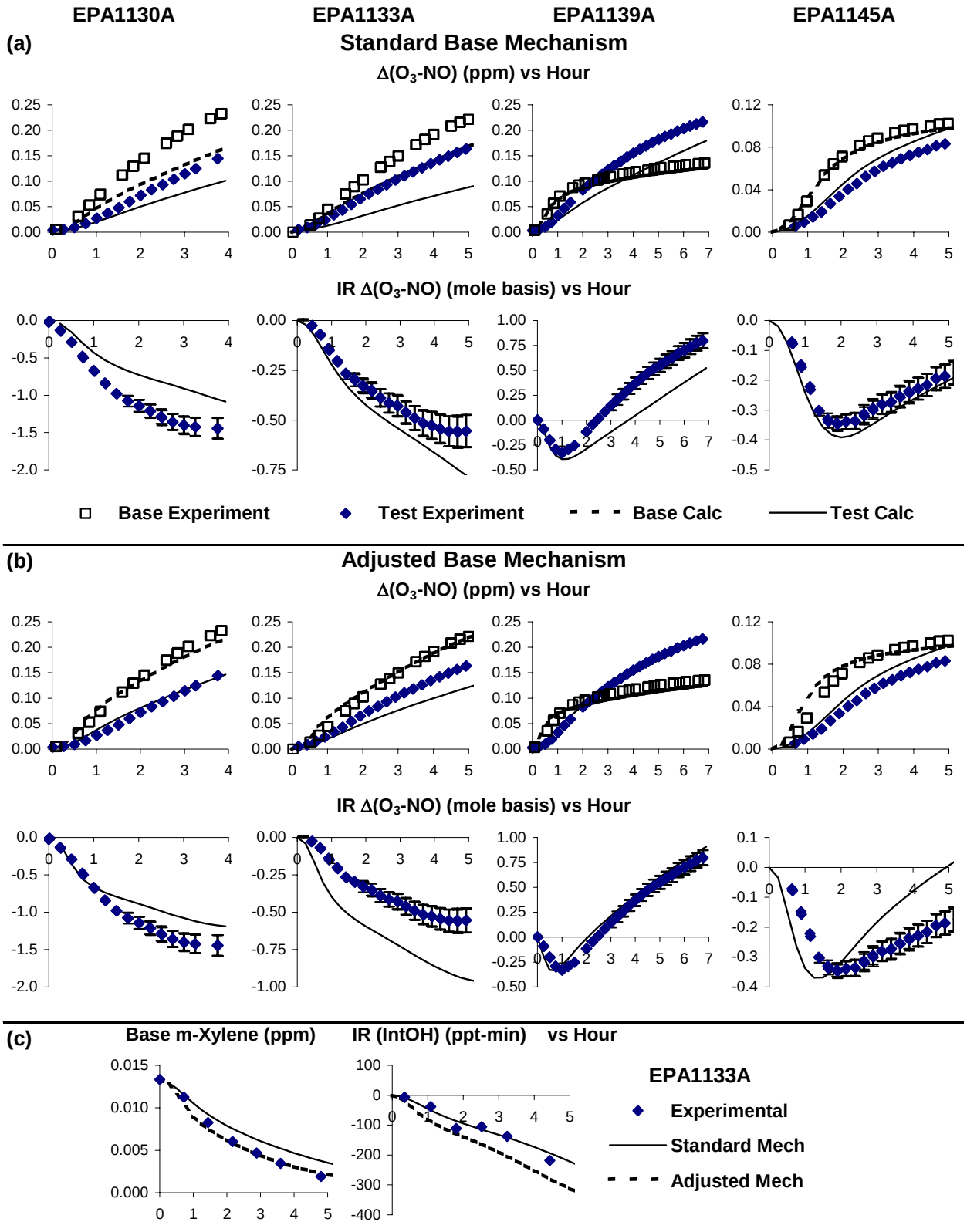

Figure 13. Plots of experimental and calculated Δ([O_3]-[NO]), m-xylene, and IntOH reactivity data for the surrogate - NO_x + EMKO reactivity experiments.

and O_3 formation and to the integrated OH yields in the experiment (EPA1133) with such data[2] suggesting that the mechanism is appropriately representing the extent of radical termination in the EMKO reactions. The ability of the adjusted mechanism to very closely simulate the enhancement of O_3 in the very NO_x - limited experiments also suggests that the model is probably predicting NO_x yields from these reactions reasonably well. Note that the estimated mechanism has very high (76%) radical terminating and NO_x formation yields.

Figure 13 shows that very similar incremental reactivity simulations are obtained with the adjusted aromatics mechanism as obtained with the standard mechanism, despite the significantly better fits to the base case experiments simulating MIR conditions. However, there are differences, with incremental reactivities in two of the experiments (one MIR and one more NO_x - limited) being fit somewhat better with the standard mechanism, and the other two being fit better with the adjusted mechanism. Probably the fits using the adjusted mechanism should be given greater weight because of the lack of bias in simulating the base case experiments. However, it is interesting that although both mechanisms fit the base cases for the more NO_x - limited experiments EPA1139 and EPA1145 reasonably well, the simulations of the incremental reactivity results are different. But in any case simulations with either mechanism do not indicate strong biases in the EMKO mechanism overall, and no adjustments to the mechanism could be found that gave better results.

Except for the choice of the MEK + NO_2 formation mechanism as the major route following reaction at the C=NOH group, the fits shown on Figure 13 were obtained without any other adjustments to the EMKO mechanism. In particular, the estimate of the rate constant for the reaction of OH at the C=NOH group is very uncertain and the overall rate constant could not be measured, so adjustments of this rate constant would not be inappropriate if necessary. However, when effects of varying this rate constant were assessed, it was found that the best fits were obtained with a rate constant reasonably close to the estimated value, so the estimated rate constant was used without change in the final mechanism.

Because it gave reasonably good simulations of the chamber data obtained in this project, the mechanism developed for EMKO was considered suitable for assessments of its atmospheric reactivity. Therefore, this compound was added to the list of compounds for which atmospheric reactivities can be estimated, and reactivity values were calculated for the MIR, MOIR, EBIR and the base case incremental reactivity scales, and the results are summarized on Table 6. Incremental reactivities of the ambient mixture used to represent VOC emissions from all sources in the reactivity calculations (the base ROG mixture) and of NO_x are shown on the table for comparison. The calculation methods employed were the same as used to calculate the reactivities of other compounds in these scales, and are summarized in the Modeling Methods section above and in more detail by Carter (2010a).

EMKO is unusual in that its incremental reactivity is calculated to be negative under MIR conditions but becomes positive and increases as conditions become more NO_x - limited. This is indicated on Table 6 and is shown even more clearly on Figure 14a, which plots the incremental reactivities of EMKO, the base ROG mixture, and NO_2 against the ROG/NO_x ratio in the averaged conditions scenario. Figure 14b also shows incremental reactivities EMKO and NO_x, but with the NO_x reactivities scaled to give the same incremental reactivities under MIR conditions to give a clearer comparison of differences in incremental reactivities under lower NO_x conditions. For further comparisons, Figure 14b also includes scaled reactivities for benzaldehyde and hexamethyldisiloxane, which are representative of other types of compounds calculated to have negative MIR values. Benzaldehyde is chosen as a representative of compounds that have negative reactivities because they have both radical and NO_x sinks, and

[2] Because of GC problems, the other experiments did not have sufficiently high quality m-xylene data to reliably estimate integrated OH levels.

Table 6. Summary of atmospheric incremental reactivities calculated for EMKO, the base ROG mixture representing VOC emissions from all sources, and NO_x in the various SAPRC-07 reactivity scales.

Compound or Mixture	Incremental reactivity (gm O_3 / gm compound) MIR	MOIR	EBIR	Base
EMKO	-1.27	0.42	1.14	0.7 ± 0.7
Base ROG Mixture	3.60	1.44	0.81	1.2 ± 0.5
NO	-8.41	-0.578	3.02	1.0 ± 2.9
NO_2	-4.35	0.207	2.42	1.2 ± 1.8

hexamethyldisiloxane is chosen because the parameterized representation used for this compound has only radical sinks (Carter et al, 1992; Carter, 2010a)[3].

The results indicate that the reactivity characteristics of EMKO are more like NO_x than a typical VOC. For most VOCs, the highest reactivity occurs under relatively high NO_x MIR conditions (which is why those conditions are referred to as "maximum incremental reactivity") and decreases and in some cases become negative as NO_x is reduced. On the other hand, the reactivity of NO_x is strongly negative under MIR conditions, is zero under MOIR conditions (by definition)[4], and becomes significantly positive as NO_x is reduced further. EMKO shows the same behavior, as indicated on Figure 14. This behavior is different than for benzaldehyde and most other compounds with negative reactivities, which have NO_x sinks rather than NO_x sources in their mechanisms, and consequently have negative reactivities under all conditions. The radical sinks cause the reactivities to be negative when NO_x is high, and the NO_x sinks cause them to be negative when NO_x is limited.

The only compounds currently represented in the SAPRC-07 chemical mechanism that are predicted to have similar reactivity characteristics as EMKO are the volatile siloxanes such as hexamethyldisiloxane that are represented by parameterized mechanisms that only have radical sinks. The true mechanisms for these compounds may well have NO_x sinks, but there were no NO_x - limited reactivity experiments to evaluate this for these compounds and rule out the parameterized mechanism that was originally developed (Carter et al, 1992; Carter, 2010a). In any case, the current representation of hexamethyldisiloxane is useful to indicate reactivity characteristics of compounds with only radical sinks and no direct effects on NO_x sources or sinks. Note that as NO_x approaches zero the reactivities of hexamethyldisiloxane, like most other VOCs, will approach zero, since NO_x is required for ozone formation. On the other hand, the reactivities of EMKO, like NO_x, will continue to increase as NO_x is reduced. This is consistent with the trends in the reactivities at NO_x levels lower than EBIR as shown on Figure 14.

[3] The reactions of hexamethyldisiloxane are represented by the highly simplified parameterized mechanism OH + SIOME6 → 0.68 {xHO2 + RO2C + yR6OOH}, which was derived based on simulations of chamber experiments representing MIR conditions.

[4] MOIR conditions are defined as NO_x levels that yield the highest O_3 concentration when all other conditions are held the same. By the principles of mathematics the partial derivative of O_3 with respect to NO_x, or the incremental reactivity, is necessarily zero under those conditions.

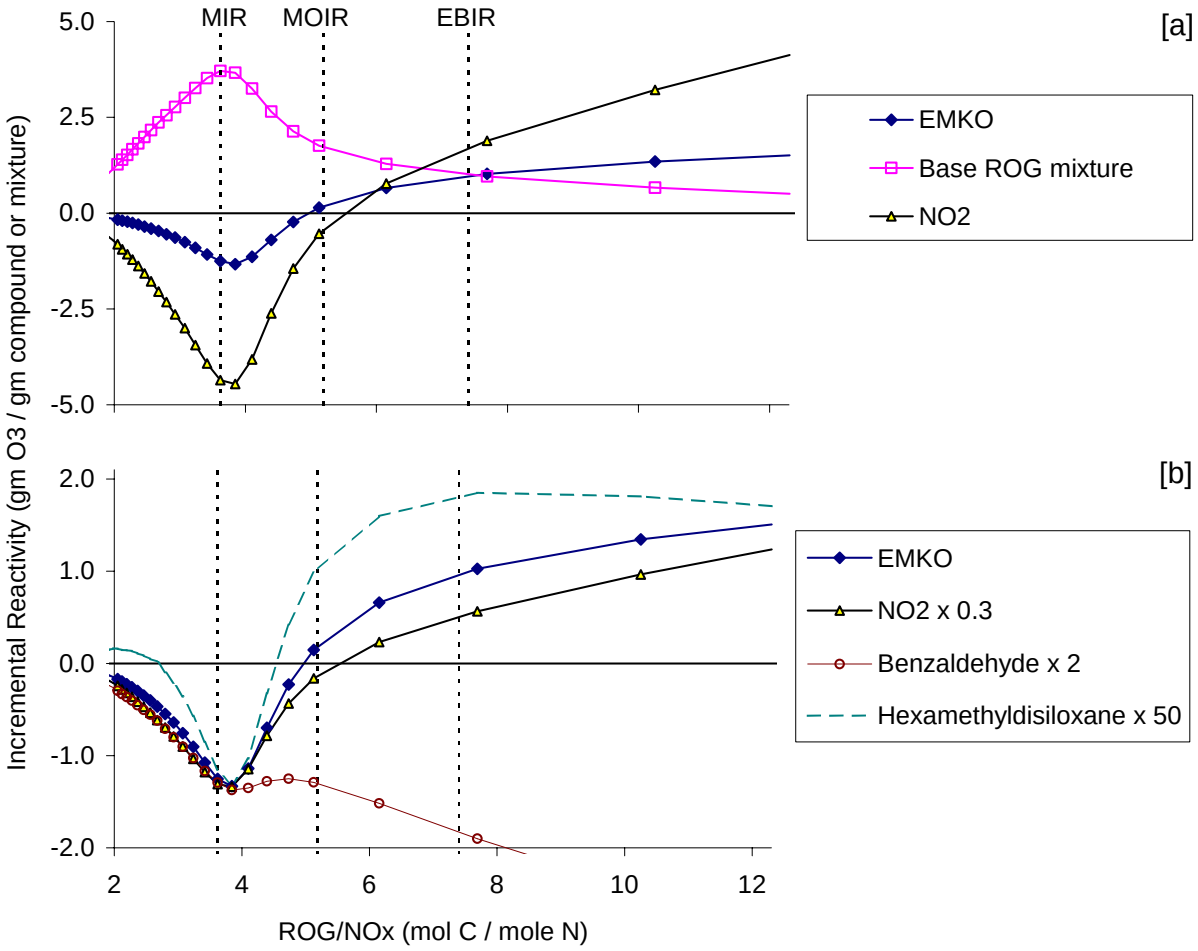

Figure 14. Plots of incremental reactivities of EMKO and other representative compounds and mixtures against the ROG/NO_x ratio for the averaged conditions scenarios.

Reactivity Results for Representative Soy Ester Constituents

The CARB staff requested that we include in this project experiments to reduce uncertainties in atmospheric reactivity estimates of soy ester mixtures that are used in some coatings formulations. Soy ester solvents are mixtures of methyl esters of various C_{17+} fatty esters, and only limited data are available concerning their compositions. An analysis of the available composition data of soy ester solvents was beyond the scope of this project, but the CARB staff provided an estimated composition (CARB, 2009) that was used as a basis for our current reactivity estimates for these solvents (Carter, 2010a,b). This composition is given on Table 7, which also gives the structures of the compounds, their estimated vapor pressures, and the current MIR estimates for these compounds. Footnote [b] to the table indicates how the MIR estimates were derived. These data give an MIR value of 1.58 grams O_3 per gram VOC that is used for soy ester mixtures in the current MIR tabulation (Carter, 2010a,b). Note that these MIR estimates are based entirely on estimated mechanisms that have not been evaluated using any experimental data.

As shown on Table 7, the vapor pressures for these constituents are very low, especially for the major constituents methyl linoleate and methyl oleate. In particular, with the possible exception of methyl

Table 7. Representative composition of soy methyl ester solvents, as estimated by CARB staff (CARB, 2009).

Wt. %	Name	Structure	VP [a] (ppb)	MIR [b]
10%	methyl hexadecanoate (methyl palmitate)	$CH_3(CH_2)_{13}C(O)OCH_3$	62	0.44
5%	methyl octadecanoate (methyl stearate)	$CH_3(CH_2)_{15}C(O)OCH_3$	18	0.40
5%	methyl linolenate (methyl cis,cis,cis-9,12,15-octadecatrienoate)	$CH_3CH_2CH=CHCH_2CH=CHCH_2CH=CH-(CH_2)_7C(O)OCH_3$	7	2.32
55%	methyl linoleate (methyl cis,cis-9,12-octadecadienoate)	$CH_3(CH_2)_4CH=CHCH_2CH=CH(CH_2)_7C(O)-OCH_3$	5	1.84
25%	methyl cis-9-octadecenoate (methyl oleate)	$CH_3(CH_2)_7CH=CH(CH_2)_7C(O)OCH_3$	8	1.54

[a] Vapor pressure at 298^{o}K estimated using the SRC PhysProp Database at the web site http://www.syrres.com/what-we-do/databaseforms.aspx?id=386.

[b] Atmospheric maximum incremental reactivity in units of grams O_3 per gram VOC calculated using the SAPRC-07 mechanism (Carter, 2010a) as provided to the CARB for regulatory applications and used for the current MIR estimate for soy ester constituents, based on the composition given in the first column of this table. Methyl linolenate and methyl linoleate are represented explicitly, methyl palmitate and methyl stearate are represented by assuming the same per-molecule reactivity as methyl pentadecanoate, and methyl oleate is represented by assuming the same per-molecule reactivity as methyl cis-9-pentadecenoate. The mechanisms used for the explicitly represented compounds and the compounds used to represent the mechanisms of the other compounds were derived using the SAPRC-07 mechanism estimation system (Carter, 2010a), with all rate constants and mechanistic parameters estimated.

hexadecanoate, it is probably not feasible to quantitatively inject these compounds into the gas phase at levels necessary to conduct incremental reactivity experiments. Therefore, the preferred approach would be to conduct experiments with lower molecular weight analogues with higher vapor pressures that have similar structures and therefore similar mechanisms. This would permit at least an evaluation of whether the SAPRC mechanism estimation system used to derive the mechanisms used to calculate the current MIR scale performs satisfactorily for chemically similar compounds.

Methyl decanoate, or $CH_3(CH_2)_8C(O)OCH_3$, was chosen as a lower molecular weight analogue for the saturated fatty ester constituents methyl hexadecanoate and methyl octadecanoate, and two incremental reactivity experiments with this compound were carried out (see Table 5). Unfortunately, we were unable to find commercial samples of lower molecular weight analogues for the unsaturated fatty esters constituents in the quantities needed for environmental chamber experiments; the only available option was methyl linoleate itself. This is unfortunate because the estimated mechanisms for the unsaturated constituents are much more uncertain than for the saturated constituents, and they have the largest contributions to the overall reactivity of the mixture (see Table 7).

The possibility of conducting reactivity experiments with commercial soy ester mixtures was also considered, and we were provided samples of such materials from Soy Technologies, LLC for potential study. Unfortunately, we were not provided quantitative composition information about these samples, so their utility for mechanism evaluation purposes is questionable even if quantitative experiments were feasible. Because methyl linoleate is expected to be a major constituent of these samples (see Table 7), it was decided that if experiments with such low volatility materials are feasible at all, it would be best to study methyl linoleate first, since at least the results have potential utility for evaluating our ability to estimate mechanisms for all the unsaturated constituents of the soy ester mixtures. If experiments with methyl linoleate are successful, we can consider whether it is worth requesting the industry sources to conduct the quantitative analyses of the solvents needed for experiments with them to be useful. Therefore, as indicated on Table 5, two experiments with methyl linoleate were attempted as part of this project.

Selected results of the experiments with methyl decanoate and methyl linoleate are summarized on Table 5 and shown on Figure 15. Results of model simulations using the estimated mechanisms for these compounds are also shown on Figure 15. The figure only shows calculations using the adjusted mechanism, since incremental reactivity results using the standard mechanism are similar, as indicated in Figure 11 through Figure 13, above, for other compounds.

It can be seen that the experiments with methyl linoleate were not successful, as indicated by the base case and the added methyl linoleate experiments had essentially the same result, at least for gas-phase species (see Table 5 and Figure 15). The only observed effect of the methyl linoleate addition was a much earlier onset of particle formation and a slight increase in measured particle levels, but the change in particle levels was relatively small considering the size of the molecule. If injected into the gas phase, the compound is expected to react rapidly and have measurable effects at least on integrated radical levels if not O_3 formation and NO oxidation, but no such effects were seen within the uncertainty of the measurement. Such a high molecular weight compounds would be expected to have relatively strong effects in reducing integrated OH levels because of radical termination caused by organic nitrate formation, and if radical termination were, for some reason, much less than expected then one would expect measurable enhancements of ozone formation and NO oxidation resulting from the photooxidation reactions.

The experiments with methyl decanoate were more successful, showing measurable effects on NO oxidation, O_3 formation and radical levels (see Figure 15). The effects were qualitatively similar to model predictions, though the model consistently underestimated the effects of the methyl decanoate addition on $\Delta([O_3]-[NO])$ and integrated OH levels. The calculations shown on Figure 15 used initial methyl decanoate levels derived from the calculated amount of compound injection, which is based on assuming that the methyl decanoate was efficiently injected into the gas phase. The GC measurements made during the experiment indicated that the gas-phase methyl decanoate concentration was about half that, and using GC-derived initial concentrations to derive the initial methyl decanoate concentration for modeling made the underprediction discrepancy worse.

The relatively poor model performance in simulating the methyl decanoate experiments suggests either experimental problems or (more likely considering the nature of the bias) problems with the estimated methyl decanoate mechanism. Investigating this further would require reactivity experiments with additional saturated fatty ester compounds, including especially compounds with lower molecular weights where experimental and analytical difficulties would be reduced. However, the saturated fatty esters are relatively minor constituents of the soy esters (accounting for only 15% of the mixture in terms of mass fraction and accounting for only 4% of the reactivity according to Table 7), so the additional experiments would be a relatively low priority for this project. Therefore, the additional experiments

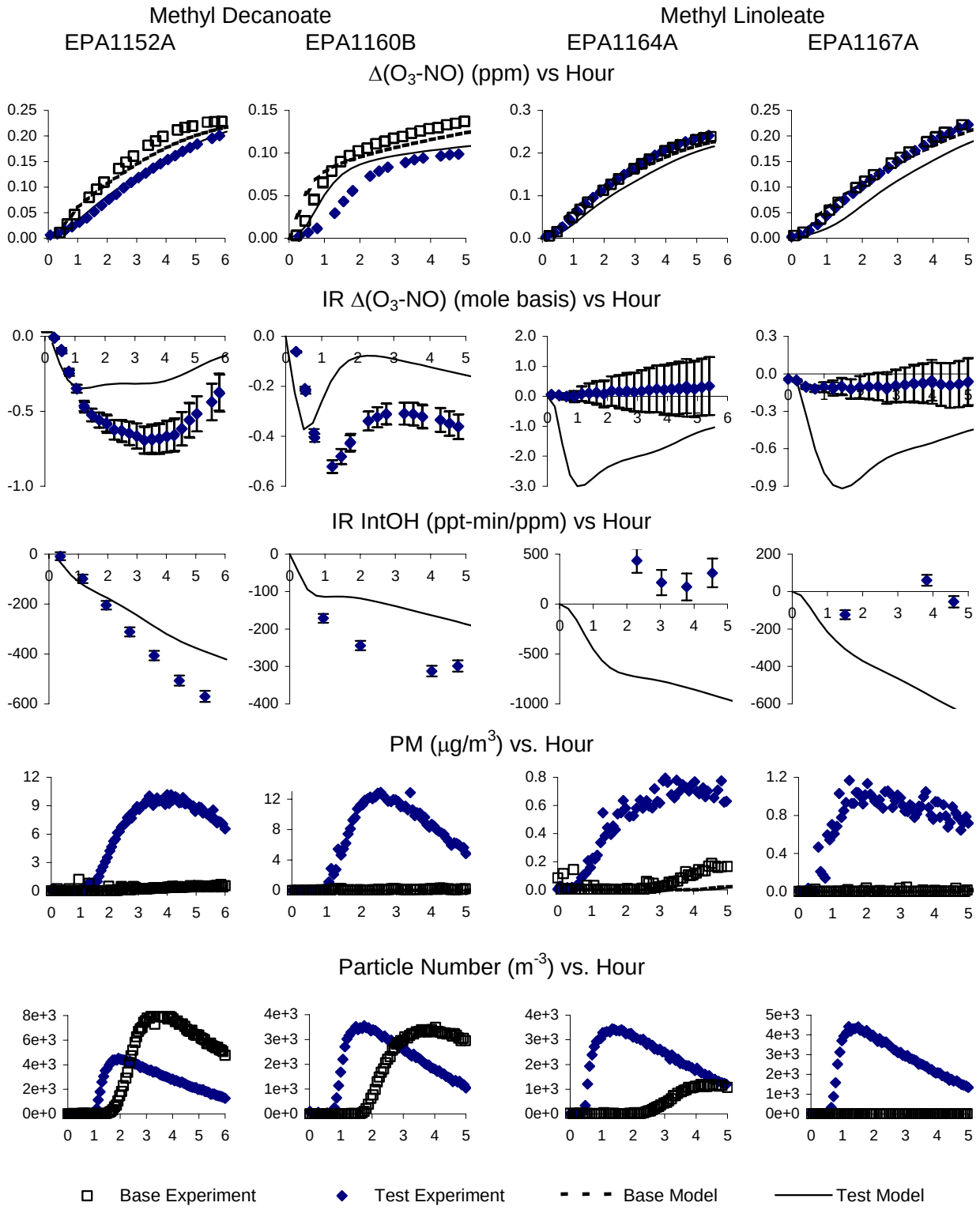

Figure 15. Plots of experimental and calculated results for the surrogate - NO_x + methyl decanoate and methyl linoleate reactivity experiments. Calculations of gas-phase species used the adjusted aromatics mechanism.

required to assess this apparent discrepancy, and to serve as a basis for modifying the mechanism estimates for saturated fatty esters, were not carried out.

Table 5 and Figure 15 also show that the addition of methyl decanoate causes a significant increase in particle formation. This is presumably due to secondary organic aerosol (SOA) formation caused by the formation of low volatility oxidation products. Model simulations of the observed SOA are not shown because the current SAPRC-07 mechanism does not have this capability, though work is underway to develop updated versions of SAPRC that have this capability. One would expect even higher SOA yields from the reactions of the saturated soy ester constituents, since they all have significantly higher molecular weights than methyl decanoate, and they would form even lower volatility products.

Results of Added H_2O_2 Surrogate Reactivity Experiments

The results of the modeling assessment of chamber vs. atmospheric reactivities, discussed above, indicated that adding H_2O_2 to base case surrogate - NO_x incremental reactivity experiments could result in significant improvements of correlations between experimental and atmospheric incremental reactivities, at least for the alkane-like compounds that are important in most coatings solvents. Therefore, experimental tests with several representative compounds with known mechanisms and coatings constituents were carried out for this project. The conditions and the selected results are summarized on Table 4 for the base case experiments and on Table 5 for the experiments with the added test compounds, and concentration time plots of $\Delta([O_3]-[NO])$ and $\Delta([O_3]-[NO])$ reactivities are shown on Figure 16 and Figure 17. Figure 16 also shows the results of the surrogate - NO_x + H_2O_2 side equivalency test that was carried out, where good side equivalency was seen.

Results of model calculations with the standard and adjusted aromatics mechanisms are also shown on Figure 16 and Figure 17. The differences between the standard and adjusted mechanisms in the simulations of the base case experiments were much less than observed in the experiments without added H_2O_2. This is expected since the presence of the added radical initiator should decrease the sensitivity of the experiment to other radical sources such as the photolysis of the photoreactive aromatic oxidation products whose yields were increased in the adjusted mechanism. The calculated incremental reactivities were also about the same with the two mechanisms, except for the experiment with m-xylene where the mechanism for the test compound was adjusted. Note that the aromatic mechanism adjustments do not significantly affect the calculations for Aromatic-100 because only the toluene and m-xylene mechanisms were adjusted, and the composition of the mixture used for modeling Aromatic-100 had no toluene and negligible amounts of m-xylene (Carter, 2010a).

The incremental reactivities measured in these experiments were reasonably consistent with model predictions in most cases, though there was a tendency for the model to underestimate the measured incremental reactivities in some cases. The greatest underprediction appear to be for Aromatic-100 (excluding the experiment with the excessive amount added, where the model fit was good) and the ASTM-1A primarily alkane mixture that had the highest aromatic content (see Table 2). This may be due to problems with the aromatics mechanism, as indicated by the fact that the incremental reactivities of m-xylene predicted using the adjusted mechanism fit the data reasonably well. However, there are insufficient data in this limited number of exploratory experiments to serve as a basis for modifications to the standard aromatics mechanism at this point.

Figure 18 shows plots of the atmospheric MIR values calculated for the test compounds against experimentally measured reactivities in these surrogate - NO_x - H_2O_2 incremental reactivity experiments. (The results for EPA1342 are excluded because the amount of Aromatic-100 added is far in excess of an appropriate value for an incremental reactivity measurement.) The chamber reactivities have been converted to mass units to be comparable to the units used for atmospheric MIR. It can be seen that the

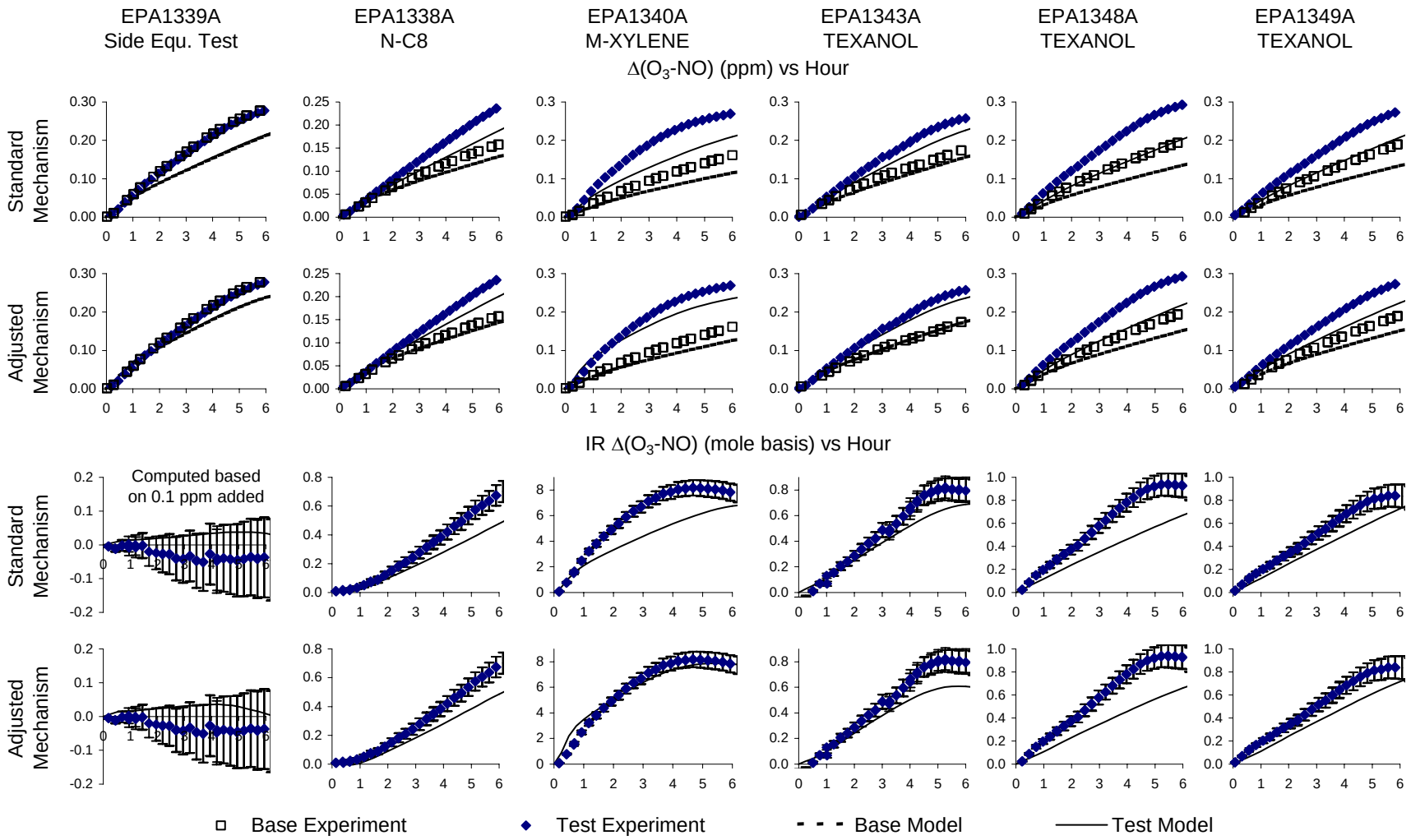

Figure 16. Plots of experimental and calculated Δ([O_3]-[NO]) data for the surrogate - NO_x - H_2O_2 reactivity experiments with n-octane, m-xylene, and Texanol®

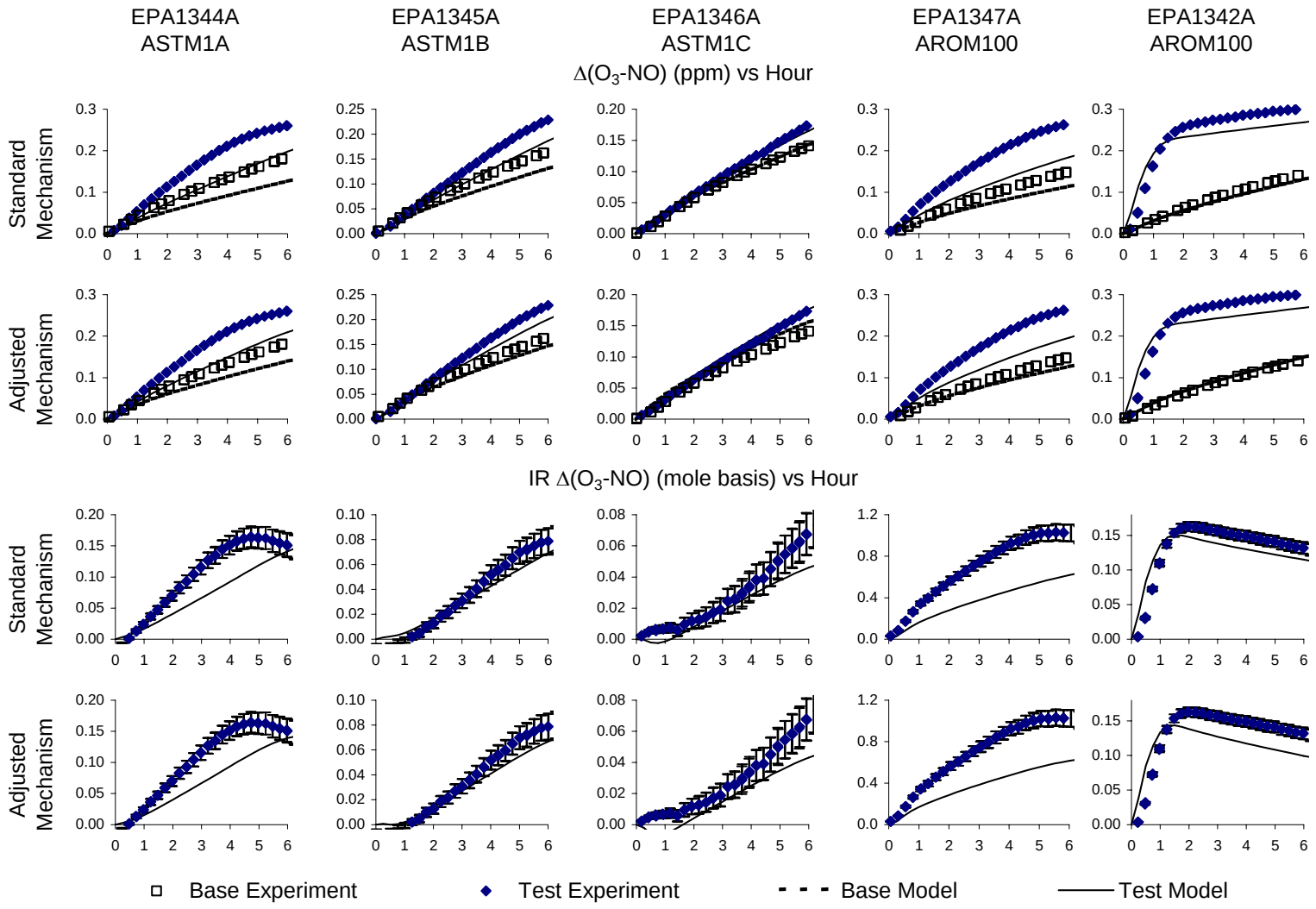

Figure 17. Plots of experimental and calculated $\Delta([O_3]-[NO])$ data for the surrogate - NO_x - H_2O_2 reactivity experiments with ASTM 1A, 1B, 1C, and Aromatic-100

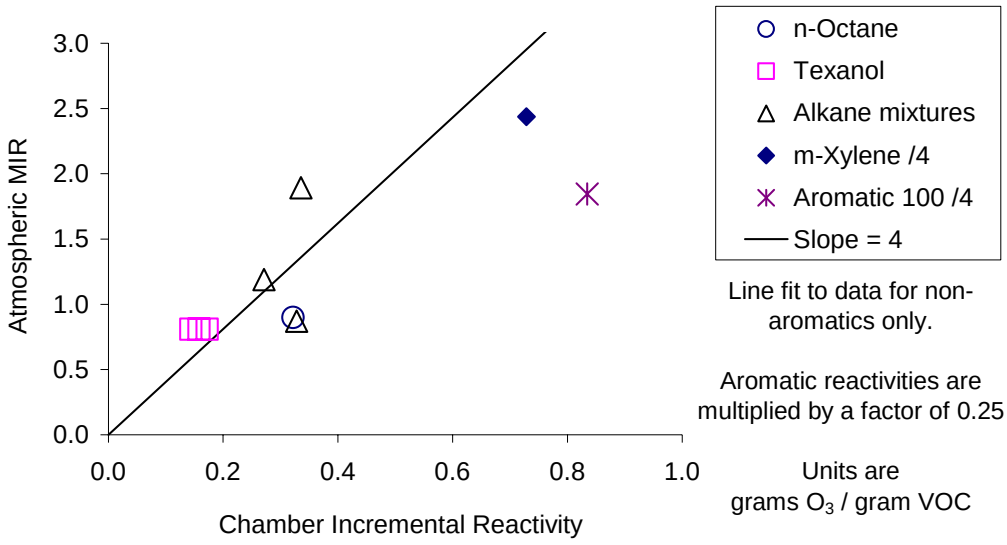

Figure 18. Plots of atmospheric MIR values against experimental reactivities of the compounds studied in the surrogate - NO_x - H_2O_2 environmental chamber experiments carried out for this project.

correlations between experimental reactivities and calculated atmospheric MIR values are reasonably good (with a correlation coefficient of 82% for the non-aromatic compounds or mixtures), consistent with the predictions of our modeling study of chamber vs. atmospheric reactivities. The modeling study also predicted that the points for aromatic compounds would fall below the regression line defined by the alkanes and alkane-like mixtures or compounds (see Figure 6c), and the results of these experiments were also consistent with this prediction. In any case, these experiments gave far better correlations with atmospheric reactivities than the previous "MIR" reactivity experiments, which gave negative reactivities for the higher alkanes and alkane mixtures, and essentially zero reactivities for Texanol®.

Effects of VOCs on Secondary Organic Aerosol Formation

Although the major objectives of this project focused on the effects of coatings VOCs on ozone formation, data were also obtained during the reactivity experiments on the effects of the studied compounds on secondary organic aerosol (SOA) formation. Measurements were made of total particle matter (PM) number and volume during most chamber experiments using the Scanning Mobility Particle Spectrometer (SMPS) described on Table 1, and five-hour and final PM volume levels measured in the base case surrogate - NO_x experiments are given in Table 4, and changes in final PM levels caused by the addition of the test compounds in the reactivity experiments are given in Table 5, above. These results can be combined with results of previous reactivity experiments in our laboratory where PM measurements were made (Carter et al., 2005c, 2010; Carter and Malkina, 2007; Carter, 2008) to enhance our database of effects of various coatings and solvent VOCs on SOA formation.

A summary of the averages of the incremental effects of the addition of the various coatings or solvent VOCs that have been studied are given on Table 8, and these data are compared graphically on Figure 19. The incremental SOA reactivities are derived from the change in PM mass after 5 hours of irradiation caused by the addition of the test compound, divided by the mass of test compound added. The

Table 8. Summary of averages of 5-hour SOA formation reactivities for various coatings and solvent VOCs measured in the UCR EPA chamber.

Compound or Mixture	5-hour Incremental SOA Reactivity (mass basis, uncorrected for wall losses) [a]				Ref. [b]
	Surrogate - NO_x		Surrogate - H_2O_2 - NO_x		
	Runs		Runs		
	No.	Average	No.	Average	
d-Limonene	3	21.9 ± 4.0%			2
m-Xylene			1	0.1%	1
Ethylene Glycol	4	-0.2 ± 0.1%			3
Propylene Glycol	4	0.0 ± 0.1%			3
2-Butoxyethanol	2	3.4 ± 1.9%			3
3 methoxy-3 methyl-1-butanol	5	0.0 ± 0.0%			5
Benzyl alcohol	2	8.9 ± 0.1%			3
2-(2-butoxyethoxy)-ethanol	2	2.5 ± 1.4%			3
Methyl Decanoate	2	1.7 ± 0.4%			1
Texanol®	6	0.0 ± 0.1%	3	0.0 ± 0.0%	1,3
CS2	3	0.6 ± 0.0%			4
Ethanolamine	4	22.8 ± 9.7%			2
MITC	4	1.1 ± 0.4%			4
EMKO	3	0.0 ± 0.0%			1
AMP	5	8.3 ± 3.4%			2
EPTC	4	1.0 ± 0.3%			4
Aromatic 100	4	0.6 ± 0.8%	2	1.1 ± 0.1%	1,3
Kerosene	4	4.4 ± 0.5%			4
Petroleum Distillate ASTM-1A (19% aromatics)	3	0.7 ± 0.5%	1	3.9%	1,3
Petroleum Distillate ASTM-1B (6% aromatics)	3	0.7 ± 0.4%	1	1.9%	1,3
Petroleum Distillate ASTM-1C (no aromatics)	2	0.2 ± 0.5%	1	1.3%	1,3
VMP Naphtha	2	-0.1 ± 0.1%			3
ASTM-3C1	4	-0.1 ± 0.3%			3

[a] Differences in PM volume measured after 5 hours of irradiation (uncorrected for wall loss) (converted to μg/m^3 by assuming unit particle density) between the experiment with added test compound and the base case experiment, divided by the amount of test VOC added (in μg/m^3).

[b] References for the reports where the experiments are discussed are as follows:
1 This work 2 Carter (2008) 3 Carter et al (2005c)
4 Carter and Malkina (2007) 5 Carter et al (2010)

effects of the VOCs on PM volume formation after 5 hours of irradiation are shown to place all the data on the same basis and because most experiments were carried out for at least that long. The data on Table 8 are given in the order they appear on reactivity tabulations (e.g., Carter, 2010b), and the data on Figure 19 are given in approximate order of PM formation potential. Previously studied compounds found to have negligible SOA reactivities are not shown on Figure 19.

The results indicate that the experimental SOA reactivities tend to be higher in the new surrogate - NO_x + H_2O_2 reactivity experiments developed for this project, but the ordering of SOA impacts appear to be approximately the same. The added H_2O_2 experiments appear to be more sensitive to differences

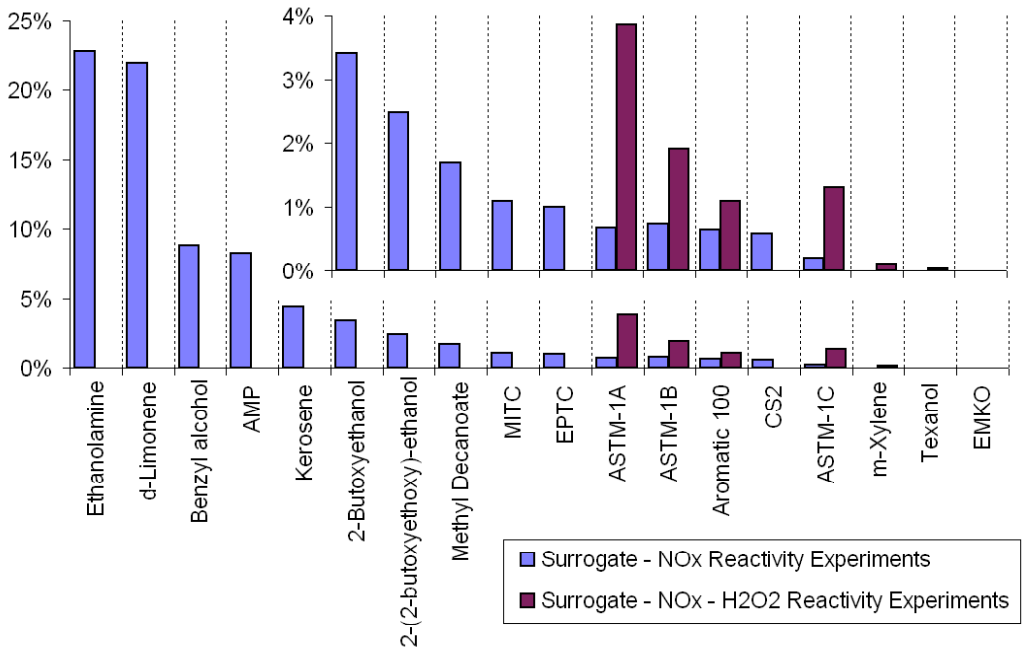

Figure 19. Comparison of average SOA formation incremental reactivities measured in various incremental reactivity experiments in the UCR EPA chamber.

among VOCs, though more replicate experiments are needed to verify the reproducibility of the results for compounds that are SOA precursors. If the results are found to be reproducible, the greater sensitivity would mean that the added H_2O_2 incremental reactivity experiments should be more useful for evaluating differences among VOCs on SOA impacts than the previous types of reactivity experiments. However, because of the larger number of compounds studied, the results of the previous experiments are more useful for comparisons among different types of compounds.

Of the compounds studied for this project, methyl decanoate appears to have the highest SOA forming potential based on the results of the surrogate - NO_x experiments, though it is still quite a bit lower than a number of other compounds that were previously studied. The experiments for this project confirmed that Texanol® has a very low SOA forming potential, even in the more sensitive reactivity experiments with added H_2O_2. Of the petroleum distillates that were studied using the added H_2O_2 experiments, the 19% aromatic mixture (ASTM-1A) had the highest SOA forming potential, while the other mixtures, including Aromatic-100, were comparable. The previous types of experiments gave the lowest SOA formation potential for the no-aromatics ASTM-1C mixture and comparable results for the others. More experiments with the added H_2O_2 would be useful to confirm the trends, because except for aromatic-100 only one added H_2O_2 experiment was conducted for each mixture. However, the SOA incremental reactivity results for the two aromatic-100 experiments were very similar, despite the very large differences in the amount of aromatic-100 added.

The relatively low or similar SOA formation potentials observed in the added H_2O_2 experiments with aromatic-100 and m-xylene compared to the primarily alkane mixtures are somewhat surprising because aromatics are considered to be more important SOA precursors than alkanes. However, these experiments are designed to represent high NO_x MIR conditions, and aromatics tend to have higher SOA formation potentials under lower NO_x conditions. More data are needed to evaluate this further.

DISCUSSION AND CONCLUSIONS

Chamber vs. Atmospheric Reactivities and Implications for Mechanism Evaluation

This project was successful in addressing the problem of apparent inconsistencies between chamber and atmospheric reactivities for compounds of interest in coatings applications such as Texanol® and petroleum distillates. These are manifested by the fact that higher alkanes and other compounds with similar mechanisms have negative effects on O_3 formation in our chamber experiments designed to represent MIR conditions but positive effects on O_3 in the atmospheric MIR scale. The modeling assessment carried out for this project provided useful information for assessing the reasons for the differences between chamber and atmospheric reactivities and indicated an alternative experimental approach that should give better correlations in this regard, at least for VOCs of interest for coatings applications. Experiments carried out to evaluate this approach successfully demonstrated its utility for several representative coatings VOCs where the correlation with atmospheric reactivity in previous experiments was poor, and much better correlations with atmospheric reactivities were obtained in these new experiments.

The modeling assessment indicated that the reason for this is that the experiments we have been using to simulate MIR conditions have significantly lower integrated radical levels and significantly greater sensitivity to radical termination processes than calculated for atmospheric MIR scenarios. The lower integrated OH levels resulted in the chamber simulations having lower sensitivity to secondary reactions of organic products compared to the atmosphere, and contributed to, but did not entirely account for, the higher sensitivity of the experiments to radical termination processes. Increasing the light intensity and duration of the irradiation to closer to ambient levels resulted in integrated OH levels approaching those of ambient simulations, but did not completely address the problem of the higher sensitivity of the experiments to radical termination processes compared to atmospheric conditions of interest. It was found that, adding H_2O_2 as a radical initiator to the experiments addressed this problem, and resulted in an experimental approach by which very good correlations between chamber and atmospheric reactivities could be obtained for the alkanes and alkane-like compounds of interest to coatings applications.

Integrated OH radical levels are important because most VOCs react in the atmosphere predominately with OH radicals under conditions where O_3 formation occurs, and increasing their integrated levels increases the extent of reaction and also opportunity for the organic oxidation products to react and contribute to O_3 formation. The fact that the previous chamber experiments were much less sensitive to reactions of VOC oxidation products than in the atmosphere is a problem not only because it contributed to reduced correlations with atmospheric reactivity in some cases, but also because it meant that chamber experiments did not provide a good evaluation of this aspect of the mechanism. Mechanisms for the reactions of VOC oxidation products in general tend to be more uncertain than mechanisms for the parent VOCs because in many cases the exact distribution of the products are uncertain, they are generally less well studied, and in most cases their reactions are represented using only a limited number of lumped model species. Improving the sensitivity of the experiments to this relatively uncertain aspect of the mechanism will be important to improving the quality of the mechanism evaluations, especially for multi-day simulations where reactions of oxidation products become increasingly important.

However, simply duplicating atmospheric integrated OH radical levels was found not to be sufficient for eliminating cases where coatings VOCs with positive MIRs had negative reactivities in chamber experiments. The much higher sensitivity of the chamber experiments to the radical termination processes appears to be the more important factor in this regard. Radical termination due to alkyl nitrate

formation from peroxy + NO reactions increases with the size of the molecule, is an important factor causing the reduced or (in chamber experiments) negative reactivities of the higher alkanes and other high molecular weight compounds. Adding additional radical initiators to the system decreases the sensitivity to radical termination (and initiation) processes because they make the system less limited by radical availability. Increasing integrated OH radical levels by increasing run duration increases initiation due to formation of photoreactive product species, but not to the same extent as adding radical initiators at the beginning of the experiment. In particular, even after increasing light intensity we found that adding a radical initiator was required to reduce the sensitivity of the experiments to radical termination processes sufficiently for the chamber reactivities of these coatings VOCs to correlate satisfactorily with atmospheric MIRs. The addition of H_2O_2 was found to serve this purpose quite well without introducing new experimental difficulties and uncertainties.

The modeling assessment resulted in deriving a reactive organic gas (ROG) surrogate - NO_x - H_2O_2 experimental system that appeared to be optimal for obtaining results that correlate with atmospheric reactivities for VOCs of interest. The correlation is not perfect, but the difference is probably within the range of variability of atmospheric reactivities calculated using different scenarios or methods. This new type of incremental reactivity experiment required the upgraded light intensity that was achieved as part of this project, but did not require longer run times that turned out to be difficult for us to achieve in practice. This system was tested experimentally and found to perform as predicted. Experiments conducted with n-octane, Texanol®, and petroleum distillate mixtures with varying aromatic content all gave positive incremental reactivities that had an 82% overall correlation with atmospheric MIR values (see Figure 18, above), despite some of these having negative or near-zero reactivities in the previous experiments.

Note that the addition of H_2O_2 to the reactivity experiments to improve the correlation with atmospheric MIR does not necessarily mean it exactly duplicates chemical conditions in the atmosphere. In fact, H_2O_2 is not emitted to any significant extent in current atmospheric models, and such models predict that that the formation of H_2O_2 is minor under higher NO_x, MIR conditions. The purpose of the added H_2O_2 is to make up for the deficiencies in radical sources in the chamber experiments compared to the atmospheric simulations. The exact reasons for these deficiencies have not been adequately investigated, but probably involve a combination of factors such as the O_3 aloft or the aldehydes or other reactive compounds in the base ROG mixture used in the ambient simulations that are not in the simplified ROG surrogate used for the chamber experiments. Attempting to simulate atmospheric conditions more closely to better represent these additional atmospheric radical initiation processes might give a more realistic atmospheric simulation, but doing so would make the experiments more difficult and expensive to carry out, and would probably be more difficult to conduct under controlled or reproducible conditions, making them less useful for mechanism evaluation. The addition of H_2O_2 in conjunction with increasing the light intensity provided what is needed to give reactivities corresponding to those in the atmosphere while minimizing experimental difficulties and cost. It also has the advantage of not requiring extended irradiation times, which turned out to be difficult to achieve in practice for our particular chamber configuration, and in any case would reduce the number of experiments that can be carried out with a given level of funding.

It should be recognized, however, that the objective of conducting environmental chamber experiments to assess reactivity is not to exactly duplicate reactivity in the atmosphere, but is to test the ability of models to correctly simulate reactivities under varying atmospheric conditions. Experimentally duplicating all relevant atmospheric conditions is not practical in any case because the atmosphere is highly variable, and air quality models provide the only practical way to assess how reactivities vary with time and space in realistic atmospheric scenarios. Although this project demonstrated that it is possible to develop an experimental system that gives chamber reactivity reasonably well correlated with atmospheric MIR, these experiments only test the mechanisms under one set of chemical conditions. The

ideal approach is to conduct experiments that are sensitive to different aspects of the mechanisms, so that together they can test all the aspects that might be important under varying atmospheric conditions. For example, the effects of the VOCs' reactions on NO_x sinks (or sources, in the case of EMKO) are critical for accurate predictions of reactivities under NO_x-limited conditions, but experiments simulating MIR conditions are insensitive to these effects. Reactivities under higher NO_x or MIR conditions are sensitive to radical sources and sinks in the mechanism, but the previous types of MIR experiments actually provided better tests in this regard because of their higher sensitivity to these factors than the new experiments that give better correlations with atmospheric reactivity. The new, added H_2O_2 experiments should provide a better test of the mechanism to secondary reactions than other types of experiments we have investigated.

Based on these considerations, we recommend that a minimum set of incremental reactivity experiments for mechanism evaluation should include not only these new experiments to better simulate reactivities under atmospheric MIR conditions, but also the previous type of "MIR" experiment to give more sensitive tests of aspects of the mechanism concerning radical processes, as well as low NO_x experiments needed to test mechanisms under NO_x - limited conditions. The previous experiments that are highly sensitive to radical termination effects are particularly useful in conjunction with the new added H_2O_2 experiments because together they provide a means to test effects of mechanisms for reactions of organic products with less concern about compensating errors concerning radical sinks and secondary reactions that could occur if only one type of experiment were employed. The experiment that is more sensitive to radical sinks can test that aspect of the mechanism, allowing the experiment that is sensitive to both effects to test the aspects of mechanisms concerning secondary reactions. Obviously, the NO_2 - limited experiments are necessary in any case, since the new experiments are not sensitive to NO_x sources and sinks in the mechanisms being evaluated.

Although the main objective for developing the modified reactivity experiments was obtaining data concerning ozone reactivity, the new, added H_2O_2 reactivity experiments also appear to be an improvement over the previous experiments in terms of assessing effects of VOCs on SOA formation. Although only a limited number of experiments were conducted with SOA precursor VOCs, the data obtained indicate that the new experimental system gives higher SOA yields from SOA precursors than the previous experiments, indicating that this system potentially provides a more sensitive measure of reactivity towards SOA formation. A wider variety of SOA precursors and more replicate experiments are needed to evaluate the utility of this type of experiment for assessing SOA reactivity, but the results thus far are encouraging.

Progress in Reducing Uncertainties in Atmospheric Ozone Impacts of Coatings VOCs

The second objective of this project concerned obtaining data to reduce uncertainties of reactivity estimates for selected coatings VOCs of interest to the CARB. This included conducting experiments with previously studied compounds such as Texanol® and representative petroleum distillates using the new reactivity measurement method discussed above, and the results indicated generally satisfactory model performance in simulating the data as well as better correlations with atmospheric MIR. This also included conducting reactivity experiments for compounds for which experimental reactivity data not available. The materials chosen for study for this aspect of the project were ethyl methyl ketone oxime (EMKO) and soy ester solvents, both of which are present in solvent emissions inventories. EMKO was chosen because its mechanism was unknown and there were no reactivity data for any chemically similar compound, and soy esters were chosen because of their importance in the inventory, and the expectation that their emissions may increase.

It turned out that we were unable to successfully conduct experiments to assess ozone impacts of soy ester constituents because of their low volatility and the lack of commercial availability of appropriate

lower molecular weight model compounds to represent them. Experiments were attempted with methyl linoleate, a major constituent of soy ester mixtures according to a CARB analysis (CARB, 2009), but we were unable to inject a sufficient quantity into the gas phase to have any measurable results on the reactivity experiment. However, for such low volatility materials the major uncertainty concerning its atmospheric ozone impact is not the chemical mechanism for its gas-phase reactions, it is its availability to enter the atmosphere and react in the gas phase in the first place. If we cannot get this material in the gas phase to react despite making every attempt to do so, one might think it would be unlikely to get into the atmosphere when it is used normally. Nevertheless, the vapor pressure of methyl linoleate and similar soy ester constituents are sufficiently high that it is possible for them to exist in the gas phase in sufficient concentrations at normal temperatures to react once they have mixed in the atmosphere. This can occur if they are emitted slowly over time, albeit slower than practical for chamber experiments. But this extra time provides the opportunity of other loss routes such as deposition on surfaces or aerosols that will reduce its availability for reactions to form ozone. Therefore, we recommend that studies of atmospheric availability be given priority over studies of atmospheric reactivity for such low volatility materials.

On the other hand, we were successful in obtaining data needed to develop and evaluate an ozone reactivity mechanism for EMKO, and in obtaining MIR and other atmospheric reactivity estimates for this compound. There were no previously evaluated or even estimated mechanisms for this compound, or any other oxime for that matter, prior to this study. The results indicate that the major reaction pathway (~75%) is formation of NO_2 and a stable product (probably MEK), with the NO_2 formation process involving radical termination. The environmental chamber reactivity data could only be simulated if radical termination and NO_x formation are major routes in the mechanism. These results can be explained if it is assumed that OH reacts with the C=NOH group forming H_2O and C=NO·, which then reacts with O_2 forming NO_2 and a carbonyl (MEK in this case). However, the kinetic data for the reactions of OH radicals with the oximes CH_2=NOH and CH_3CHNOH are more consistent with the initial process being OH addition to the C=N double bond, rather than abstraction from the OH group, and our EMKO reactivity results are best simulated if the OH + EMKO rate constant is estimated based on this addition mechanism. It appears that the initial reaction may be addition to the double bond, but the adduct must decompose or rearrange to form the same products as one would expect from H extraction from the NOH group.

The atmospheric reactivity of EMKO is unusual in that it calculated to have reactivity characteristics more like that of NO_x than a VOC. In particular, it is calculated to inhibit O_3 formation under MIR conditions (with an MIR of -1.27 gm O_3 /gm VOC) but have positive and increasing incremental reactivities under NO_x -limited conditions, with an MOIR of 0.42 and an EBIR of +1.14. This is similar to NO_x, though the magnitudes of the reactivities of EMKO (positive or negative) are about 30% those of NO_2. Thus, the O_3 impacts of emitting EMKO are more like those of emitting NO_x than emitting other types of VOCs. This has implications on the suitability of the MIR scale for such compounds, as discussed below.

In the course of investigating model compounds to represent soy ester constituents, we conducted a few experiments with methyl decanoate [$CH_3(CH_2)_8C(O)OCH_3$] as an analogue for the higher molecular weight saturated fatty esters present in soy ester mixtures. The results suggest that the current SAPRC-07 mechanism may be somewhat overestimating the atmospheric reactivity of this saturated fatty ester, based on the fact that the model somewhat underpredicted the extent to which these compounds inhibited O_3 formation in the MIR experiments (without H_2O_2) that are highly sensitive to radical termination processes. (The experiments with these compounds were conducted before the new type of reactivity experiments was developed.) However, these saturated esters are believed to represent only ~15% by mass and only ~5% by reactivity of whole soy ester mixtures, and the unsaturated esters, for which lower molecular weight analogues are apparently not available, are calculated to be much more reactive and have much more uncertain mechanisms. Therefore, further experiments with these compounds were not

carried out once we realized we could not adequately assess the reactivities of the more important and uncertain soy ester constituents. But if saturated fatty esters are important in emissions from other sources, then additional experiments studying these compounds would be needed, including the added H_2O_2 reactivity experiments that were developed as part of this project.

There were insufficient time and resources in this project to utilize this new method for conducting reactivity experiments for assessing mechanisms for any VOCs other than those with Texanol® and petroleum distillates used to test the new reactivity measurement method with previously studied compounds, as discussed above. In particular, the method was finalized and tested around the end of the project, so it wasn't employed in the tests of the mechanisms for the soy ester compounds or EMKO. However, the experiments with m-xylene and the Aromatic-100 mixture that were conducted to test the method suggest that the SAPRC-07 chemical mechanism may be underpredicting reactivities of aromatics in these experiments. Because of the better correlation between reactivities obtained using this method and atmospheric MIR, this suggests that the atmospheric MIR estimates for the aromatics may be too low, though the extent of this underprediction would require further investigation. The uncertain portions of the mechanisms can be adjusted to give better simulations of these new reactivity results as well as the results of the base case surrogate - NO_x experiments, but this would result in mechanisms that overpredict the reactivities of the aromatic - NO_x experiments that were used as the basis for developing the present mechanisms. Additional experiments of using this new reactivity assessment method may be useful in providing a more comprehensive evaluation database for aromatics mechanisms, which remain a significant uncertainty in present atmospheric models.

Implications of the EMKO Reactivity Results to Use of the MIR Scale

As discussed above, EMKO was found to be unusual in that it has relatively large negative reactivities in the MIR scale, but non-negative positive reactivities under more NO_x - limited conditions. For example, despite its negative MIR, the MOIR value for EMKO is positive and about the same as the MIR of ethane, and its MOIR value is ~4 times greater than the MIR of ethane, on a mass basis. (The MIR of ethane is used as the metric for comparison in this context because it measures its highest ozone impact.) Thus if ethane is used as a criterion for defining "negligible" ozone reactivity as is the standard practice of the EPA when granting VOC exemptions (Dimitriades, 1999), then it would not be appropriate to grant EMKO a VOC exemption under this criterion, despite its negative MIR. Most other compounds with negative MIR values have NO_x sinks in their mechanism, and thus have negative reactivities under all conditions. EMKO is the only compound in the current reactivity scale that has this reactivity characteristic, other than the volatile siloxanes, whose mechanisms are almost certainly oversimplified and neglect NO_x sinks that may in fact be present, and have very low magnitude reactivities in any case.

The concept behind using the MIR scale is that it reflects the maximum ozone impacts of the VOCs, and thus is an appropriate basis for regulating VOCs under conditions where changing VOC emissions is most effective (CARB, 1993; Carter, 1994a). Most VOCs indeed have their maximum reactivity under MIR conditions, which is why it is named the "maximum incremental reactivity" scale. But clearly the MIR scale does not represent the maximum incremental reactivity of EMKO, which means that use of the MIR value is not an appropriate basis for making an exemption decision for this compound. The only other compounds in the present Carter reactivity scales where this problem exists are the volatile siloxanes, whose mechanisms are probably incorrect and whose maximum reactivity values are still much lower than the MIR of ethane in any case. How these compounds should be treated in regulatory applications where use of a single scale is required is a policy issue that is beyond the scope of the present report. However, the existence of these cases needs to be considered when the regulatory reactivity scale is updated.

REFERENCES

Atkinson, R. and J. Arey (2003): "Atmospheric Degradation of Volatile Organic Compounds," Chem. Rev. 103, 4605-4638

CARB (1993): "Proposed Regulations for Low-Emission Vehicles and Clean Fuels -- Staff Report and Technical Support Document," California Air Resources Board, Sacramento, CA, August 13, 1990. See also Appendix VIII of "California Exhaust Emission Standards and Test Procedures for 1988 and Subsequent Model Passenger Cars, Light Duty Trucks and Medium Duty Vehicles," as last amended September 22, 1993. Incorporated by reference in Section 1960.

CARB (2000): "Initial Statement of Reasons for the Proposed Amendments to the Regulation for Reducing Volatile Organic Compound Emissions from Aerosol Coating Products and Proposed Tables of Maximum Incremental Reactivity (MIR) Values, and Proposed Amendments to Method 310, 'Determination of Volatile Organic Compounds in Consumer Products'," California Air Resources Board, Sacramento, CA, May 5.

CARB (2008): "Architectural Coatings – Reactivity Page," California Air Resources Board web page at http://www.arb.ca.gov/coatings/arch/reactivity/reactivity.htm, May 23.

CARB (2009): Carla Takemoto, California Air Resources Board Stationary Source Division, personal communication, August 26.

CARB (2010): "Final Statement of Reasons for Rulemaking: Public Hearing to Consider Proposed Amendments to the Tables Of Maximum Incremental Reactivity (MIR) Values," California Air Resources Board, Sacramento, California, July, 2010. Available at http://www.arb.ca.gov/regact/2009/mir2009/mir2009.htm

Carter, W. P. L. (1994a): "Development of Ozone Reactivity Scales for Volatile Organic Compounds," J. Air & Waste Manage. Assoc., 44, 881-899.

Carter, W. P. L. (1994b): "Calculation of Reactivity Scales Using an Updated Carbon Bond IV Mechanism," Report Prepared for Systems Applications International Under Funding from the Auto/Oil Air Quality Improvement Research Program, April 12.

Carter, W. P. L. (2000a): "Documentation of the SAPRC-99 Chemical Mechanism for VOC Reactivity Assessment," Report to the California Air Resources Board, Contracts 92-329 and 95-308, May 8. Available at http://cert.ucr.edu/~carter/absts.htm#saprc99 and http://www.cert.ucr.edu/~carter/reactdat.htm.

Carter, W. P. L. (2000b): "Implementation of the SAPRC-99 Chemical Mechanism into the Models-3 Framework," Report to the United States Environmental Protection Agency, January 29. Available at http://www.cert.ucr.edu/~carter/absts.htm#s99mod3.

Carter, W. P. L. (2002): "Development of a Next Generation Environmental Chamber Facility for Chemical Mechanism and VOC Reactivity Research," Draft Research Plan and First Progress Report to the United States Environmental Protection Agency Cooperative Agreement CR 827331-01-0, January 3. Available at http://www.cert.ucr.edu/~carter/epacham.

Carter, W. P. L. (2004): Evaluation of a Gas-Phase Atmospheric Reaction Mechanism for Low NO_x Conditions," Final Report to California Air Resources Board Contract No. 01-305, May 5. Available at http://www.cert.ucr.edu/~carter/absts.htm#lnoxrptf

Carter, W. P. L. (2008). "Reactivity Estimates for Selected Consumer Product Compounds," Final Report to the California Air Resources Board Contract 06-408, February 19. Available at http://www.cert.ucr.edu/~carter/absts.htm#aminrep.

Carter, W. P. L. (2009a): "Investigation of Atmospheric Ozone Impacts of Trans 1,3,3,3-Tetrafluoropropene," Final Report to Honeywell International Inc, February 9.

Carter, W. P. L. (2009b): "Investigation of Atmospheric Ozone Impacts of 2,3,3,3-Tetrafluoropropene," Final Report to Honeywell International Inc, June 2.

Carter, W. P. L. (2009c): "Investigation of Atmospheric Ozone Impacts of 1-Chloro-3,3,3-Trifluoropropene," Final Report to Honeywell International Inc, June 8.

Carter, W. P. L. (2010a): "Development of the SAPRC-07 Chemical Mechanism and Updated Ozone Reactivity Scales," Revised Final report to the California Air Resources Board Contract No. 03-318. January 27. Available at www.cert.ucr.edu/~carter/SAPRC.

Carter, W. P. L (2010b): "Updated Maximum Incremental Reactivity Scale and Hydrocarbon Bin Reactivities for Regulatory Applications," Report to the California Air Resources Board, Contract 07-339, January 28, available at http://www.cert.ucr.edu/~carter/SAPRC/MIR10.pdf.

Carter, W. P. L., J. A. Pierce, and I. L. Malkina (1992): "Investigation of the Ozone Formation Potential of Selected Volatile Silicone Compounds," Final report to Dow-Corning Corporation, November.

Carter, W. P. L., D. Luo, I. L. Malkina, and D. Fitz (1995): "The University of California, Riverside Environmental Chamber Data Base for Evaluating Oxidant Mechanism. Indoor Chamber Experiments through 1993," Report submitted to the U. S. Environmental Protection Agency, EPA/AREAL, Research Triangle Park, NC, March 20.

Carter, W. P. L., J. H. Seinfeld, D. R. Fitz, and G. S. Tonnesen (1999): "Development of a Next-Generation Environmental Chamber Facility for Chemical Mechanism and VOC Reactivity Evaluation," Proposal to the U. S. Environmental Protection Agency, February 22. Available at http://www.cert.ucr.edu/~carter/epacham.

Carter, W. P. L. and I. L. Malkina (2005): "Evaluation of Atmospheric Impacts of Selected Coatings VOC Emissions," Final report to the California Air Resources Board Contract No. 00-333, March 21. Available at http://www.cert.ucr.edu/~carter/absts.htm#coatrpt.

Carter, W. P. L., D. R. Fitz, D. Cocker, III, I. L. Malkina, K. Bumiller, C. G. Sauer, J. T. Pisano, C. Bufalino, and Chen Song (2005a): "Development of a Next-Generation Environmental Chamber Facility for Chemical Mechanism and VOC Reactivity Research," Final Report to the United States Environmental Protection Agency Cooperative Agreement CR 827331-01-0. June 27

Carter, W. P. L., D. R. Cocker III, D. R. Fitz, I. L. Malkina, K. Bumiller, C. G. Sauer, J. T. Pisano, C. Bufalino, and C. Song (2005b): "A New Environmental Chamber for Evaluation of Gas-Phase Chemical Mechanisms and Secondary Aerosol Formation", Atmos. Environ. 39 7768-7788.

Carter, W. P. L., I. L. Malkina, D. R. Cocker III, and C. Song (2005c): "Environmental Chamber Studies of VOC Species in Architectural Coatings and Mobile Source Emissions," Final Report to the South Coast Air Quality Management District Contract No. 03468, July 5. Available at http://www.cert.ucr.edu/~carter/absts.htm#scaqcham.

Carter, W. P. L. and I. L. Malkina (2007): "Investigation of the Atmospheric Impacts of Selected Pesticides," Final Report to the California Air Resources Board Contract 04-334, January 10. Available at http://www.cert.ucr.edu/~carter/absts.htm#pestrep.

Carter W. P. L, Wendy S. Goliff, Roger Atkinson, Janet Arey and Sara M. Aschmann (2010): "Investigation of Atmospheric Ozone Impacts of 3-Methoxy-3-Methyl-1-Butanol," Final Report to the Kuraray Co. Ltd, July 8. Available at http://www.cert.ucr.edu/~carter/absts.htm #MMBrept

Cocker, D. R., R. C. Flagan, and J. H. Seinfeld. (2001). "State-of-the-Art Chamber Facility for Studying Atmospheric Aerosol Chemistry," Environ. Sci. Technol. 35, 2594-2601.

Dimitriades, B. (1999): "Scientific Basis of an Improved EPA Policy on Control of Organic Emissions for Ambient Ozone Reduction," J. Air & Waste Manage. Assoc. 49, 831-838

Dodge, M. C. (2000): "Chemical Oxidant Mechanisms for Air Quality Modeling, Critical Review Paper for 1998 Ozone Assessment," Atmos. Environ, 34, 2103-2130.

Horne, D. G. and R. G. W. Norrish (1970): "The Flash Photolysis of Oximes," Proc. Roy. Soc. London A, 315, 287-300.

Jaques, A. (2003): "Hydrocarbon Solvent Test Materials for Chamber Experiments," Letter provided by the Hydrocarbon Panel of the American Chemistry Council to W. P. L. Carter dated March 24, 2003.

Jaques, A (2004): "Sample Analysis for Products sent to Dr. W. Carter for CARB Architectural Coatings Research," revised compositional information provided by the Hydrocarbon Panel of the American Chemistry Council on March 8, 2004.

Jeffries, H.E.; Gery, M.W.; and Carter, W.P.L. (1992) Protocol for evaluating oxidant mechanisms for urban and regional models. Report for U.S. Environmental Protection Agency Cooperative Agreement No. 815779, Atmospheric Research and Exposure Assessment Laboratory, Research Triangle Park, NC.

Lowi, A. L., and W. P. L. Carter (1990): "A Method for Evaluating the Atmospheric Ozone Impact of Actual Vehicle Emissions," Presented at the SAE International Congress and Exposition, Detroit, Michigan, February 26 - March 2, 1990.

Song, C, Na., B. Warren, Q. Malloy, and D. R. Cocker, III (2007): "Secondary Organic Aerosol Formation from m-Xylene in the Absence of NOx," Environ. Sci. Technol, 41, 7409-7416

Zafonte, L., P. L. Rieger, and J. R. Holmes (1977): "Nitrogen Dioxide Photolysis in the Los Angeles Atmosphere," Environ. Sci. Technol. 11, 483-487.

APPENDIX A. SUPPLEMENTARY MATERIALS

Table A-1. Compositions of mixtures used in various calculations discussed in this report.

Wt. Fraction	Component	Wt. Fraction	Component
	Base ROG Mixture for Atmospheric Reactivity Scale Calculations		ASTM-1A Mixture (Regular mineral spirits, Primarily C_{10}-C_{12} mixed alkanes with 19% aromatics)
3.54%	ethane	0.45%	n-octane
4.35%	propane	0.96%	branched C8 alkanes
7.33%	n-butane	0.24%	C8 bicycloalkanes
3.20%	isobutane	0.78%	C8 cycloalkanes
3.09%	n-pentane	1.20%	n-nonane
7.64%	isopentane	2.56%	branched C9 alkanes
0.35%	cyclopentane	0.64%	C9 bicycloalkanes
0.79%	n-hexane	2.08%	C9 cycloalkanes
0.14%	branched C6 alkanes	4.35%	n-decane
0.28%	2,2-dimethyl butane	9.28%	branched C10 alkanes
0.57%	2,3-dimethyl butane	2.32%	C10 bicycloalkanes
2.13%	2-methyl pentane	7.54%	C10 cycloalkanes
1.52%	3-methyl pentane	5.85%	n-undecane
0.40%	cyclohexane	12.48%	branched C11 alkanes
0.94%	methyl cyclopentane	3.12%	C11 bicycloalkanes
0.84%	n-heptane	10.14%	C11 cycloalkanes
0.78%	2,3-dimethyl pentane	2.70%	n-dodecane
0.42%	2,4-dimethyl pentane	5.76%	branched C12 alkanes
0.89%	3-methyl hexane	1.44%	C12 bicycloalkanes
1.46%	branched C7 alkanes	4.68%	C12 cycloalkanes
0.08%	C7 cycloalkanes	0.45%	n-tridecane
0.47%	methyl cyclohexane	0.96%	branched C13 alkanes
0.59%	n-octane	0.24%	C13 bicycloalkanes
3.22%	branched C8 alkanes	0.78%	C13 cycloalkanes
0.14%	ethyl cyclohexane	0.07%	toluene
0.67%	n-nonane	0.12%	ethyl benzene
1.53%	branched C9 alkanes	0.27%	m-xylene
1.83%	n-decane	0.39%	o-xylene
1.55%	branched C10 alkanes	0.10%	p-xylene
0.18%	n-undecane	0.66%	n-propyl benzene
0.18%	branched C11 alkanes	0.10%	isopropyl benzene (cumene)
0.39%	n-dodecane	0.55%	m-ethyl toluene
0.39%	branched C12 alkanes	2.13%	o-ethyl toluene
0.02%	n-tridecane	0.55%	p-ethyl toluene
0.02%	branched C13 alkanes	0.63%	1,2,3-trimethyl benzene
2.64%	ethene	0.65%	1,3,5-trimethyl benzene
0.93%	propene	0.32%	C10 monosubstituted benzenes
0.45%	1-butene	2.40%	C10 disubstituted benzenes
0.06%	C4 terminal alkenes	0.46%	m-diethyl benzene
0.45%	isobutene	2.89%	C10 trisubstituted benzenes
0.36%	cis-2-butene	1.14%	C10 tetrasubstituted benzenes
0.45%	trans-2-butene	0.43%	methyl indanes
0.06%	C4 internal alkenes	0.17%	naphthalene
0.23%	1,3-butadiene	0.26%	C11 monosubstituted benzenes
0.39%	1-pentene	0.65%	C11 disubstituted benzenes
0.16%	3-methyl-1-butene	2.13%	pentyl benzenes

Table A-1 (continued)

Wt. Fraction	Component	Wt. Fraction	Component
0.21%	C5 terminal alkenes	0.78%	methyl naphthalenes
0.45%	2-methyl-1-butene	0.26%	C12 trisubstituted benzenes
0.25%	2-methyl-2-butene	0.24%	hexyl benzenes
1.55%	C5 internal alkenes	0.63%	C12 monosubstituted naphthalene
0.62%	isoprene (2-methyl-1,3-butadiene)		
0.20%	1-hexene		ASTM-1B Mixture (Reduced Aromatics Mineral Spirits, Primarily C_{10}-C_{12} mixed alkanes with 6% aromatics.
1.31%	C6 terminal alkenes		
0.59%	C6 internal alkenes		
0.10%	cyclohexene	0.14%	n-octane
0.80%	C7 cyclic olefins or di-olefins	0.31%	branched C8 alkanes
0.30%	C7 terminal alkenes	0.10%	C8 bicycloalkanes
0.13%	C7 internal alkenes	0.39%	C8 cycloalkanes
0.19%	C8 terminal alkenes	1.12%	n-nonane
0.17%	C8 internal alkenes	2.48%	branched C9 alkanes
0.46%	C9 terminal alkenes	0.80%	C9 bicycloalkanes
0.22%	C9 internal alkenes	3.12%	C9 cycloalkanes
0.09%	C10 terminal alkenes	3.92%	n-decane
0.09%	C10 internal alkenes	8.68%	branched C10 alkanes
0.18%	3-carene	2.80%	C10 bicycloalkanes
0.48%	alpha-pinene	10.92%	C10 cycloalkanes
0.21%	C11 terminal alkenes	5.60%	n-undecane
0.21%	C11 internal alkenes	12.41%	branched C11 alkanes
1.80%	benzene	4.00%	C11 bicycloalkanes
5.94%	toluene	15.59%	C11 cycloalkanes
0.95%	ethyl benzene	2.80%	n-dodecane
1.62%	m-xylene	6.20%	branched C12 alkanes
1.35%	o-xylene	2.00%	C12 bicycloalkanes
1.62%	p-xylene	7.80%	C12 cycloalkanes
0.13%	C9 monosubstituted benzenes	0.42%	n-tridecane
0.30%	n-propyl benzene	0.93%	branched C13 alkanes
0.16%	isopropyl benzene (cumene)	0.30%	C13 bicycloalkanes
2.07%	C9 disubstituted benzenes	1.17%	C13 cycloalkanes
1.98%	C9 trisubstituted benzenes	0.02%	toluene
0.63%	1,2,3-trimethyl benzene	0.04%	ethyl benzene
0.60%	1,3,5-trimethyl benzene	0.08%	m-xylene
0.39%	C9 styrenes	0.12%	o-xylene
0.17%	C10 monosubstituted benzenes	0.03%	p-xylene
0.21%	sec-butyl benzene	0.21%	n-propyl benzene
1.44%	C10 disubstituted benzenes	0.03%	isopropyl benzene (cumene)
1.50%	C10 trisubstituted benzenes	0.17%	m-ethyl toluene
0.39%	C10 tetrasubstituted benzenes	0.67%	o-ethyl toluene
0.33%	C10 styrenes	0.17%	p-ethyl toluene
0.67%	C11 monosubstituted benzenes	0.20%	1,2,3-trimethyl benzene
0.10%	C11 disubstituted benzenes	0.21%	1,3,5-trimethyl benzene
0.10%	C11 trisubstituted benzenes	0.10%	C10 monosubstituted benzenes
0.03%	C12 monosubstituted benzenes	0.76%	C10 disubstituted benzenes
0.10%	C12 disubstituted benzenes	0.15%	m-diethyl benzene
0.10%	C12 trisubstituted benzenes	0.91%	C10 trisubstituted benzenes
1.66%	formaldehyde	0.36%	C10 tetrasubstituted benzenes
1.47%	acetaldehyde	0.14%	methyl indanes
0.28%	propionaldehyde	0.06%	naphthalene
1.25%	acetone	0.08%	C11 monosubstituted benzenes

Table A-1 (continued)

Wt. Fraction	Component	Wt. Fraction	Component
0.16%	C4 aldehydes	0.21%	C11 disubstituted benzenes
0.55%	methyl ethyl ketone	0.67%	pentyl benzenes
0.64%	C5 aldehydes	0.25%	methyl naphthalenes
0.51%	C6 aldehydes	0.08%	C12 trisubstituted benzenes
0.12%	benzaldehyde	0.08%	hexyl benzenes
1.77%	acetylene	0.20%	C12 monosubstituted naphthalene
Base ROG Mixture used in Environmental Chamber Simulations of Chamber vs. Atmospheric Reactivity		ASTM-1C Mixture (Dearomatized Mixed Alkanes, Primarily C_{10}-C_{12} mixed alkanes)	
40.03%	n-butane	0.14%	n-octane
18.15%	n-octane	0.30%	branched C8 alkanes
3.72%	ethene	0.11%	C8 bicycloalkanes
4.36%	propene	0.45%	C8 cycloalkanes
5.00%	trans-2-butene	1.12%	n-nonane
13.57%	toluene	2.40%	branched C9 alkanes
15.18%	m-xylene	0.88%	C9 bicycloalkanes
		3.60%	C9 cycloalkanes
	Aromatic-100 mixture	3.92%	n-decane
0.00%	ethyl benzene	8.40%	branched C10 alkanes
0.01%	m-xylene	3.08%	C10 bicycloalkanes
0.78%	o-xylene	12.60%	C10 cycloalkanes
0.01%	p-xylene	5.60%	n-undecane
7.12%	n-propyl benzene	12.01%	branched C11 alkanes
2.39%	isopropyl benzene (cumene)	4.40%	C11 bicycloalkanes
24.01%	m-ethyl toluene	18.00%	C11 cycloalkanes
9.40%	o-ethyl toluene	2.66%	n-dodecane
10.72%	p-ethyl toluene	5.70%	branched C12 alkanes
6.19%	1,2,3-trimethyl benzene	2.09%	C12 bicycloalkanes
18.72%	1,2,4-trimethyl benzene	8.55%	C12 cycloalkanes
12.23%	1,3,5-trimethyl benzene	0.56%	n-tridecane
0.02%	isomers of propyl benzene	1.20%	branched C13 alkanes
0.15%	C10 monosubstituted benzenes	0.44%	C13 bicycloalkanes
1.05%	n-butyl benzene	1.80%	C13 cycloalkanes
0.16%	sec-butyl benzene		
3.19%	C10 disubstituted benzenes		
0.68%	m-diethyl benzene		
0.05%	o-diethyl benzene		
1.05%	p-diethyl benzene		
1.95%	C10 trisubstituted benzenes		
0.03%	C10 tetrasubstituted benzenes		
0.08%	butylbenzenes		

Table A-2. List of example VOCs used for assessing factors affecting reactivity, and reactivities calculated for various scenarios.

Compound or Mixture	Incremental Reactivity (gm O_3/gm VOC)						
	MIR [a]	Avg. Cond MIR [b]	Chamber Reactivity Simulations [c]				
			Cham 1	Cham 2	Cham 2T	Cham 2H	Cham 2H+
Base ROG Mixture used in atmospheric reactivity simulations	3.60	3.69	0.185	0.658	0.676	0.885	0.718
		Alkanes, alcohols, ethers, glycols, etc.					
ethane	0.28	0.28	0.010	0.024	0.057	0.069	0.082
n-butane	1.15	1.17	0.030	0.078	0.219	0.290	0.349
2-methyl pentane	1.50	1.53	0.011	0.059	0.217	0.344	0.411
methyl cyclohexane	1.70	1.56	-0.034	-0.047	0.061	0.358	0.444
n-octane	0.90	0.92	-0.033	-0.077	-0.057	0.216	0.309
n-decane	0.68	0.70	-0.042	-0.118	-0.165	0.152	0.230
n-dodecane	0.55	0.57	-0.042	-0.122	-0.197	0.118	0.184
carbon monoxide	0.06	0.06	0.006	0.011	0.022	0.028	0.037
isopropyl acetate	1.07	1.10	0.049	0.191	0.331	0.391	0.421
2-propoxy-ethanol	3.30	3.71	0.211	0.547	0.825	0.986	0.903
2-(2-methoxyethoxy) ethanol	2.66	3.24	0.259	0.562	0.777	0.943	0.865
cyclohexanol	1.95	2.39	0.091	0.217	0.468	0.628	0.643
isobutyl acetate	0.62	0.64	0.021	0.054	0.159	0.241	0.308
n-butyl acetate	0.83	0.85	0.005	0.029	0.118	0.197	0.244
1-propoxy-2-propanol (propylene glycol n-propyl ether)	2.68	3.04	0.125	0.268	0.547	0.742	0.723
2-butoxy-ethanol	2.90	2.98	0.109	0.391	0.630	0.787	0.710
1-methoxy-2-propyl acetate	1.70	1.76	0.024	0.143	0.397	0.551	0.589
1-[2-hydroxypropyl]-2-propanol	2.31	2.75	0.110	0.232	0.472	0.644	0.619
n-pentyl acetate	0.84	0.98	-0.005	0.007	0.099	0.235	0.295
n-butoxy-2-propanol	2.72	2.80	0.060	0.178	0.417	0.627	0.597
ethyl 3-ethoxy propionate	3.58	3.33	0.074	0.435	0.624	0.800	0.684
1-methoxy-2-(2-hydroxypropoxy)-propane	1.98	2.51	0.112	0.244	0.460	0.693	0.665
n-hexyl acetate	0.69	0.79	-0.020	-0.037	0.009	0.191	0.262
2-butoxyethyl acetate	1.62	1.67	0.006	0.063	0.229	0.441	0.457
1-hydroxy-2,2,4-trimethylpentyl-3-isobutyrate	0.89	0.91	-0.014	0.014	0.117	0.204	0.215
3-hydroxy-2,2,4-trimethylpentyl-1-isobutyrate	0.77	0.94	-0.004	0.023	0.123	0.222	0.241
isopropyl alcohol	0.61	0.63	0.065	0.121	0.234	0.270	0.322

Table A-2 (continued)

Compound or Mixture	Incremental Reactivity (gm O_3/gm VOC)						
	MIR [a]	Avg. Cond MIR [b]	Chamber Reactivity Simulations [c]				
			Cham 1	Cham 2	Cham 2T	Cham 2H	Cham 2H+
propylene glycol	2.58	2.38	0.176	0.371	0.595	0.651	0.611
methanol	0.67	0.69	0.039	0.144	0.220	0.241	0.256
ethanol	1.53	1.55	0.047	0.134	0.318	0.381	0.420
dimethyl ether	0.81	0.83	0.086	0.170	0.327	0.383	0.473
ethylene glycol	3.13	3.22	0.137	0.357	0.710	0.830	0.808
isobutyl alcohol	2.51	2.56	0.092	0.303	0.544	0.631	0.609
n-butyl alcohol	2.88	2.94	0.102	0.320	0.560	0.650	0.620
sec-butyl alcohol	1.36	1.39	0.086	0.181	0.369	0.428	0.468
ethyl acetate	0.63	0.64	0.005	0.040	0.114	0.143	0.159
1-methoxy-2-propanol	2.44	2.73	0.176	0.353	0.637	0.780	0.776
propylene carbonate	0.28	0.29	0.007	0.028	0.069	0.080	0.096
			Alkenes				
ethene	9.00	9.22	0.598	2.139	2.427	3.053	2.776
propene	11.66	12.03	0.919	2.629	2.500	3.066	2.407
trans-2-butene	15.16	15.91	1.005	2.896	2.457	2.792	2.017
isobutene	6.29	6.54	0.979	2.252	1.762	1.987	1.625
1-pentene	7.21	7.43	0.421	1.223	1.198	1.590	1.225
isoprene	10.61	10.97	0.899	2.036	1.577	2.233	1.685
2-methyl-1-butene	6.40	6.64	0.894	2.023	1.549	1.804	1.430
2-methyl-2-butene	14.08	14.95	0.845	2.483	1.971	2.256	1.667
1-hexene	5.49	5.67	0.385	0.937	1.002	1.319	1.075
cis-2-hexene	8.31	8.66	0.576	1.573	1.280	1.495	1.020
2,3-dimethyl-2-butene	12.49	13.27	0.796	2.036	1.448	1.602	1.206
2-methyl-2-pentene	11.00	11.64	0.627	1.871	1.438	1.677	1.156
1-octene	3.25	3.36	0.015	0.235	0.470	0.733	0.635
1-decene	2.17	2.25	-0.085	-0.052	0.185	0.460	0.430
			Aromatics				
benzene	0.72	0.73	0.017	0.062	0.003	0.122	0.073
toluene	4.00	4.09	0.068	0.295	0.292	0.563	0.432
m-xylene	9.75	10.02	0.200	0.786	0.692	1.165	0.796
o-xylene	7.64	7.83	0.130	0.548	0.529	0.888	0.634
p-xylene	5.84	5.99	0.130	0.511	0.450	0.888	0.622
1,3,5-trimethyl benzene	11.76	12.13	0.382	1.202	0.998	1.349	0.947
1,2,3-trimethyl benzene	11.97	12.32	0.262	0.948	0.915	1.214	0.836
1,2,4-trimethyl benzene	8.87	9.12	0.274	0.921	0.858	1.215	0.856
ethyl benzene	3.04	3.10	0.073	0.310	0.317	0.583	0.454
			Aldehydes				
formaldehyde	9.46	9.78	0.725	2.108	2.171	1.912	1.532
acetaldehyde	6.54	6.76	0.216	1.001	1.502	1.585	1.386
			Ketones				
acetone	0.36	0.36	0.016	0.062	0.099	0.077	0.079
methyl ethyl ketone	1.48	1.52	0.025	0.119	0.185	0.205	0.182
2-pentanone	2.81	2.88	0.051	0.256	0.452	0.519	0.502

Table A-2 (continued)

Compound or Mixture	Incremental Reactivity (gm O_3/gm VOC)						
	MIR [a]	Avg. Cond MIR [b]	Chamber Reactivity Simulations [c]				
			Cham 1	Cham 2	Cham 2T	Cham 2H	Cham 2H+
4-methyl-2-pentanone	3.88	4.00	0.051	0.382	0.778	0.948	0.894
diacetone alcohol	0.60	0.61	0.005	0.035	0.088	0.110	0.114
2-heptanone	2.36	2.42	0.005	0.098	0.330	0.491	0.516
di-isobutyl ketone (2,6-dimethyl-4-heptanone)	2.68	2.77	-0.042	0.001	0.217	0.503	0.476
			Amines				
morpholine	1.98	2.06	-0.176	-0.259	-0.138	0.491	0.568
2-amino-2-methyl-1-propanol	0.25	0.26	-0.197	-0.723	-1.688	-0.580	-0.518
diethanol-amine	2.47	2.56	-0.185	-0.101	0.289	0.516	0.546
n-methyl-2-pyrrolidone	2.41	2.47	0.017	0.112	0.380	0.618	0.607
triethyl amine	3.84	4.02	0.600	1.150	0.812	1.212	0.921
			Mixtures				
Texanol ®	0.81	0.93	-0.007	0.020	0.121	0.216	0.232
Regular mineral spirits (ASTM-1A)	1.89	1.95	-0.032	0.023	0.221	0.441	0.412
Reduced Aromatics Mineral Spirits (ASTM-1B)	1.19	1.22	-0.049	-0.105	-0.060	0.252	0.306
Dearomatized C_{10}-C_{12} mixed alkanes (ASTM-1C)	0.87	0.89	-0.052	-0.135	-0.189	0.174	0.244
Aromatic-100	7.38	7.59	0.188	0.716	0.662	1.011	0.713

[a] Standard atmospheric MIR scale from Carter (2010a). Average of the incremental reactivities in the 39 city-specific scenarios with NO_x inputs adjusted to yield maximum incremental reactivities.

[b] Atmospheric reactivities calculated using the "Averaged Conditions" MIR scenario.

[c] Incremental reactivities calculated for various types of environmental chamber experiments, as follows. See Table 3. Codes for various types of experiments are as follows:

- Cham 1: Previous MIR reactivity experiments
- Cham 2: MIR experiments with higher light intensity
- Cham 2T: MIR experiments with higher light intensity and longer time
- Cham 2H: MIR experiments with higher light intensity and added H_2O_2 (as used)
- Cham 2H+: MIR experiments with higher light intensity and more added H_2O_2

Table A-3. Chronological listing of environmental chamber experiments whose results are relevant to this project.

Run	Date	Type	Purpose and Conditions [a]	Results
991	4/9/09	Surrogate + perfluoro n-hexane	Test whether using perfluorohexane as a dilution tracer in experiments affects reactivity results. 22 ppb NO_x and 1.23 ppmC ROG surrogate added to both reactors, and 3.5 ppm perfluorohexane added to Side A. Original lights used.	The added prefluorohexane had no effect on O_3 formation, NO oxidation or reactant consumption rates. See Figure 7.
	1/27/10	Fabrication of enhanced blacklights completed		
1064	10/26/09	Dilution test #1	Test the ability to conduct experiments with controlled and reproducible experiments with equal dilution in each reactor. See text.	The dilution rates were found not to be sufficiently equal in the two reactors to be suitable for incremental reactivity experiments. See text.
1066	11/5/09	Dilution test #2		
1067	11/9/09	Dilution test #3 (no air handlers)		
1073	11/23/09	Surrogate + n-octane	Test measurements of incremental reactivity of n-octane using the higher light intensity. See note [b].	See note [b] and Figure 12.
1076	12/1/09	CO - Air	Characterization experiment to test background NO_x offgasing. 55 ppm CO injected into both reactors.	Results best fit with models using HONO offgasing (RN-I) parameter values of 25 and 15 ppt/min in Sides A and B, respectively. Results in normal range. See Figure 9.
1079	12/4/09	Surrogate + n-butane	Test measurements of incremental reactivity of n-butane using the higher light intensity. See note [b].	See note [b] and Figure 11.
1081	12/9/09	Surrogate + Texanol®	Test measurements of incremental reactivity of Texanol® using the higher light intensity. See note [b].	See note [b] and Figure 12.
1083	12/11/09	Surrogate + n-Butane	Same as EPA1079. See note [b].	See note [b] and Figure 11.
1088	12/22/09	Surrogate + Texanol®	Replicate previous incremental reactivity experiments with Texanol®. See note [b].	See note [b] and Figure 12.

Table A-3 (continued)

Run	Date	Type	Purpose and Conditions [a]	Results
1103	1/22/10	CO + NO_x	Characterization experiment to test for chamber radical source. 40 ppm of CO and ~20 ppb NO_x injected into both reactors.	Results best fit with models using HONO offgasing (RN-I) parameter values of 21 and 14 ppt/min in Sides A and B, respectively. Results in normal range. See Figure 9.
1112	2/2/10	Surrogate Side Equivalency	Test equivalency of results when the same surrogate - NO_x mixture is irradiated in both reactors. See Table 4	Acceptable side equivalency obtained. See Table 4 and Figure 11.
1113	2/3/10	Surrogate (vary NO_x)	Obtain data to evaluate mechanisms and base case surrogate experiments under various surrogate and NO_x conditions with the increased light intensity. See Table 4.	See note [b]. Figure 10 gives plots of model errors against surrogate / NO_x ratios.
1122	2/17/10	Surrogate (vary NO_x)	Same as EPA1113. See Table 4.	See note [b]. Figure 10 gives plots of model errors against surrogate / NO_x ratios.
1124	2/19/10	CO - Air	Characterization experiment to test background NO_x offgasing. 30 ppm CO injected into both reactors.	Results best fit with models using HONO offgasing (RN-I) parameter values of 8 ppt/min for both reactors. Results in normal range. See Figure 9.
1128	2/24/10	Surrogate + n-octane	Same as EPA1073 except with different surrogate and NO_x levels. See note [b].	See note [b] and Figure 12.
1130	2/26/10	Surrogate + EMKO	Obtain data to evaluate mechanism for EMKO. See note [b].	See note [b] and Figure 13.
1133	3/5/10	Surrogate + EMKO	Obtain data to evaluate mechanism for EMKO. See note [b].	See note [b] and Figure 13.
1138	3/10/10	In-chamber actinometry	Measure light intensity (NO_2 photolysis rate) inside the reactors. The quartz tube actinometer was placed inside reactor A and measurements were made with only the original (old) light banks on, with only the new lights on, and with all lights on.	In chamber NO_2 photolysis rates were 0.131 min^{-1} with old lights only, 0.256 min^{-1} with the new lights, and 0.401 min^{-1} with all lights. The value with all the lights was within 4% of the sum of the old + new, and a factor of 3 higher than with only the old lights.
1139	3/11/10	Surrogate + EMKO	Obtain data to evaluate mechanism for EMKO. See note [b].	See note [b] and Figure 13.

Table A-3 (continued)

Run	Date	Type	Purpose and Conditions [a]	Results
1140	3/12/10	Surrogate + Texanol®	Replicate EPA1088 previous incremental reactivity experiments with Texanol®. See note [b].	See note [b] and Figure 12.
1144	3/16/10	Pure air irradiation	Test for background effects, particularly for background PM formation. No injections.	About 20 ppb O_3 and 1 μg/m^3 PM formed in 4 hours, within the normal range.
1145	3/17/10	Surrogate + EMKO	Obtain data to evaluate mechanism for EMKO. Only original blacklights used (lower light intensity). See note [b].	See note [b] and Figure 13.
1152	3/24/10	Surrogate + methyl decanoate	Obtain data to evaluate the mechanism for methyl decanoate, a lower molecular weight and saturated analogue of constituents of soy esters. See note [b].	See note [b] and Figure 15.
1160	4/2/10	Surrogate + methyl decanoate	Same as EPA1152. See note [b]	See note [b] and Figure 15.
1164	4/6/10	Surrogate + methyl linoleate	Obtain data to evaluate the mechanism for methyl linoleate, an analogue of constituents of soy esters. See note [b].	Results suggested that methyl linoleate was not successfully injected into the gas phase. See note [b] and Figure 15.
1165	4/7/10	CO - NO_x	Characterization experiment to test for chamber radical source. 36 ppm of CO and ~25 ppb NO_x injected into both reactors.	Results best fit with models using HONO offgasing (RN-I) parameter values of 15 and 10 ppt/min in Sides A and B, respectively. Results in normal range. See Figure 9.
1167	4/9/10	Surrogate + methyl linoleate	Second attempt to obtain data to evaluate the mechanism for methyl linoleate. See note [b]	Results also suggested that methyl linoleate was not successfully injected into the gas phase. See note [b] and Figure 15.
1177	5/7/10	Surrogate side equivalency	Test equivalency of results when the same surrogate - NO_x mixture is irradiated in both reactors. See Table 4.	Acceptable side equivalency obtained. See note [b] and Figure 11.
1230	7/24/10	H_2O_2 - Air	Characterization experiment to test background NO_x offgasing. Model simulations indicate that O_3 formation in these experiments should be very sensitive to NO_x offgasing	Results best fit with models using HONO offgasing (RN-I) parameter values of around 12 ppt/min for both reactors. Results in normal range. See Figure 9.

Table A-3 (continued)

Run	Date	Type	Purpose and Conditions [a]	Results
1338	12/13/10	Surrogate H_2O_2 + n-octane	Evaluate new surrogate - NO_x - H_2O_2 experiments for assessing reactivity with selected previously studied compounds. See note [b].	See note [b], Figure 16 and Figure 18.
1339	12/15/10	Surrogate H_2O_2 side equivalency	Test equivalency of results when the same surrogate - NO_x - H_2O_2 mixture is irradiated in both reactors. See note [b].	Acceptable side equivalency obtained. See Table 4 and Figure 16.
1340	12/16/10	Surrogate H_2O_2 + m-xylene	Same as EPA1338. See note [b].	See note [b], Figure 16 and Figure 18.
1342	12/18/10	Surrogate H_2O_2 + Aromatic-100	Same as above. Amount of injected Aromatic-100 was higher than intended, but results still usable. See note [b]	See note [b] and Figure 17.
1343	12/19/10	Surrogate H_2O_2 + Texanol®	Same as above. See note [b].	See note [b], Figure 16 and Figure 18.
1344	12/21/10	Surrogate H_2O_2 + ASTM-1A	Same as above. See note [b].	See note [b] Figure 17 and Figure 18.
1345	12/23/10	Surrogate H_2O_2 + ASTM-1B	Same as above. See note [b].	See note [b] Figure 17 and Figure 18.
1346	12/31/10	Surrogate H_2O_2 + ASTM-1C	Same as above. See note [b].	See note [b] Figure 17 and Figure 18.
1347	1/1/11	Surrogate H_2O_2 + Aromatic-100	Same as above. See note [b].	See note [b] Figure 17 and Figure 18.
1348	1/3/11	Surrogate H_2O_2 + Texanol®	Same as above. See note [b].	See note [b], Figure 16 and Figure 18.
1349	1/5/11	Surrogate H_2O_2 + Texanol®	Same as above. See note [b].	See note [b], Figure 16 and Figure 18.
1351	1/8/11	CO - NO_x	Characterization experiment to test for chamber radical source. 40 ppm of CO and ~60 ppb NOx injected into both reactors. The CO analyzer was not operational during this period so the initial CO was estimated based on the amount injected.	Results best fit with models using HONO offgasing (RN-I) parameter values of 60 and 55 ppt/min in Sides A and B, respectively. This is far outside the expected range (see Figure 9), and suggests experimental problems or contamination. There is no reason to expect such a high level of contamination for the other runs for this project with these reactors. The results of this experiment were not used for chamber characterization.

[a] Unless indicated otherwise, all the blacklights were used for maximum light intensity.

[b] Base case conditions and selected results for all useable surrogate experiments without added test compounds are summarized on Table 4 and amounts of test VOC added and selected reactivity results for experiments with added test compounds are summarized on Table 5.